

T-3472

TWO-DIMENSIONAL COMPUTER MODEL OF TRANSIENT
UNSATURATED FLOW

by

Angelina Marie Dennis

ARTHUR LAKES LIBRARY
COLORADO SCHOOL of MINES
GOLDEN, COLORADO 80401

ProQuest Number: 10782963

All rights reserved

INFORMATION TO ALL USERS

The quality of this reproduction is dependent upon the quality of the copy submitted.

In the unlikely event that the author did not send a complete manuscript and there are missing pages, these will be noted. Also, if material had to be removed, a note will indicate the deletion.



ProQuest 10782963

Published by ProQuest LLC (2018). Copyright of the Dissertation is held by the Author.

All rights reserved.

This work is protected against unauthorized copying under Title 17, United States Code
Microform Edition © ProQuest LLC.

ProQuest LLC.
789 East Eisenhower Parkway
P.O. Box 1346
Ann Arbor, MI 48106 – 1346


T-3472

A thesis submitted to the Faculty and the Board of Trustees of the Colorado School of Mines in partial fulfillment of the requirements for the degree of Master of Science in Engineering Ecology.

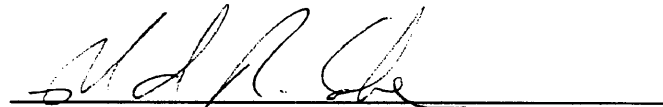
Golden, Colorado

Date 1-5-88

Signed:

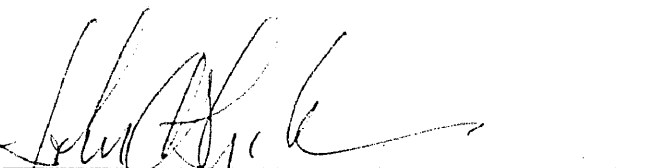

Angelina M. Dennis

Approved:


Ronald R. Cohen
Thesis Advisor
Assistant Professor of Environmental
Sciences and Engineering Ecology

Golden, Colorado

Date 1/6/88


John C. Emerick
Associate Professor of Environmental
Sciences and Engineering Ecology
Acting Head
Department of Environmental Sciences
and Engineering Ecology

ABSTRACT

Predicting leachate movement in the unsaturated zone is important in carrying out effective remediation at leaking landfill cells. This modelling project represents progress towards the ultimate goal of accurately predicting leachate flow rates and patterns under unsaturated conditions. Infiltration of water was modelled using a two-dimensional, transient flow computer program.

Computer simulation results were compared to capillary head field data from a line source leak experiment. A constant 22 inches of head was maintained on a 30 foot section of 2 inch, slotted Schedule-40 PVC well screen, protectively buried below the ground surface. Richards' (1931) transient, unsaturated flow equation is solved using finite differences and the alternating direction implicit numerical analysis method. The gravity component of flow was only added in the calculations for the column implicit iterations. Internodal capillary conductivities and water contents were calculated using a geometric mean weighting factor. Three categories of functions are tested to determine which produces results most like the field data. The functions depend on the independent variable, head, and calculate the capillary conductivity and water content values.

Most of the predicted flow rates were slower than those indicated by the field data. One of the test runs matched the field data. In this run, the influence of the gravity component for saturated conditions was increased

by one order of magnitude. Test runs excluding the gravity term erroneously indicated that the geologic units would become drier.

Saturated zones were observed in the subsurface. Head values greater than -20 cbars were designated as saturated. The question arose as to which head value should be used in saturated blocks that were not necessarily hydraulically connected to other saturated blocks. When pressure head was substituted, drying blocks were indicated. Different influence factors were applied to test the influence of the $\partial h/\partial w$ function at saturation. Best results were obtained when the influence factor was equal to unity.

Some type of transitional force must be determined for flow between saturated and unsaturated blocks. Additionally, theories need to be founded that would describe head values for saturated blocks in known unsaturated zones. Unsaturated flow models for infiltration conditions that reach saturation may need to rely on water content as the independent variable. Mass balance on liquid flux could be applied at the boundaries and conductivity would be based on water content.

TABLE OF CONTENTS

ABSTRACTiii

LIST OF FIGURES.....vii

LIST OF TABLES.....ix

ACKNOWLEDGEMENTS.....x

1.0 INTRODUCTION.....1

 1.1 Modelling Unsaturated Flow.....1

 1.2 Description of Project.....2

 1.3 Numerical Model.....3

 1.4 Unique Aspects of the ADI Model in this Project.....5

 1.5 Examples of Flow Models Employing the ADI Technique.....7

 1.6 Historical Development of Unsaturated Flow Models and
 Support for Richards' Equation.....8

2.0 FIELD CONDITIONS AND EQUIPMENT13

 2.1 Source of Field Data.....13

 2.2 Site Geology.....13

 2.3 Porosity, Water Content and Hydraulic Conductivity Values.....16

 2.4 Configuration of the Infiltration Source.....17

 2.5 Vadose Zone Monitoring System.....19

3.0 THE PHYSICAL SYSTEM.....28

 3.1 Properties of the Unsaturated Zone.....28

 3.2 Capillary Pressure.....30

 3.3 Flow Zones During Infiltration.....32

 3.4 Hysteresis in Unsaturated Flow.....34

 3.5 Similarity Theory and Scaling Factors for Capillary
 Conductivity and Water Content Functions.....35

4.0	THE CAPILLARY CONDUCTIVITY AND WATER CONTENT FUNCTIONS.....	38
4.1	The Uncertainty of the Prediction.....	38
4.2	The Brooks and Corey Power Function.....	40
4.3	Closed-form Analytical Functions.....	43
4.4	Polynomial Relationship Added to the Campbell Power Function.....	46
4.5	Comparison of Three Functions.....	49
5.0	GOVERNING DIFFERENTIAL EQUATIONS.....	50
5.1	Richards' Equation.....	50
5.2	The Influence of the Gravity Term.....	52
5.3	Support for Richards' Equation.....	54
6.0	ASSUMPTIONS INTRINSIC TO THE MODEL.....	56
7.0	NUMERICAL ANALYSIS.....	61
7.1	Approximating the Richards' Equation with Finite Differences.....	61
7.2	The Implicit Method.....	63
7.3	The ADI Method.....	64
7.4	Weighting Factors.....	68
7.5	Initial and Boundary Conditions.....	69
8.0	DISCUSSION OF INPUT PARAMETERS AND RESULTS.....	72
8.1	Explanation of Input/Output Data File Tables.....	72
8.2	General Program Flow and Constraints.....	79
8.3	Input Parameters.....	82
8.4	Discussion of Output Data.....	85
9.0	CONCLUSIONS.....	89
10.0	REFERENCES CITED.....	95
11.0	APPENDICES.....	105
11.1	Appendix A.....	105
11.2	Appendix B.....	107
11.3	Appendix C.....	124

LIST OF FIGURES

Figure 1.	CROSS SECTION PERPENDICULAR TO THE BEDDING PLANES AND UNDER THE SOURCE PIPE: LOCATION OF EQUIPMENT IN THE CENTRAL PROFILE.....	18
Figure 2.	LOCATION OF GEOLOGIC UNITS AND MONITORING EQUIPMENT.....	22
Figure 3.	W vs. H, BROOKS AND COREY, AVERJANOV AND MUALEM POWER EQUATIONS.....	108
Figure 4.	H vs. K, BROOKS AND COREY, AVERJANOV AND MUALEM POWER EQUATIONS.....	109
Figure 5.	W vs. K, BROOKS AND COREY, AVERJANOV AND MUALEM POWER EQUATIONS.....	110
Figure 6.	RELATIVE SHAPE OF THE W vs. H RELATIONSHIP FOR COMPARISON TO GENERATED CURVES.....	111
Figure 7.	W vs. H, VAN GENUCHTEN CLOSED FORM ANALYTICAL EQUATIONS.....	112
Figure 8.	H vs. K, VAN GENUCHTEN CLOSED FORM ANALYTICAL EQUATIONS.....	113
Figure 9.	W vs. K, VAN GENUCHTEN CLOSED FORM ANALYTICAL EQUATIONS	114
Figure 10.	W vs. H, VAN GENUCHTEN CLOSED FORM ANALYTICAL EQUATIONS.....	115
Figure 11.	H vs. K, VAN GENUCHTEN CLOSED FORM ANALYTICAL EQUATIONS.....	116
Figure 12.	W vs. K, VAN GENUCHTEN CLOSED FORM ANALYTICAL EQUATIONS.....	117

Figure 13. W vs. H, CAMPBELL POWER EQUATIONS WITH THE CLAPP AND HORNBERGER POLYNOMIAL VARIATION.....118

Figure 14. H vs. K, CAMPBELL POWER EQUATIONS WITH THE CLAPP AND HORNBERGER POLYNOMIAL VARIATION.....119

Figure 15. W vs. K, CAMPBELL POWER EQUATIONS WITH THE CLAPP AND HORNBERGER POLYNOMIAL VARIATION.....120

Figure 16. W vs. H, THREE TYPES OF FUNCTIONS REPRESENTED FOR COMPARISON.....121

Figure 17. H vs. K, THREE TYPES OF FUNCTIONS REPRESENTED FOR COMPARISON.....122

Figure 18. W vs. K, THREE TYPES OF FUNCTIONS REPRESENTED FOR COMPARISON.....123

Figure 19. GRID POINT SYSTEM.....61

LIST OF TABLES

Table 1. Description of Geologic Layers by Unit Numbers.....15

Table 2. Tensiometer, Lysimeter and BAT Data from the Central Profile Under the Source Pipe.....25

Table 3. Description of Column Headings in the Data File Tables.....72

Table 4. Computer Simulation Data for the Brooks and Corey Power Functions.....74

Table 5. Computer Simulation Data for the Van Genuchten Closed Form Analytical Equations.....75

Table 6. Computer Simulation Data for the Campbell Functions with a Polynomial Variation.....76

Table 7. Computer Simulation Data for Runs with Zero Influence from the Gravity Term.....77

Table 8. Computer Simulation Data for Positive Initial Head Values.....78

ACKNOWLEDGEMENTS

I would like to thank everyone who has had any part in encouraging or assisting me during my graduate school years. Professor Elisabeth Lloyd convinced me I had the abilities to study at the graduate level. Joan Armatrading and Colorado Womens Ice Hockey kept me sane my first two years. Barbara Kleeman helped me understand the emotional dynamics that accompany graduate work. She also spent considerable time helping me learn better communication skills in my professional and personal relationships. Don Gipe allowed me the flexibility to work for him at the EPA and still concentrate on my graduate studies. Thanks, Don, for all your patience. Julie Irvine, my ice hockey linemate and fellow engineer, is the best supporter and friend I could have wanted to find in Colorado. Thanks, Susan Hodgson, for showing me compassion to compliment the sometimes severe engineering training. Diane Dvorin, Bill Butler and their friends provided invaluable love and assistance during the writing of my thesis. Kata Weber is quite a woman, and her advice and assistance could not have been replaced. Ron Cohen's enthusiasm for academics and his belief in me was a bomber hold on the steep climb of graduate school. Thanks, Dr. Cohen, for standing by me and reading a long thesis many times. Lauren Weintraub served as an expert copy editor and I am not sure how to thank her enough. Probably the best thanks to her would be not to, because I want a different way with her. Lastly, and most importantly, I would like to thank my parents, Rose and Arthur Dennis. They have always wanted me to excel and have provided everything possible to see that I do.

1.0 INTRODUCTION

1.1 Modelling Unsaturated Flow

Landfill waste disposal cells can potentially leak liquids, called leachate, into the unsaturated zone. This leachate may contain hazardous or toxic chemicals. Understanding the flow characteristics of liquid in the unsaturated zone is essential to prevent leachate from entering the water cycle. In this project, results from a newly created computer model are compared to a simulated waste disposal cell leak using colored water "leachate". The goal of this project is to determine whether the model will match the field results given the proper water content, $w(h)$, and hydraulic conductivity, $K(h)$, functions (as they relate to capillary head, "h").

Porous media whose naturally occurring liquids are not hydraulically connected and do not completely fill the pores of the strata, comprise the unsaturated, or vadose zone. The capillary fringe above a water table where pores are partially to completely filled with liquid is not typically considered part of the unsaturated zone. The definition of the vadose zone often includes the capillary fringe. The strata in the unsaturated zone can adsorb and absorb the contaminants during percolation.

Unlike models of saturated flow, the conductivity in unsaturated systems is not a constant. Both the capillary head and capillary conductivity are functions of water content. As a result, any unsaturated

flow equation based on these parameters will be nonlinear. Herein lies the uncertainty in any unsaturated flow modelling attempt. The parameters required to determine the new moisture contents and conductivities are dependent on these as yet unknown moisture values. One investigative group has noted that the estimate of conductivity in the vertical direction can be in error by a factor of five for any given water content value (Van Bavel, *et al.*, 1968, p. 315).

Three types of capillary conductivity, water content and capillary head functional relationships are tested with the numerical analysis in this project to ascertain which models the field data most effectively. These relationships often require coefficients or exponents that have been shown to be somewhat related to particular soil properties. These factors are adjusted until the numerical model better simulates the field conditions. A range of values are selected based on general knowledge of the geologic strata and according to applicable values derived from research by others. Conclusions about the applicability of different researchers' functions will be discussed in the final chapter.

1.2 Description of Project

This modelling project consists of a two-dimensional numerical analysis of unsaturated water flow. The model is programmed in FORTRAN on a VAX operating system. A parabolic, partial differential equation is solved using a finite difference grid scheme and the Alternating Direction Implicit (ADI) solution technique. The results are compared to field data

from an infiltration study. The field data is composed of capillary head measurements obtained from monitoring equipment installed beneath a simulated waste disposal cell leak. Comparisons of capillary head are made between spacially located computer simulation results and point measurements from the field data. The simulation is adjusted by different functional inputs and numerical parameters to most closely emulate the field data. The saturated conductivity, residual water content and porosity were empirically derived by geologic and hydrologic testing. These parameters are not changed in an attempt to fit the data. No formal sensitivity analysis is performed, but the effects of changing the magnitude of various parameters in the numerical and modelling procedure are discussed.

Sand units in the field area are noted as extremely heterogeneous in textural terms. Idealized solutions often rely on simplifying assumptions such as homogeneity. In spite of these inconsistencies, other workers have obtained reasonable results in heterogeneous systems by using analyses of idealized solutions (Singh, 1965, p. 20).

1.3 Numerical Model

In this research, Richards' equation is used to model the physical system of unsaturated flow (Richards, 1931). The foundations of this equation are based on the theories of capillary conductivity and the equation of continuity. As shown below, the equation assumes transient conditions with respect to the water content-time relationship.

$$\frac{\partial w}{\partial h} \frac{\partial h}{\partial t} = \frac{\partial K}{\partial x} \frac{\partial h}{\partial x} + \frac{\partial K}{\partial z} \frac{\partial h}{\partial z} + \frac{\partial K}{\partial z}$$

The characters denote the following: w is water content; h is capillary head; t is time; K is capillary conductivity; and x and z are the horizontal and vertical directions, respectively. The physical assumptions in Darcy's theories that volume flow rate is proportional to conductivity and head are inherent in Richards' equation.

Richards' original work considered three dimensions but only two are used in this simulation. Two dimensions should effectively model this system because aquifer tests (in similar strata to that of the test area) have shown the hydraulic conductivity perpendicular to the bedding planes is several orders of magnitude less than that parallel to bedding, .

The ADI numerical analysis technique is used to solve Richards' equation. This method was selected for several reasons. Primarily, the ADI scheme is well suited to the two-dimensional, parabolic version of the Richards' equation (Luthin, *et al.*, 1975, p. 973). The inventors of ADI, Peaceman and Rachford (1955) have shown the iterative ADI method is unconditionally stable for any size time increment. This stability is essential because portions of the field data extend to 119 days. Being restricted to small time steps could make the computational requirements unnecessarily time consuming.

A specific application of gravity forces is made possible by the configuration of the ADI numerical solution technique into two iteration steps. The gravity component is only added in the calculations for the column implicit mode. Gravity forces do not affect horizontal flow, and so the gravity term is excluded from the row implicit iteration. The idea of adjusting for the influence of gravity will be discussed further in later sections.

1.4 Unique Aspects of the ADI Model in this Project

Another goal of this modelling project is to determine whether or not the force of gravity is important in a two-dimensional unsaturated flow model. Many infiltration problems are handled with one-dimensional analyses because the gravity term only influences flow in the vertical direction. If vertical flow is studied, the gravity term is included with the vertical component; but if horizontal flow is being considered, only the horizontal component is used. By including the gravity term in the calculation of the horizontal components, as would occur in a numerical solution of an equation containing all three terms (horizontal, vertical and gravity), the horizontal flow components would be influenced by gravity forces. Adding the gravity influence into the horizontal calculation does not produce an accurate mathematical model (Bear, 1972, p. 497). This problem is circumvented herein by applying the ADI method. As mentioned above, the gravity component will only be present in the calculations where the vertical components are considered implicit. This method will

effectively keep the horizontal component from the erroneous influence of gravity. The formulae are shown in the chapter entitled "Numerical Analysis".

Wang and Anderson (1982, pp. 106-107) have shown the iterative ADI method converges much quicker if the newly calculated values are updated with each iteration. In this project, the newly calculated head values replace the old ones with each iteration. An iteration represents the solution of one set of simultaneous equations. As mentioned above, the capillary conductivity and the capillary head are functions of water content. The Richards' equation used in this project is written in terms of hydraulic head. Functions are accordingly transformed so that the capillary conductivity and the water content are written in terms of head. New values for capillary conductivity and water content are calculated for each iteration. In other words, during the same time level for each implicit-explicit iteration the new head is utilized whenever available to get the most current capillary conductivity and water content values. This method could be considered entirely iterative. Advance to the next time level does not occur until the cumulative difference between the implicit-explicit and explicit-implicit solutions of head values is sufficiently small.

The geometric mean weighting method is the averaging method used in this project. Three studies have shown the geometric mean method as highly effective for unsaturated flow modelling (Haverkamp and Vauclin, 1979 and 1981; Schnabel and Richie, 1984). Finite difference methods

partition a continuous medium into discrete parts. Obviously, the physical properties of the medium do not conveniently divide themselves into the blocks chosen by the investigator. Averaging methods are used to smooth the errors created by the strict limits set by the discretizations.

1.5 Examples of Flow Models Employing the ADI Technique

Three unsaturated flow models and one ground-water model using the ADI technique are noted for comparison to this project. Each gave acceptable results in describing the flow systems. Using the diffusivity form of the Richards' equation, Selim and Kirkham (1973) studied infiltration from trench shaped sources for comparison to their ADI analysis. They concluded the ADI method accurately solved two-dimensional, unsteady and unsaturated flow systems. The ADI model by Luthin and co-workers (1975) incorporates unsaturated and saturated flow systems. Richards' equation is set in terms of radial coordinates to model an experimental configuration simulating water table flow to an extraction well. Prickett and Lonquist (1971) utilize the transmissivity form of the Richards' equation in a ground-water model and analyze the system with the ADI method. One study used the same differential form of the Richards' equation as employed in this project (Rubin, 1968). Rubin (1968) compared laboratory experiments of horizontal infiltration and drainage to his ADI model. The differential forms of Richards' equation utilized in each case are given in Appendix A.

1.6 Historical Development of Unsaturated Flow Models and Support for Richards' Equation

Models of unsaturated flow were first published in the early 1900's. Buckingham was the first worker to show a dependence of capillary head on water content (1907). Green and Ampt, in 1911, developed an equation to determine the vertical depth of the wetting front after a specified period of time. Required parameters for one form of their equation are: the depth of ponded water at the surface, an infiltration rate, and the capillary conductivity function with respect to head (Neuman, 1976, p. 564). The Green and Ampt equation is one-dimensional and does not consider the effects of gravity. In contrast, Richards (1931) showed that unsaturated flow could be described in three-dimensions using a parabolic partial differential equation. Richards' equation considers the gravity force in unsaturated flow but does not intrinsically provide for the phenomenon of hysteresis. However, hysteresis is easily incorporated into a numerical solution of the Richards' equation by altering $w(h)$ and $K(h)$ functions under specified conditions. The hysteresis phenomenon is discussed in the chapter entitled, "The Physical System".

Richards' equation can be derived from the same theories as those of Darcy's law for saturated flow (Narasimhan and Witherspoon, 1977, p. 657). Theoretically, the Green and Ampt equation and the Richards' equation represent the same physical phenomenon. This similarity was demonstrated by Mein and Larson (1973) who achieved similar results

the Green and Ampt model and a particular numerical analysis of the Richards' equation.

The use of the Green and Ampt model is not warranted in this project. A major reason for not using the Green and Ampt model is because information regarding the capillary head (and therefore the water content) is desired for the entire test area. The Green and Ampt equation provides only the depth of the wetting front and no information from the surface down to that point. Additional grounds for using the Richards' equation over the Green and Ampt equation are discussed in the following paragraphs.

The Richards' equation is employed over the Green and Ampt equation because the infiltration rate is unknown. The Green and Ampt equation requires a knowledge of the infiltration rate. One might correctly deduce that the infiltration rate is precisely the unknown parameter one is trying to predict. The Richards' equation (1931) used herein requires a knowledge of the appropriate $w(h)$ and $K(h)$ functions but not that of the infiltration rate. The numerical solution of the Richards' equation is based on determining the infiltration rates as the conditions change in each discretization block.

A two-dimensional model is more appropriate than a one-dimensional model considering the hydrogeologic conditions at the test site and the three-dimensional freedom of the test liquid. The preferential flow directions in the field strata are parallel to bedding making a two-

dimensional assumption plausible and applicable. No physical boundaries other than a finite length of source water and natural geologic conditions were imposed on the test area. The Green and Ampt equation is strictly a one-dimensional viewpoint on unsaturated flow.

By using the Richards' equation the force of gravity can be included in the calculations, whereas, the Green and Ampt equation has no gravity components. The case for applying the gravity force is discussed in a later section. Briefly, under saturated or near saturated conditions, gravity flow has been shown to be significant even for initially unsaturated flow conditions. The field results show that substantial portions of the monitored zone reached saturation during the experiment.

Many workers have attempted to model unsaturated flow via numerical solutions of various flow equations. The term "numerical methods" is used herein to represent series of arithmetic operations with options to procedural branches based on Boolean type decisions (Carnahan, *et al.*, 1969, p. 1). Numerous one-dimensional numerical analyses of steady-state and transient unsaturated flow have been tested including Hanks and Bowers (1962); Kraijenhoff and van De Leur (1962); Rubin and Steinhardt (1963); Remson, *et al.* (1965); Wang and Lakshminarayana (1968); Rubin (1969); Warrick, *et al.* (1971); Ahuja (1973); Bresler (1973); Unger, *et al.* (1976); Reeder, *et al.* (1980); Dane and Mathis (1981); Haverkamp and Vauclin (1981); Straub and Lynch (1982). Examples of two-dimensional numerical studies for the case of steady-state unsaturated flow include: Nelson (1962); Reisenauer (1962 & 1963); Bouwer (1964);

Burejev and Burejeva (1969); Raats (1970); Zachmann and Thomas (1973). Past works on numerical analyses of transient unsaturated flow were performed by Singh (1965); Rubin (1968); Amerman (1969); Hornberger, *et al.* (1969), Taylor and Luthin (1969); Selim and Kirkham (1973); Taylor (1974); Van der Ploeg and Benecke (1974); Luthin, *et al.* (1975); Narasimhan and Witherspoon (1976 & 1977); Narasimhan (1978).

Certain workers, *e.g.*, Narasimhan, Neuman and Witherspoon, have used the finite element numerical technique to model multi-dimensional, unsaturated flow (Narasimhan and Witherspoon, 1976 & 1977; Narasimhan, 1978). Integrals of the governing equations are used in the development of a finite element numerical procedure (Wang and Anderson, 1982, p. 153; Narasimhan and Witherspoon, 1976, p. 57). Any unsaturated flow equation is highly nonlinear because of the dependence of the water content and capillary conductivity on the capillary head. Integrating this nonlinear equation produces a complicated solution that will probably require simplifications to solve numerically. Narasimhan and co-workers overcame this problem by assuming that the water content and capillary conductivity were constant for the theoretical numerical analysis, and they imposed the nonlinearity functions during the computational execution (Narasimhan and Witherspoon, 1976, p. 57; Narasimhan, *et al.*, 1978, p. 871). Their technique is clearly not mathematically rigorous. These same workers only verified the convergence for the linear cases of their formulations and numerical analyses (Neuman and Narasimhan, 1977). In addition, Wang and Anderson point out that for the transient flow equation

the finite element method is merely a "hybrid" of finite difference and finite element techniques (1982, p. 152). Thus, the remaining advantage for using a finite element procedure in this project would be to better describe the boundary conditions. However, the boundary conditions are relatively simple and easy to describe with the finite difference technique.

2.0 FIELD CONDITIONS AND EQUIPMENT

2.1 Source of Field Data

The data used for this study was obtained from a January, 1987 report entitled "Kettleman Hills Vadose Zone Demonstration" (hereafter referred to as "the demonstration"). The work was conducted by Dames and Moore Associates and Kaman Sciences Corporation, Tempo Division, both of Santa Barbara, California. The field experiment was performed in Kings County, California at the Kettleman Hills Facility. Chemical Waste Management, Inc owns and operates the facility. Kings County is in South Central California approximately 60 miles inland. The field configuration was designed to test the suitability of different types of unsaturated zone monitoring equipment in the dry, heterogeneous sediment conditions of the test area. In addition, the source of water was situated below the ground surface to simulate a waste cell disposal leak.

2.2 Site Geology

The test site lies in the Central Valley physiographic province. The geologic units of interest are part of the Pliocene San Joaquin Formation. Many different depositional environments occurred during the Pliocene including open marine, shallow marine and embayment settings. This created sediments that ranged from saline to brackish water types. Typical transgressive and regressive sediment patterns were observed

along with lower energy bay sediments. The sandstones are calcareously cemented, contain numerous shell fragments and show signs of bioturbation in some stratigraphic intervals. Relative amounts of silts or claystone to sandstones along with the presence of certain shell species delineate the stratigraphic intervals. In all, 15,000 feet of marine and nonmarine sediments were deposited.

Erosion, folding and faulting during the Pleistocene left 2,300 feet of Pliocene sediments in three large anticlinal domal structures trending northwest. After the orogenic events, additional erosion removed the crests of the anticlines, exposing older sediments located in the core of the anticlines. The test site, on the southwest flank of the North Dome, lies on one of these exposed, older sediment layers (the San Joaquin Formation). No secondary faulting or folding has been detected. The North Dome is a doubly plunging anticline eighteen miles long and five miles wide. The axis strikes 50 degrees west of north and has ends plunging northwest at seven degrees and southeast at six degrees.

The San Joaquin Formation contains alternating units of sandstones, siltstones and claystones exhibiting lensing and interfingering. Varying sea levels affected the energy of the depositional setting, therefore creating many layers of different textures. Although faults were created perpendicular to the axis of the anticlines during the upfolding events, these faults are not believed to affect the overall hydraulic conductivity. The units underlying the experimental leak strike north 50 degrees west and dip to the southwest at 25 to 30 degrees. Although the units are not

well sorted, they are regionally continuous as noted from outcrops in the area. A brief description and numbering system for the units underlying the infiltration source are given in Table1 (Dames & Moore and Kaman Tempo, 1987, p. 2-11).

TABLE 1
Description of Geologic Layers by Unit Numbers
Listed on Figures 1 and 2
(Modified from: Dames & Moore and Kaman Tempo, 1987, p. 2-11)

- 1 Blue grey, fine to medium sand; friable, clean.
- 2 Siltstone unit containing three feet of green-grey siltstone, one foot of red-brown oxidized fine grained sand, and three feet of dark brown claystone at the base.
- 3 Blue-grey silty fine sandstone, friable near surface, becoming indurated with depth.
- 4 Dark green-grey claystone, internally laminated and mottled with black staining. Unit contains thin (1 foot thick) siltstone layers. Upper and lower portions of unit are dark brown claystone. Gypsum observed filling some cracks and fractures.
- 5 Light tan-grey silty very fine sand. The basal portion contains gypsum filled cracks and a thin red iron oxide stained layer.
- 6 Dark brown claystone.
- 7 Light tan-grey, fine to medium silty sand with thin red-brown laminations containing medium sand.

2.3 Porosity, Water Content and Hydraulic Conductivity Values

Representative porosity and residual water content values were taken from a survey conducted in the immediate vicinity of the test area. Twenty-one soil samples were collected at depths ranging from 10 to 60 feet (Meredith/Boli and Associates, Inc., 1985, p. 47, Table 5-1). A simple average of the values yielded a porosity of 42.0% and a residual water content of 15.5%. These are the values employed in the computer simulation. No further statistical analysis is warranted for these sample values in view of the extreme heterogeneous conditions noted at the test site.

Pumping test data of hydraulic conductivities for sandstones in the San Joaquin Formation range from $2.0 \cdot 10^{-4}$ to $1.7 \cdot 10^{-3}$ cm/s (Sisk, 1986, p. 32; Supplement to RCRA Part B Permit Application, 1985, p. B.2, 3.0-45). The saturated conductivity value used in the computer simulation is $1.0 \cdot 10^{-3}$ cm/s. Saturated conductivity is equivalent to hydraulic conductivity. Packer and laboratory conductivity tests exhibit similar values but with larger ranges. The conductivity value was chosen from pumping test data, because that type of aquifer test best represents an average value of conductivity for the entire stratigraphic interval in which the test was conducted.

The claystone intervals underlying the infiltration source were considered to be aquitards. Hydraulic conductivities for claystone units from packer test values range from $1.0 \cdot 10^{-5}$ to less than $1.0 \cdot 10^{-8}$ cm/s

(Sisk, 1986, p. 32; Supplement to RCRA Part B Permit Application, 1985, p. B.2, 3.0-35). Laboratory core analyses of vertical conductivity of claystone cores are less than $1.0 \cdot 10^{-8}$ cm/s. The vertical hydraulic conductivity for sandstone cores is also less than $1.0 \cdot 10^{-8}$ cm/s. This low vertical conductivity adds credibility to the selection of a two-dimensional flow model for this project.

2.4 Configuration of the Infiltration Source

A line-source configuration was constructed beginning with the excavation of a one-foot deep trench into previously undisturbed sediments. The line source was oriented perpendicular to the strike of the beds, and it crossed four different stratigraphic units in the area. Figure 1 shows the location of the line source with respect to the geologic units described in Table 1. Geofabric was placed in the trench as a permeable liner, and a three inch layer of sand and gravel was laid on the bottom. Next, a factory slotted, two inch diameter, schedule-40 PVC pipe was laid horizontally in the trench. Approximately three inches of additional coarse sand and gravel were then poured over the pipe. The geofabric was then folded on top. Any excess overlap was cut away. The trench was filled to surface level with a mixture of clayey site soils, bentonite, and water. With compaction, the permeability of the cover is rated at less than 10^{-7} cm/s. More than adequate precautions were taken to prevent evaporation by covering the trench with the following layers: powdered bentonite,

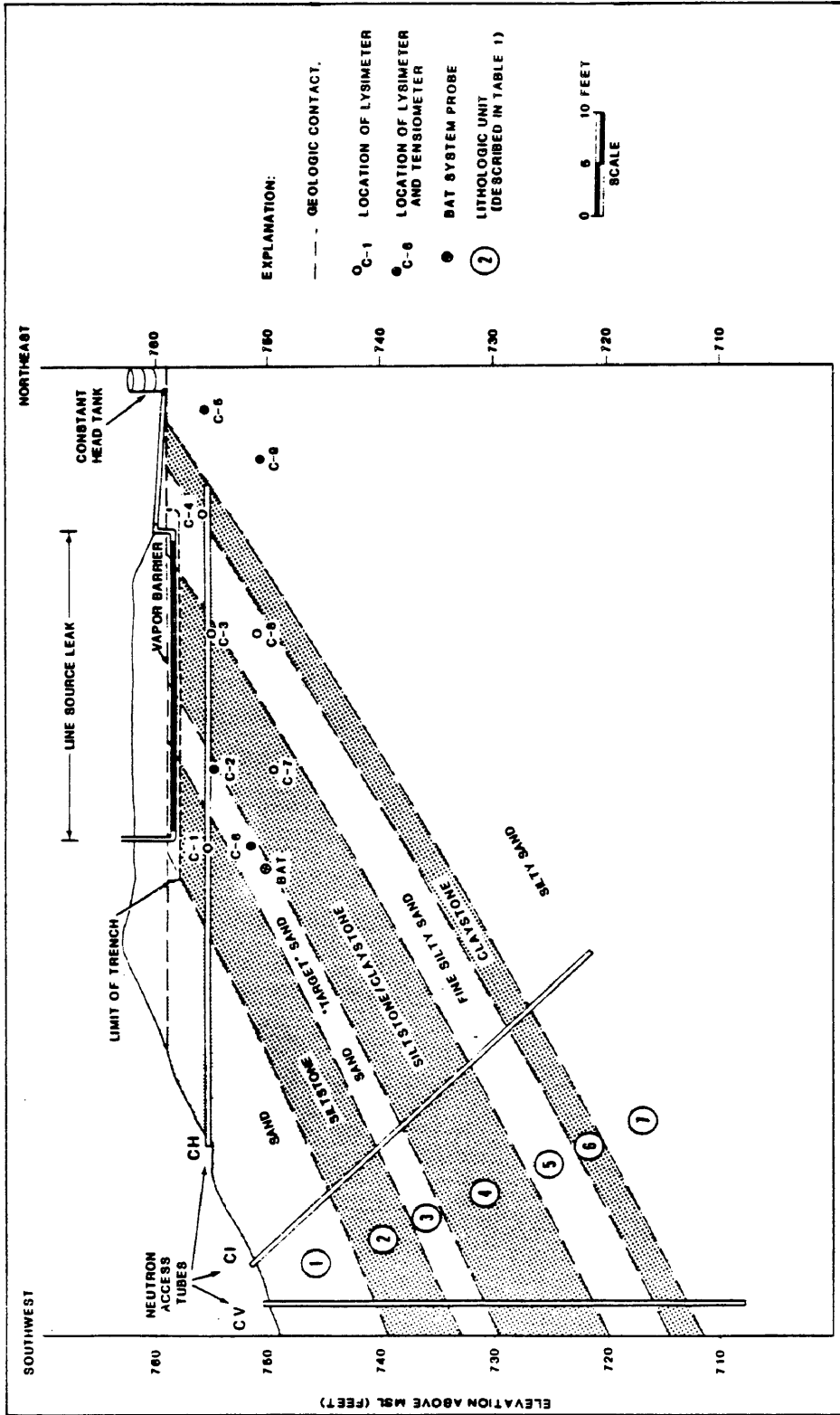


Figure 1
CROSS SECTION PERPENDICULAR TO THE BEDDING PLANES
AND UNDER THE SOURCE PIPE:
LOCATION OF EQUIPMENT IN THE CENTRAL PROFILE
(Modified from: Dames & Moore and Kaman Tempo, 1987, p. 2-6)

geofabric, 6 mil PVC vapor barrier, geofabric, and two to three feet of natural material.

The 30 foot long slotted source pipe was connected to a constant head control tank by standard schedule 40 one inch diameter PVC pipe. Two 1000 gallon storage tanks provided water to the control tank. The head in the control tank was kept as close as possible to one foot above ground surface for the duration of the experiment. The source pipe was ten inches below the ground surface. Head measurements at the opposite end of the source pipe showed no head loss occurred over the length of the pipe. The average flow rate for the experiment was calculated based on total water used and total time elapsed. A constant 200 gallons per day flowed into the source pipe for 119 days.

2.5 Vadose Zone Monitoring System

A vadose zone monitoring system, including many different types of instruments, was installed surrounding the infiltration source pipe. Figures 1 and 2 illustrate the relative locations of the monitoring devices, source pipe and geologic units (Dames & Moore and Kaman Tempo, 1987, pp. 2-6 & 2-5, respectively). Neutron probes, earth resistivity, tensiometers, lysimeters and the BAT system comprised the monitoring system. The extremely dry initial conditions throughout the strata prohibited obtaining background data from some of the instruments. These restrictions, a brief explanation of the equipment and a discussion of data obtained from each

device are presented in the following paragraphs. Measurement times are expressed in hours or days from commencement of the leak.

The vadose zone monitoring device called the neutron moisture probe is similar to a neutron-gamma type, down-well, geophysical logging device. A Cambell Pacific Nuclear Model 503 hydroprobe using a 50 m curie americium-beryllium source was used in the demonstration. Briefly, high energy neutrons are emitted from the probe and are thermalized to gamma type thermal neutrons by light atomic nuclei, e.g., hydrogen atoms present in water molecules (Wilson, 1981, p. 35). The more water present, the greater the number of thermalized neutrons and the higher the counts. Relative count readings are also affected by clay materials which produce higher counts than sands.

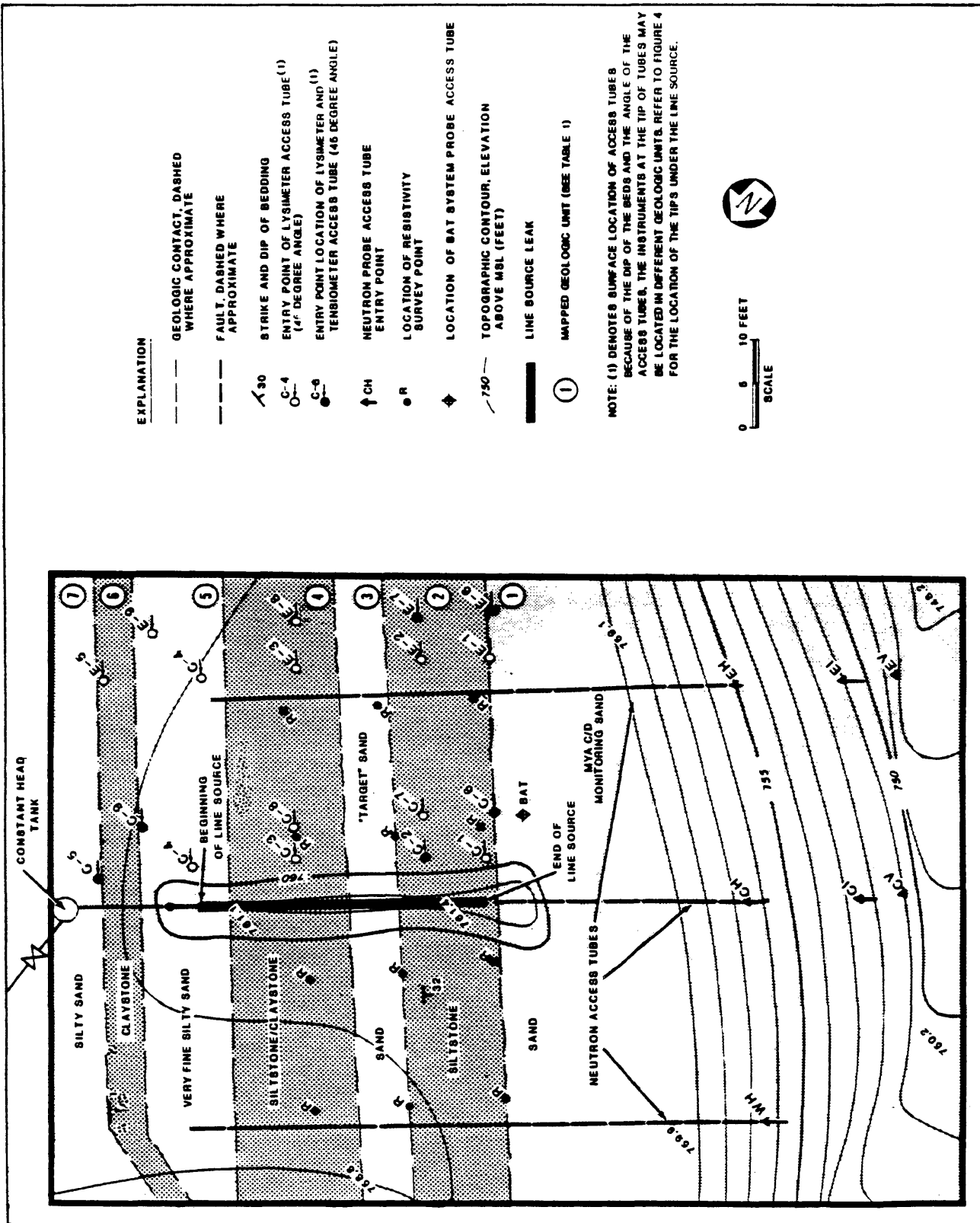
The probes traveled through stainless steel 2 1/2 I.D. x 1/8 wall type 304 tubing that was completed in a 3 inch drilled hole. None of the annuli for the horizontal access tubes could be backfilled, thereby leaving a potential fluid migration path. Even the diagonal and vertical holes that were backfilled created potential preferential flow paths. This disturbance of natural conditions is one of the biggest drawbacks of the neutron logging method.

Data from the probe is sent to the surface electrically encoded, and it can be recorded on computer or other data collection systems. Note that all the thermalized neutrons in a spherical area two to three feet in diameter are interpreted during one counting episode (Dames & Moore and

Kaman Tempo, 1987, p. 3-12). Consequently, the actual depth of a moisture content may not match the depth recorded by the data collection system (Wilson, 1981, p. 39). The depth measurements as they relate to strata placement must not be interpreted rigidly when analyzing the neutron counts as they compare to recorded depth.

Neutron probes were installed along three profiles parallel to the direction of the line source as shown in Figure 2. Each profile included horizontal, inclined and vertical access tubes. One profile was situated directly beneath the source, and the orientation of its three tubes are depicted in Figure 1. Only the central-horizontal probe recorded moisture levels above background readings prior to day 130. At that time, the west-horizontal probe first displayed elevated moisture levels. The central-horizontal probe was located approximately 3.5 feet below the source pipe. Although calibration of the neutron probe can be made to convert count readings to water content values, this calibration relationship was not given with the data. Therefore, the neutron probe data is used to qualitatively assess whether the computer model is generally reproducing when moisture reached the central-horizontal probe.

After 30 hours, the first indications of moisture appeared at the base of sand unit 1. Migration along the access tube is believed to account for this early reading. On day four, the presence of moisture in the middle sand unit, 3, became apparent. By day six, increased moisture levels in unit 3 were well established by elevated neutron probe counts, and sand unit 5 showed slightly elevated readings. On day eight, a sharp increase in



EXPLANATION	
---	GEOLOGIC CONTACT, DASHED WHERE APPROXIMATE
- - -	FAULT, DASHED WHERE APPROXIMATE
↘ 30	STRIKE AND DIP OF BEDDING
○-4	ENTRY POINT OF LYSIMETER ACCESS TUBE (1) (4° DEGREE ANGLE)
●-4	ENTRY POINT LOCATION OF LYSIMETER AND (1) TENSIOMETER ACCESS TUBE (45 DEGREE ANGLE)
↑ CH	NEUTRON PROBE ACCESS TUBE ENTRY POINT
● R	LOCATION OF RESISTIVITY SURVEY POINT
◆	LOCATION OF BAT SYSTEM PROBE ACCESS TUBE
~ 750	TOPOGRAPHIC CONTOUR, ELEVATION ABOVE MSL (FEET)
—	LINE SOURCE LEAK
①	MAPPED GEOLOGIC UNIT (SEE TABLE 1)

NOTE: (1) DENOTES SURFACE LOCATION OF ACCESS TUBES BECAUSE OF THE DIP OF THE BEDS AND THE ANGLE OF THE ACCESS TUBES, THE INSTRUMENTS AT THE TIP OF TUBES MAY BE LOCATED IN DIFFERENT GEOLOGIC UNITS. REFER TO FIGURE 4 FOR THE LOCATION OF THE TIPS UNDER THE LINE SOURCE.



0 5 10 FEET
SCALE

Figure 2
LOCATION OF GEOLOGIC UNITS AND MONITORING EQUIPMENT
(Modified from: Dames & Moore and Kaman Tempo, 1987, p. 2-5)

neutron counts for sand unit 5 verified the presence of moisture. Also on day eight, the siltstone unit, 2, exhibited comparably high neutron counts. The moisture is believed to have migrated from sand unit 1 along the access tube to the siltstone. By day twenty, one section of the siltstone/claystone unit (unit 4) still showed background level counts indicating no increased moisture levels. This data adds credibility to the hypothesis that this strata acts as an effective aquiclude.

Earth resistivity is also known as the four probe electrical method. In this technique, four electrodes are arranged in specified patterns with current passing through the outer two electrodes. The inner two electrodes measure the voltage (Wilson, 1983, p. 157). As the water content increases, the resistivity decreases.

Figure 2 shows the placement of three resistivity profiles parallel to the strike of the units and across the source pipe. The orientation parallel to the bedding planes is necessary because the resistivity measurements depend on lithology as well as water content. Hence, results obtained from electrodes passing through different types of strata would be difficult to interpret (Wilson, 1983, p. 162).

The earth resistivity measurements are of little use to this project. Basically, the resistivity measurements showed that by day 37, the upper three to four feet of sediment in sand units 3 and 5 had become saturated. However, on day 23, the sediment was not saturated. No data was given between these two times.

One important resistivity finding is that by day 37, the resistivity profile over siltstone unit 2 indicated unsaturated conditions. This piece of data indicates that the high neutron probe counts reported in unit 2 are probably erroneous. Therefore, the theory that water flowed along the open annulus of the central-horizontal access tube into unit 2 is most likely true.

The lysimeter and BAT instruments are used to collect pore-liquid samples. The BAT instrument is more fragile than the lysimeters but is much more capable of maintaining the integrity of samples containing volatile organic compounds (Dames & Moore and Kaman Tempo, 1987, p. 3-20). Both have a porous ceramic cup through which the sample is collected. The porous cup reaches equilibrium with the surrounding porous medium, allowing soil moisture to flow in or out of the cup (Johnson, *et al.*, 1981, p. 56). The cup is attached to a short length of PVC well type tubing and is buried at the desired location. The top of the PVC tubing is sealed with a rubber stopper. Smaller tubing runs up to the surface to a vacuum pump and sample bottle. By applying a vacuum on the discharge tube, the sample is drawn to the surface. A vacuum can also be applied inside the cup to obtain samples in dry conditions. One group performed tests with ceramic, suction lysimeters and concluded the effective operating range was between 0 and 60 centibars of suction (Everett and Mc Million, 1985, p. 58).

As stated previously, the natural capillary head conditions at the demonstration site are greater than 200 centibars (Dames & Moore and

Kaman Tempo, 1987, p. 1-1). Samples were obtained when the moisture front reached one of the sampling devices. Unfortunately, the exact times over which the samples flowed into the cups are not known, and only qualitative comparisons can be made with the computer model results. The location of the lysimeters and BAT are shown in Figures 1 and 2. A listing of lysimeter and BAT data along with tensiometer data is given in Table 2.

TABLE 2
Tensiometer, Lysimeter and BAT Data
from Central Profile Under Source Pipe

(Modified from: Dames & Moore and Kaman Tempo, 1987, Appendix B)

Location Code	Instrument	Data
C1	lysimeter	No sample through day 14. 690 ml red sample day 22.
C2	tensiometer	Out of range, day 4. 18 centibars (cb), day 9. 10 cb, day 12. 8 cb, day 14. 3 cb, day 22.
C2	lysimeter	No sample through day 4. 10 ml red sample day 9. 560 ml red sample day 14. 670 ml red sample day 22.
C3	lysimeter	No sample through day 14. 800 ml red sample day 22.

(continued)

TABLE 2 (continued)

C4	lysimeter	680 ml red sample day 2. (attributed to surface leakage at access tube).
C5	tensiometer	Out of range, day 120.
C5	lysimeter	No sample through day 120.
C6	tensiometer	Out of range, day 41. 45 cb, day 43. 40 cb, day 48. 17 cb, day 55. 10 cb(?), day 79. (questionable datum) 15 cb, day 97.
C6	lysimeter	No sample through day 41. 450 ml red sample day 43.
C7	lysimeter	No sample through day 90. Red water sample on day 97.
C8	lysimeter	No sample through day 22. 755 ml red sample day 28.
C9	tensiometer	Out of range, day 120.
C9	lysimeter	No sample through day 120.
BAT	BAT(lys/tens)	Tensiometer out of range, day 9. Lysimeter, Red water sample on day 55.

The tensiometer measurements are the most useful data for this project. Figures 1 and 2 show the location of the tensiometers and the tensiometer data is given in Table 2. Like the lysimeter and BAT systems,

a porous ceramic cup is fastened to the PVC tubing of the tensiometer. The differences are that the cup is initially filled with water and a pressure gauge is attached to the surface tubing. As the liquid in the cup reaches equilibrium with the surrounding strata, the pressure is indicated on the gauge. A major problem encountered during the demonstration was all the water being sucked into the very dry soil before the wetting front of the leak approached. The effects of 1) hysteresis and 2) overcoming air entry pressure skew the pressure readings at the surface and make the results unreliable (Wilson, 1981, p. 40). To overcome this problem, each tensiometer was refilled with water every day until the wetting front reached each one. Model 1920 tensiometers manufactured by Soilmoisture Equipment, Inc. were used and could only measure capillary head up to 90 centibars of suction. This limitation is imposed by the micropores of the ceramic cup in conjunction with the maximum maintainable vacuum pressure inside the tubing.

3.0 THE PHYSICAL SYSTEM

3.1 Properties of the Unsaturated Zone

Porosity is the pore spaces or voids in a porous medium. In modelling unsaturated flow, the key factor is knowing the extent to which these pores are filled by liquids as a wetting or drying event progresses. Liquids in an unsaturated porous medium do not completely fill the pore spaces. If two or more immiscible fluids are present, whether or not the pores are filled, each is considered unsaturated in that porous medium. Example combinations of immiscible fluids are water and air, water and hydrocarbons, air and hydrocarbons or the three together. In this project, only water in a liquid phase will be considered. In terms of occupying space or contributing pressure, air and water vapor will be considered negligible (Swartzendruber, 1969, p. 216).

In an unsaturated system, not only is the porosity important to flow considerations but also to how much of the porosity, or void space, is filled with liquid. The volume of water in a unit volume of soil, otherwise known as the water content, is denoted by "w". With "n" representing porosity, the degree of saturation, "s" is defined as follows:

$$s = \frac{w}{n}$$

The degree of saturation can be considered the fraction of the porosity filled by liquid.

Additional physical parameters of note include inactive and threshold moisture contents. Inactive moisture is liquid trapped in pores and/or liquid bound to particle surfaces in moisture films. This liquid does not contribute to total flow. The amount of inactive moisture, for a given soil, decreases as the degree of saturation increases, because the additional liquid alters the directions of molecular forces in the moisture films (Singh, 1965, pp. 21-22). A parameter related to inactive moisture is threshold moisture. Threshold moisture is the degree of saturation at which flow begins. As can be seen, the moisture which flows in an unsaturated medium is the threshold minus the inactive moisture. The threshold moisture is not constant because the inactive moisture is not constant.

As mentioned in the previous chapter, capillary conductivity is a function of water content. Most empirical and theoretical formulae relating water content and capillary conductivity include the residual moisture value (the moisture content below which flow does not occur, also called threshold moisture). Mualem (1978, p. 327) points out that the immobile or ineffective portion of the water content significantly increases as the overall water content decreases. The variability of this basic physical parameter enhances the complexity of modelling unsaturated flow.

In an unsaturated system containing only water and air, pressure gradients are the result of pressure differences across air-water

interfaces. The air pressure is at the ambient atmospheric pressure, and the water pressure is lower than that of the air (Bear, *et al.*, 1968, p. 226; Swartzendruber, 1969, p. 218). Many terms have been applied to this sub-atmospheric pressure in unsaturated systems. Some of these terms are: underpressure, soil moisture tension, capillary potential, pressure deficiency, capillary head, and suction head (Bear, *et al.*, 1968, p. 40; Singh, 1965, p. 9; Swartzendruber, 1969, p. 219).

Henceforth, either the term "head" or capillary head will be used in this paper. The head values are assigned negative values and are expressed in terms of height measured in centimeters. Centimeters of head are easily converted to bars of pressure for comparison with the field data as will be shown in a later chapter. Even though the height convention is used to denote pressure in the numerical analysis, the head actually represents the moisture suction described above.

3.2 Capillary Pressure

The physical laws directing unsaturated fluid flow are different than those of saturated flow. The main driving force in saturated, unconfined flow is total head, which depends on the pressure derived from the total height of the water column and the elevation head, i.e., the height of the saturated zone. The conductivity in saturated flow is considered constant for any given geologically oriented direction. For unsaturated flow, however, capillary pressure drives water flow, and the capillary

conductivity is not constant but is a function of the water content (Richards, 1931, p. 323).

Capillary pressure, also known as capillary conduction and capillary suction, depends on the relative surface tension and the radius of curvature at the interface of two immiscible fluids (Richards, 1931, pp. 319-320). Capillary pressure is actually a potential created by a pressure difference at the interface of immiscible fluids. The capillary law equation shown below represents an air-water interface (Richards, 1931, p. 319).

$$P_W - P_A = T_1 \left[\frac{1}{R_1} + \frac{1}{R_2} \right]$$

P represents pressure with the subscripts w and A denoting water and air, respectively. T is the surface tension in the wetting fluid. And the quantity in brackets is the mean curvature between the two fluids, where R represents the radius of curvature. This equation shows that the pressure difference is measured at the point of mean curvature on the surface between the two fluids (Bear, *et al.*, 1968, p. 41). The degree of curvature depends on the relative surface tension between the fluids, the effective cross-sectional area of the pores, pore geometry, wettability (produces different contact angles), water content, temperature, gravity, and atmospheric pressure (Bear, *et al.*, 1968, p. 43). Additionally, Bear and co-authors state the following details: "The effects of capillarity are more pronounced in the smaller pore sizes and at lower moisture contents, for

there the area of the air-water interfaces and their curvature increases." (1968, p. 41).

Following the laws of hydrodynamics, water in an unsaturated state flows from higher to lower head (Richards, 1931, p. 318; Bear *et al.*, 1968, p. 226). The lower water content corresponds to lower capillary head (lower capillary head implies moving towards a more negative head value); therefore, water flows from more saturated areas to less saturated areas. Gravity contributes to vertical flow near saturation, but capillary conduction is a much stronger force in unsaturated flow conditions (Singh, 1965, pp. 7-8).

As long as the moisture in an unsaturated porous medium is continuous, flow will occur (Singh, 1965, p. 21). The differential equation used as the basis for the numerical analysis in this project is founded on the hydrodynamic principles of continuity. Overall, however, unsaturated hydraulic conductivities are less than those for the same porous medium under saturated conditions. For further discussions on theories for this difference see Swartzendruber (1969), pp. 278-279 and Bear *et al.* (1968), pp. 226-227.

3.3 Flow Zones During Infiltration

One could easily be misled by certain workers' portrayal of two studies performed by Bodman and Colman (1943) and Colman and Bodman (1944). Bodman and Colman (1943) measured the distribution of moisture

profiles during infiltration experiments. A constant head was maintained at the top of a soil column, but the duration of flow was not allowed to last until water reached the bottom of the column. Basically, these workers measured moisture distributions at the front of the wetting zone, and their conclusions have no bearing on moisture distributions over long periods of time where an excess of water is available for infiltration. With an excess of water and over long periods of time, the porous media may become saturated. Long periods are defined here as meaning the time necessary to allow maximum water accumulation in the soil column. Bear (1972), Singh (1965) and other workers discuss Bodman and Colman's work as if their water content distribution zones held true for all infiltration problems. The field data used in this project showed that after long periods of time, saturation was reached above the wetting front. No saturated zones were observed in any of Bodman and Coleman's experiments. Additional problems, such as the appropriate head value to apply in saturated blocks, are associated with modelling an infiltration problem that includes saturated areas. Therefore, infiltration rate conclusions based on Bodman and Colmans' work do not apply to this project.

The wetting front in unsaturated flow does not advance in a smooth parabolic shape but in a fingering pattern. This pattern of fingering is predicted by the principles of hydrodynamic stability analysis. Diment, *et al.*, note many authors who have studied the analytical formulations and have proposed various numerical solutions for this fingering phenomenon (1982, pp. 1248-1249). The field data used in this project was restricted

to point and line measurements. These limited data points preclude judgements on whether or not fingering did occur. No special considerations are made in the model to account for this phenomenon.

3.4 Hysteresis in Unsaturated Flow

Briefly stated, hysteresis is the difference between the wetting and drying curves for a given soil under unsaturated conditions. The curves refer to the relationships among water content, head and capillary conductivity. Observations also show that the wetting and drying properties depend on the wetting history of the porous medium. The wetting and drying curves depend on past pressure events. They do not depend upon the period of time over which they occurred nor on the rate at which the current event takes place (Miller and Miller, 1956, p. 327). Richards (1931, p. 320) gives an eloquent discourse on hysteresis, citing adhesive forces as the primary cause. He states that during initial wetting, the adhesive forces play a major role in fluid movement. Upon rewetting or additional draining, the adhesive forces contribute inconsequentially by only altering the fluid-particle contact angles via the moisture films already formed on the particle surfaces.

Several authors cite the relative magnitude of hysteresis observed among the water content, head and capillary conductivity. Little or no hysteresis is observed between the water content and capillary conductivity relationship by numerous authors (Bear, 1972, p. 503; Talsma, 1970, p. 964; Topp, 1971, p. 914; Mualem, 1976b, p. 1248; Van Genuchten,

1980, p. 897; Mualem and Klute, 1984, p. 994). Both capillary conductivity and the water content relative to head are well established as hysteretic functions.

These conclusions about hysteresis become important in developing functions for the water content, capillary conductivity and head relationships. These functions are necessary in all unsaturated flow models. However, this model is designed solely for infiltration into 1) previously unperturbed geologic units or 2) units that have had an opportunity to reach ambient conditions. For the case of the experiment modelled herein, the initial conditions were that of extremely dry geologic strata. Hysteresis is not applicable to this modelling project because of the restriction to infiltration, which does not extend to any drainage periods, and because of the dry initial conditions.

3.5 Similarity Theory and Scaling Factors for Capillary Conductivity and Water Content Functions

One approach for determining conductivity and head functions with respect to water content is called the scaling technique. Miller and Miller (1956) originated the scaling technique based on their theory of similitude. The theory is microscopic in nature and assumes homogeneous, isotropic, and permanent soil conditions. In terms of the liquid behavior in their theory, the liquid is assumed to follow the physical laws of surface tension and viscous flow. Additionally, they assume the liquid has no isolated liquid drops or gas bubbles (Miller and Miller, 1956, p. 325). Considering

the instability observed in unsaturated flow systems (Diment, et al., 1982) and the heterogeneity of the field conditions under study, these ideal assumptions seem to have little applicability.

The scaling technique also assumes the position of the wetting front is directly proportional to the square root of time from the start of infiltration (Reichardt, et al., 1975, p.167). The slope of this linear relationship is used as the basis for scaling factors. Philip (original work in Australian J. of Physics 10:29, 1957) and Klute (original work in Soil Science 73:105, 1952) first developed the time-wetting front relationship mentioned above via a Boltzman transformation for one-dimensional infiltration. The infiltration problems they studied apply only to horizontal flow and do not hold for large values of time (Philip, 1969, p. 473). In a separate work, Philip states the relationship does not hold for two- or three-dimensional problems (Philip, 1969, p. 503). Swartzendruber (1969, p. 228) sites several workers who have not had good results matching this infiltration solution to experimental data. However, Rogers and Klute (1971, p. 695) site other workers who have observed significant discrepancies between actual simulations and the square root of time relationship. In this project, the use of a two-dimensional equation and the inclusion of gravity term immediately presume that the relationship between the depth of the wetting front and the square root of time is not linear.

Several workers have shown that for actual soil systems the scaling theory gives poor results (Klute and Wilkinson, 1958; Wilkinson and Klute,

1959; Elrick, et al., 1959). Reichardt and co-workers have had success using the characteristic length method of soil scaling (Reichardt, et al., 1975). The characteristic length is a statistically averaged length of a geometric measurement involving grain orientations, grain shapes and pore sizes (Miller and Miller, 1956, p. 328). Warrick and his co-workers (1977) deduce that if a medium can be measured with a characteristic length, then that material must have constant particle and pore size distributions. They go on to state that strata rarely exhibit such strict homogeneity. In addition, swelling and shrinking almost always occur in the unsaturated zone. Warrick and his co-workers refute the similarity theory based on simple, practical observations (Warrick, et al., 1977, p. 355). Philip maintains through rigorous mathematical arguments that the similarity theory does not apply to unsaturated flow regimes (Philip, 1969, p. 505). In conclusion, similitude applications and interpretations are not used in this project.

4.0 THE CAPILLARY CONDUCTIVITY AND WATER CONTENT FUNCTIONS

4.1 The Uncertainty of the Prediction

No laboratory data for the $K(h)$ or $w(h)$ functions were available to augment the model of the field experiment. This lack of data is not surprising, because reasonably accurate measurements of these functions are difficult to obtain and rather expensive (Clapp and Hornberger, 1978, p. 601; Schuh and Bauder, 1986, p. 848). Moreover, in-situ measurements pertain to single points in space, and laboratory measurements of field samples are imposed on disturbed strata that may not give results indicative of field conditions (Schuh and Bauder, 1986, p. 848). Considering this information in addition to the heterogeneity of the system, laboratory results would not be very helpful.

Important unknown elements in this, as in any, unsaturated flow model are the estimations of the $K(h)$ and $w(h)$ functions. Keep in mind that general conjectures for the conductivity and water content values in the dry wetting front conditions should suffice, because the head fluctuates several orders of magnitude in short time periods (Clapp and Hornberger, 1978, p. 603). At the opposite extreme, when near saturation, gravity begins to affect flow and the influence of air pockets becomes significant. The goal is to determine average functions that optimize the re-creation of observed field events.

Three categories of functions are tested in this model. The functions are 1) power relationships by Brooks and Corey (1964, 1966) and Averjanov (1950); 2) closed-form analytical equations by Van Genuchten (1980); and 3) power relationships by Campbell (1974) with a polynomial variation near saturation as theorized by Clapp and Hornberger (1978). Each of these functions provides three parameters for use in the model. These parameters are water content, capillary conductivity, and the derivative of head with respect to water content ($\partial h/\partial w$). The water content is needed to test for saturation. At saturation, the saturated conductivity value is employed and $\partial h/\partial w$ is set equal to one so as to have no effect.

In the following sections, each category of function is discussed, and the equations for each parameter are given. Three graphs have been produced for each function. These graphs are water content versus capillary head (log), capillary head (log) versus relative capillary conductivity (log) (K/K_{sat}), and water content versus relative capillary conductivity (log). Different input parameters for the functions are shown on each graph to illustrate the input's effects on the positioning of the curves and their shapes. The graphs are presented in Appendix B and are briefly discussed in the following sections.

The slope of the capillary head versus water content curve, $\partial h/\partial w$, is one component of the coefficient for the head values in the Richards' equation. This coefficient arises from the particular numerical scheme

employed in the model. (See "Numerical Analysis.") The coefficient is shown below.

$$U = \frac{\text{time}}{\Delta x} \frac{\partial h}{\partial w}$$

"U" is a dummy variable used in the example discrete equations listed in Appendix C. Capillary conductivity is also a component in the coefficients for the head values. Actually, the $\partial h/\partial w$ graphical relationship is log-linear, making the value of the slope equal to $\Delta(\log h)/\Delta w$. Computational problems arise when this curve becomes horizontal or becomes asymptotic to the vertical axis. Example curves for each category of function were studied for the log capillary head versus water content graphs, and a reasonable maximum value for $\partial h/\partial w$ was determined as 200 cm. This value is of an appropriate magnitude for this numerical scheme. A lower limit of 0.001 is provided to avoid an erroneous zero multiplication during the simulation. Lower and upper limit values for $\partial h/\partial w$ maintain the integrity of the numerical analysis.

4.2 The Brooks and Corey Power Function

The "power function" originated by Brooks and Corey is based on experimental data from dozens of soils (1964, 1966). In their equation, the capillary conductivity and the effective saturation are presumed to be exponentially related to the capillary head.

$$K = K_{\text{sat}} \left[\frac{h}{h_{\text{bub}}} \right]^{-e}$$

In the above equation, K_{sat} is the saturated hydraulic conductivity; h_{bub} is the capillary pressure head at which air movement occurs as bubbles (also known as the air-entry pressure or bubbling point); and e is an exponent related to soil characteristics such as texture or organic content (e is not the natural log, \ln , value often represented by e). Brooks and Corey found the above equation to be a best estimate of the $K(h)$ function and do not claim the function perfectly fits all soil types (Van Genuchten, 1980, p. 895).

Schuh and Bauder (1986) compared field results of unsaturated flow characteristics to $K(h)$ power functions. They examined the possibilities of calculating e with functions derived from soil indices. The indices exhibiting rather strong correlation were sand to silt ratio, geometric mean particle diameter, and organic carbon content (Schuh and Bauder, 1986, p. 851). Some investigators have obtained good results with power relationships (Ward, *et al.*, 1983, p.854; Campbell, 1974, p. 313). However, Green and Corey in a later paper, stated that they found rather poor correspondence using the power function in their earlier work (1971, p. 3).

Mualem questions whether this simple function is applicable to finer textured soils that often exhibit $w(h)$ functions with two or more inflection points (1978, p. 327). As previously mentioned though, the field strata in this study area would probably not be considered fine textured.

When the $w(h)$ curve is irregularly shaped, Mualem suggests adding parameters to the exponent to better represent the $K(h)$ curve. His adaption of the Brooks and Corey equation as used in the computer program is given below (Mualem, 1976, p. 514).

$$K = K_{\text{sat}} \left[\frac{h}{h_{\text{bub}}} \right]^{(-2 - 2.5 e)}$$

Laliberte, *et al.*, (1966) proposed a similar exponent of $(-2 - 3.0 e)$, where e is a measure of the pore-size distribution index. Mualem derived his estimate of $(-2 - 2.5 e)$ from thorough statistical analysis of deviations of conductivity calculations. His rigorous analyses and good results warrant use of his exponent in this project (Mualem, 1976, p. 516).

A $w(h)$ function exhibiting a similar exponential relationship was presented by Averjanov (1950), as shown below.

$$S_e = \frac{w - w_{\text{res}}}{w_{\text{sat}} - w_{\text{res}}} = \left[\frac{h}{h_{\text{bub}}} \right]^{(-e)}$$

The water content subscripts represent residual (res) and saturated (sat) water contents. S_e is effective saturation as represented by the compound fraction. Again, the exponent, e , is an empirical value related to soil characteristics. The form of the Averjanov equation solved by the computer program to calculate moisture content is shown below.

$$w = w_{\text{res}} + (w_{\text{sat}} - w_{\text{res}}) \left[\frac{h}{h_{\text{bub}}} \right]^{(-e)}$$

The $\partial h/\partial w$ equation computed in the program is also based on the Averjanov equation and is given below.

$$\frac{\partial h}{\partial w} = \frac{e}{(\log 10)(w - w_{res})}$$

The same e values are used in each of the above equations for one computer run. Typical e values found by Brooks and Corey (1966) range from 1.8 to 7.3 (Mualem, 1978, p. 325).

Figures 3 through 5 depict the Averjanov and Brooks & Corey equations. The exponent, e , is assigned values of 0.5, 2.0, 4.0, 8.0. For the water content versus head graph, the displayed relationship is purely exponential. This type of relationship is probably a good estimation of the physical system with the exception of near saturation. Here the head should decrease (become less negative) much quicker. Figure 6 exhibits a more typical curve for water content versus head (Hillel, 1982, p. 76). The head versus capillary conductivity relationship is linear. Once again, near saturation, this relationship may not be valid. In the model for this project, saturated conductivity is applied when the calculated water content indicates saturated conditions. This provision should minimize any errors.

4.3 Closed-form Analytical Functions

The second type of relationship is closed-form analytical expressions derived by Van Genuchten (1980) and based on the statistical

theories of unsaturated flow by Mualem (1976a). Both papers show that these function definitions yield statistically better results than those obtained by several other workers equations: Brooks and Corey's power functions (1964); Averjanov's variation on the power functions (1950); Burdine's statistical-integral theories (1953); and the finite sum procedures by Childs and Collis-George (1950) and Millington and Quirk (1961). The latter two quantitatively divide the porous medium into representative blocks based on pore size distributions. The water content and conductivity values for each block are then summed.

Mualem's theories are statistical in nature and account for the relatively greater influence of unsaturated flow in larger pores (1976a, p. 520). He begins with the premises that partitions are based on pore size distribution, that conduction through these pores can be approximated by cylindrical tubes, and that the capillary law inversely relates capillary pressure to pore radius. By doing this Mualem produces a generic function for $K(w)$ (1976a, pp. 513-514). In the same paper, Mualem tested 45 soils to determine the optimum value for the exponent of the effective saturation parameter (Mualem, 1976a, p. 515). This exponent is also incorporated in Van Genuchten's work.

Stephens and Rehfeldt (1985) have shown, with comparisons between laboratory and computed results, that a well-fitting $w(h)$ curve produced by a Van Genuchten equation does not mean the $K(h)$ curve produced by the same method is as valid. The values could be inaccurate up to one order of magnitude (Stephens and Rehfeldt, 1985, p. 18). In contrast, Mualem

p. 517) and Van Genuchten (1980) have shown very positive results from the closed-form analytical method.

The Van Genuchten (1980) closed-form analytical equations utilized in this project are given below. Note that a definite functional relationship has not been established between the exponents used for the power functions, e , and the exponent, N , seen in the following equations.

$$w = w_{res} + \frac{w_{sat} - w_{res}}{(1 + (\alpha h)^N)^M}$$

$$\frac{\partial h}{\partial w} = \frac{(w_{sat} - w_{res}) S_e^{((1-M)/M)}}{(\log 10) M N (w - w_{res})^2 (S_e^{1/M} - 1)}$$

$$K = \frac{K_{sat} \left[1 - (1 - [1 + (\alpha h)^N]^{-1})^M \right]^2}{(1 + (\alpha h)^N)^{M/2}}$$

where $M = 1 - 1/N$, and $N > 1$.

The α term is related to the inverse of the air entry pressure (Van Genuchten, 1980, p. 895). Dane and Hruska (1983, p. 620) have shown that the N and α values can be determined by the shape of the $w(h)$ curve. Unfortunately, the $w(h)$ curve is not available. Research by Stephens and Rehfeldt (1985) is used for an empirically determined α value. The N value is varied until a best fit of the field study is obtained, as is done for the power function exponent, e , in the other two categories of functions.

Stephens and Rehfeldt (1985) applied Van Genuchten's (1978, 1980) curve fitting method to check the statistical validity of his closed-form analytical equations. They determined empirical relationships for $K(h)$ and $w(h)$ on seven cores of fine- to medium- grained sands and silty sands. By applying Van Genuchten's model, they found the statistically best α value of 0.031 (Stephens and Rehfeldt, 1985, p. 17). This is the value employed in the program. Stephens and Rehfeldt do note, however, that the results are quite sensitive to the selection of residual saturation. Interestingly enough, the Averjanov equation for water content is also very sensitive to the residual saturation.

Figures 7 through 12 illustrate Van Genuchten's relationships. In the first three figures (7-9), N is varied over 1.5, 2.5, 4.0 and 8.0 holding α constant at 0.007. In the next three figures (10-12), α is varied over 0.009, 0.007, 0.005 and 0.01 for N constant at 2.5. Except for the low N value of 1.5, the curves produced by the Van Genuchten equations exhibit shapes extremely similar to empirical curves for head, conductivity and water content relationships. Assuming ideal conditions, the Van Genuchten equations should produce the best results.

4.4 Polynomial Relationship Added to the Campbell Power Function

Campbell (1974) derived power functions similar to those developed by Brooks & Corey (1964) and Averjanov (1950). The difference among the equations lies in the definition of "effective" or "relative" water content. Whereas, Averjanov employs S_e as shown above, Campbell believes that a

simpler relative water content term suffices. Relative water content is the ratio of water content to saturated water content. The Campbell's power function equations applied in this model are listed below (Campbell, 1974, p. 312):

$$w = w_{\text{sat}} \left[\frac{h}{h_{\text{bub}}} \right]^{(-1/e)}$$

$$K = K_{\text{sat}} \left[\frac{h}{h_{\text{bub}}} \right]^{(-2-2/e)}$$

$$\frac{\partial h}{\partial w} = \frac{-e}{w (\log 10)}$$

As with the other power functions, the same e value is used in each equation. Campbell (1974, p. 313) found reasonable agreement comparing his equations to empirical data, but he did note discrepancies. In comparisons with empirical data, Campbell used e values in the range 0.14 to 13.3 (1974, p. 313).

Clapp and Hornberger (1978, p. 601) propose using the Campbell equations in combination with a polynomial function that relates head to water content in order to better fit empirical curves. Van Genuchten compared the numerical fit of Brooks and Corey's power functions to results obtained with his closed-form equations (1980, p. 894). Significant discrepancies were apparent in the $K(h)$ function at water contents approaching saturation (Van Genuchten, 1980, p. 896). Clapp and Hornberger claim the polynomial is warranted due to the phenomenon of

gradual air entry near saturation. This point of transition on the head versus water content curve is seen as an inflection point where the slope of the function changes from increasing to decreasing. Adding the polynomial equation to the Campbell equations should better approximate the $K(h)$ and $w(h)$ functions above the water content corresponding to this inflection point.

In this project, the polynomial function is applied when the relative water content (w/w_{sat}) is above a percentage pore saturation. This parameter is given as input at the beginning of the simulation. The capillary conductivities and water contents are calculated by the regular Campbell power function below that percentage. If the pore saturation exceeds the designated percentage, a new capillary head value is calculated using the polynomial shown below (Clapp and Hornberger, 1978, p. 601). This new head value is then used to recalculate conductivity and water content values for use in the numerical analysis.

$$h = m (W - n) (W - 1) \quad \text{where, } W = w/w_{sat}$$

In the above equation, m and n are calculated by the following expressions:

$$m = \frac{h_i}{(1 - W_i)^2} - \frac{h_i e}{W_i (1 - W_i)}$$

$$n = 2 (W_i) - \left[\frac{h_i e}{m W_i} \right] - 1$$

where, h_i is the head at the inflection point and W_i is the relative water content at the inflection point (Clapp and Hornberger, 1978, p. 601).

The Campbell relationships with the Clapp and Hornberger variation are shown in Figures 13 through 15. The Clapp and Hornberger technique is invoked near saturated water contents, but differences between using that versus the Campbell technique are negligible. These graphs resemble the general shape of the Averjanov and Brooks & Corey curves. This similarity is not surprising because both are power functions.

4.5 Comparison of Three Functions

An example curve for each of the three types of functions is presented on each one of the graphs in Figures 16 through 18. These graphs can be used to compare the relative shapes of the curves. For the head versus water content graph, the two power functions produce very similar curves, quite different from the closed-form analytical equation . In the graph of head versus conductivity, the Van Genuchten function produces a steeper slope than that of the power functions but shows a gradual approach to saturated conductivity as the capillary head becomes small. The water content versus capillary conductivity graph shows similar curves for all three functions. This similarity stems from the particular form of the exponents chosen by the respective researchers for their power functions. The expressions for these exponents are based on the same theories as Van Genuchten's equations. Because both water content and conductivity are derived from the same parameter, head, the influence of these exponents can be more clearly seen.

5.0 GOVERNING DIFFERENTIAL EQUATIONS

5.1 Richards' Equation

The conservation of mass equation can be applied to unsaturated flow if no sources or sinks occur within the flow domain (Bear, 1972, p. 495). The term flow domain denotes all the interior locations as defined for a problem. It does not include the boundaries (Norrie and de Vries, 1973, p. 4). The conservation of mass equation is shown below.

$$\frac{\partial(\rho w)}{\partial t} + \text{div}(\rho \hat{q}) = 0$$

Where ρ is the water density, t is time and \hat{q} is the volume flow rate (vector quantity). By imposing the reasonable assumption that water is incompressible, the mass conservation equation becomes the continuity equation:

$$\frac{\partial w}{\partial t} = - \text{div} \hat{q}$$

Now an applicable motion equation must be applied. Richards (1931, p. 323) states that unsaturated flow can be considered saturated flow with reduced porosity (which is one reason for reduced capillary conductivities). Darcy's law depends on head differences and conductivities and not on the particle sizes or the geometry of the pores. Therefore, Darcy's law can be

applied to unsaturated flow (Richards, 1931, p. 323; Bear, 1972, p. 496). Darcy's law is shown below.

$$\hat{q} = -k \text{ grad}(H + Z)$$

In the above equation, k is hydraulic conductivity, H is the pressure head and Z is the height above a datum or the elevation head (Freeze and Cherry, 1979, p. 21). Putting the above equations in terms of unsaturated flow, k becomes the capillary conductivity, K , (which is a function of capillary head), H becomes capillary head, h , and two of the head terms are zero (Richards, 1931, p.324). The third head term is actually representing the influence of gravity and will hereafter be called the gravity term.

$$\frac{\partial Z}{\partial x} = \frac{\partial Z}{\partial y} = 0; \quad \frac{\partial Z}{\partial z} = 1;$$

$$\hat{q} = -K \left[\frac{\partial h}{\partial x} + \frac{\partial h}{\partial y} + \frac{\partial h}{\partial z} + 1 \right].$$

Where x and y are horizontal directions and z is positive downward. Combining Darcy's equation with the continuity equation gives the following:

$$\frac{\partial w}{\partial t} = - \text{div } \hat{q} = - \left\{ - K \left[\frac{\partial h}{\partial x} + \frac{\partial h}{\partial y} + \frac{\partial h}{\partial z} + 1 \right] \right\}.$$

Considering a profile type of restriction to spacially reduce the problem to two-dimensions, the above equation can be written as a general form of the Richards' equation as shown below.

$$\frac{\partial w}{\partial t} = \frac{\partial K}{\partial x} \frac{\partial h}{\partial x} + \frac{\partial K}{\partial z} \frac{\partial h}{\partial z} + \frac{\partial K}{\partial z}$$

Using the chain rule, the equation is changed to the form used for the numerical analysis in this project.

$$\frac{\partial w}{\partial h} \frac{\partial h}{\partial t} = \frac{\partial K}{\partial x} \frac{\partial h}{\partial x} + \frac{\partial K}{\partial z} \frac{\partial h}{\partial z} + \frac{\partial K}{\partial z}$$

It is assumed that the water content, $w(h)$, and the capillary conductivity, $K(h)$, are independent functions of capillary head, h . These functions are also assumed to be independent of the hydraulic gradient by the use of Darcy's equation (Rogers and Klute, 1971, p. 695). The rate of change of capillary head should not effect the functions either (Miller and Miller, 1956, p. 327).

5.2 The Influence of the Gravity Term

The gravity term is used in this project to account for the difference between the vertical and lateral wetting front progressions observed in the field. Anisotropic conditions are often mimicked by tilted beds (Sposito, 1978, p. 479). The spacial differences in infiltration could be due to anisotropy, and the model could be adjusted with different capillary conductivities in the horizontal and vertical directions. Instead, the gravity term is used to simulate the field data because the along strike and down-dip conductivities (horizontal and vertical, respectively) are similar, as stated previously. As already pointed out and as might be logically deduced, gravity does not affect horizontal flow (Bear, *et al.*, 1968, p. 259;

Bear, 1972, p. 498). Consequently, the gravity term is not included in horizontal calculations. However, the influence of gravity on the vertical flow in head ranges from 0 to -0.5 bars (near saturation) is well established (Clapp and Hornberger, 1978, p. 603). The field data shows saturation does occur. If gravity is an important force in saturated conditions and saturation occurs, then gravity should be included in the calculations of vertical flow.

Raats sites three workers who have shown the insignificance of gravity as a force if the infiltration source is small and the strata is fine textured (1970, p. 91). For one, the field strata is probably not considered a fine texture under this ambiguous textural quantification. This author read two of Raats' citations and found no solid empirical proof for the above claim. One of the citations is a mathematical presentation having no experimental comparisons (Miller and Miller, 1956). The other citation includes a mathematical treatise as well as a laboratory experiment (Kraijenhoff van de Leur, 1962). Kraijenhoff van de Leur's work is one-dimensional with respect to the mathematics and laboratory configuration. The single experimental tank was 262 centimeters in length but only 1.2 centimeters wide (Kraijenhoff van de Leur, 1962, p. 4350). The field experiment studied herein is on a completely different scale. It consists of a four-inch diameter source pipe thirty feet in length and no physical boundaries restricting flow in any direction.

Philip performed mathematical calculations based on radial sources and concluded that gravity effects decrease as the radius of the source

decreases (Philip, 1969a, p. 503). The theoretical equations were in two- and three-dimensions using radii at 10 and 50 centimeters (Philip, 1969, p. 510). Again no field or laboratory work was compared to these conclusions.

Based on the evidence researched, no judgements can be made on the gravity effects as related to source size.

5.3 Support for Richards' Equation

Richards' equation was chosen for this project for several reasons. Independently of one another, at least three other workers have used his equation for numerical applications of unsaturated flow, as described in the introduction.

The transient nature of the equation is well suited to unsaturated flow. A steady-state solution assumes that the same amount entering a delineated zone, leaves that zone over a given period of time. In other words, the total flux (volume outflow minus volume inflow) is constant and no water is stored. Within the confines of the field area, large amounts of water were stored during the experiment. An initial wetting event took place, and steady-state conditions in terms of inflow at the surface equalling outflow at the deepest monitoring point were not reached in 120 days.

Richards' equation and other equations used to describe unsaturated flow are often applied in a diffusivity form. Klute (1952) developed the diffusivity term $D(w)$ as shown below:

$$D(w) = K \frac{\partial h}{\partial w}$$

The diffusivity form is not applicable to this project because portions of the flow domain reach saturation. Whenever saturation is observed, the inverse of the differential term approaches zero causing the diffusivity to approach infinity (Rubin, 1969, p. 443; Whisler and Klute, 1969, p. 454).

6.0 ASSUMPTIONS INTRINSIC TO THE MODEL

A mathematical model is presented in this project. Mathematical models are intended to replicate physical events with the laws of physics and applied mathematics. Unfortunately, our computational facilities and numerical analyses can not solve many theoretical formulas without compromising on simplifying assumptions. In addition, the theoretical equations that form the base of a model often incorporate simplifications and assumptions, because the actuality of the field situation is too complicated to describe with mathematical equations (Wang and Anderson, 1982, p. 2). Anytime simplifications are applied, the observed reality will not be precisely represented by the model. Some analytical solutions do provide exact results, but these solutions often involve simplifications and are not always applicable to every problem. The two-dimensional form of Richards' equation used in this project is not solvable by analytical methods. The following paragraphs discuss the assumptions and simplifications behind the numerical analysis of and the theory behind the Richards' equation. Assumptions that have already been discussed will not be reiterated in this section.

The medium is considered homogeneous and granular (Singh, 1965, p. 14). Of course, the medium is not homogeneous; but the averaging formulas used to write the differential equation and the iterative nature of the numerical analysis are an attempt to smooth over many of the inconsistencies. Assuming the material is granular, a valid assumption in

this case, is necessary because the Richards' equation is founded in the physical laws of capillary conductivity. Capillary conductivity occurs when the forces of surface tension and gravity act to reach equilibrium. A granular material provides the surface area and pore spaces for capillary forces.

Isotropy of the field strata has not been determined in field or laboratory experiments. One author points out that tilted beds often emulate anisotropic conditions (Sposito, 1978, p. 479). However, the capillary conductivity values in both the horizontal and vertical directions will be the same in this project. Any anisotropy will be accounted for by including the gravity term alternately in the numerical solution as described earlier.

The continuity equation applies to flow of incompressible fluids in a fully connected state. At the atmospheric and sub-atmospheric pressures in this experiment, assuming water to be incompressible is sound. Continuity is an aptly chosen description for this equation because the theory is valid only as long as moisture is continuous. If the flowing fluid is not continuous on a microscopic level, then the continuity equation is not valid in a differential form.

The water is presumed to follow the physical laws of Newtonian fluid flow. Electrostatic forces in clays can create nearly plastic water flow characteristics in unsaturated flow (Bear, *et al.*, 1968, p. 33). The

relatively low clay content in the field strata and the heterogeneity of the system do not warrant consideration of plastic flows.

The water is assumed to contain no substantial concentrations of chemical agents. In addition, no considerations for chemically activated soil-water interactions are made. One author states that diffusion type equations do not apply if salts are present in solution (Wang and Lakshminarayana, 1968, p. 329). Singh sites particular electrolytes that can cause flocculation in a solution when flowing through clay materials (1965, p. 19). Other authors warn that significant surface flows are produced by high solute concentrations, surfactants (change wetting characteristics) and/or chemically induced electrical gradients (Bear, *et. al.*, 1968, p. 228). Drinking water dyed with red food coloring was used in the field experiment. Large amounts of the water will probably be adsorbed upon initial infiltration given the extremely dry natural conditions at the site. This adsorption will be accounted for by adjustments in the $K(h)$ and $w(h)$ functions. Naturally occurring chemical actions facilitated by the addition of the water could explain inconsistencies between the computational results and the field data.

Bacteria and other microorganisms can reduce the effective permeability of a porous medium (Singh, 1965, p. 18). Higher order organisms, such as worms creating channels, can effect flow paths. Indigenous species actions are dependent on climate, season and environmental conditions. No allowance is made in this project for any biological intervention.

The flow is considered isothermal and independent of changes in ambient atmospheric pressure. The experiment took place from August through November of 1986 in Kings County, California. Considering the size of the storage tanks and the average flow rate of 200 gallons per day, the temperature of the water probably was not raised significantly from ambient ground-water temperature. Temperatures in the test zone were most likely similar. Although changes in the barometric pressure increase the hydraulic head, the capillary head does not change appreciably because the hydraulic head increase is compensated for by increased suction (Bear, *et al.*, 1968, p. 259). The suction increases because the radii of curvature decreases as the atmospheric pressure rises.

Evaporation is considered negligible. The burial of the source pipe below ground surface and the maintenance of a constant head via the control tank effectively prevent any possible evaporation effects on the field data.

Many assumptions surround the estimation of the $K(h)$ and $w(h)$ functions. Empirical and theoretical equations will be discussed at length in an upcoming section. The basic premise for all of these equations is that the functions are only contingent upon capillary head (or the water content depending on how the functions are written) and empirical input factors. The functions do not depend upon the rate of head change or the flow status being dynamic or static (Rogers and Klute, 1971, p. 695; Bear, *et al.*, 1968, p. 490; Wang and Lakshminarayana, 1968, p. 329). One more

pertinent relationship to this project is that Richards' equation assumes that capillary conductivity is subject only to changes in head (Irmay, 1954, p. 463).

7.0 NUMERICAL ANALYSIS

7.1 Approximating the Richards' Equation with Finite Differences

The points of reference for the finite difference method used in this model are at the intersection of two sets of perpendicular lines and are called grid points, node points or mesh points in most literature. Grid points are utilized over mesh-centered ones because head values, not flux values, are designated at the boundaries. The horizontal position is denoted by the subscript "a" and the vertical position is denoted with the subscript "b". An example grid point system is shown below in Figure 19. The horizontal, x, and vertical, z, dimensions of each block are equal. Similarly, the Δx and Δz values are equal in the numerical analysis.

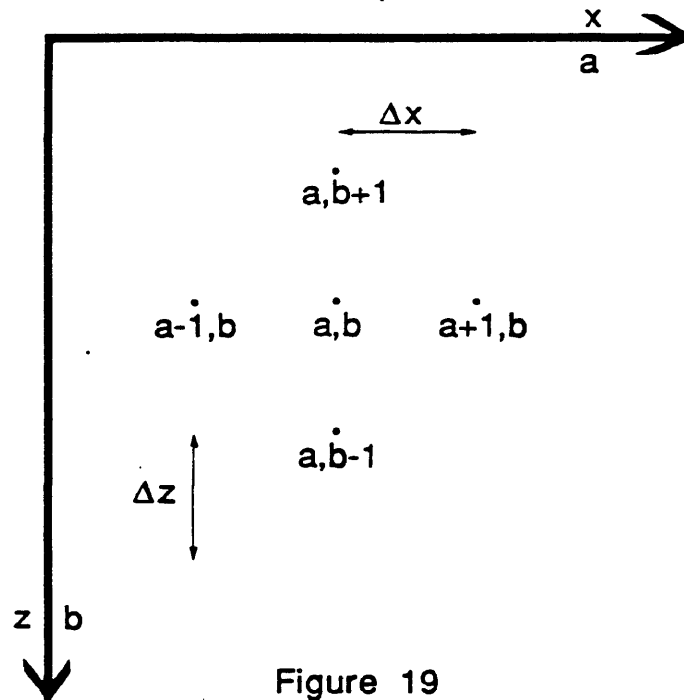


Figure 19
GRID POINT SYSTEM

The first derivative gravity term is estimated using a block-centered, central-difference scheme as shown below.

$$\frac{\partial K}{\partial z} \approx \frac{(K_{a,b+1/2} - K_{a,b-1/2})}{\Delta z}$$

The second derivative terms in the Richards' equation are actually a combination of two first derivatives. The two first derivatives are the capillary conductivity and head in the numerator. A spacial second derivative is in the denominator. By adding the backward and forward difference equations in the form of Taylor series expansions, a finite difference equation is obtained for the second derivative (Carnahan, *et al.*, 1969, pp. 430-431). An example adapted to the double first derivative in the numerator is given below. The weighting formula for calculating the block-centered capillary conductivity values will be discussed in another section of this chapter.

$$\frac{d K}{d x} \frac{d h}{d x} \approx$$

$$\frac{(K_{a-1/2,b} h_{a-1,b}) - (K_{a-1/2,b} h_{a,b}) - (K_{a+1/2,b} h_{a,b}) + (K_{a+1/2,b} h_{a+1,b})}{(\Delta x)^2}$$

The discretization or truncation error associated with the finite difference form of the ADI solution method is $[(\Delta t)^2 + (\Delta x)^2]$, assuming that $\Delta x = \Delta z$ (Carnahan, *et al.*, 1969, p. 453). This truncation error is the result of approximating a complete and continuous area by predetermined, finite blocks. Because the estimation of the water content and capillary conductivity relies on the variable being discretized (head), the ADI

truncation error may be larger in the case of unsaturated flow. A geometric mean weighting factor method is employed in an attempt to minimize any additional error that may be created by the nonlinearity of the unsaturated equation.

The two left-hand-side terms of the Richards' equation must also be expressed in discrete terms. The water content with respect to head term is expressed as a function and is discussed in the chapter concerning the $K(h)$ and $w(h)$ functions. The head with respect to time term is discussed in the following section on the implicit method.

7.2 The Implicit Method

Numerical methods for solving nonlinear, partial differential equations consist of various iterative schemes to estimate space values at advanced time levels. If the new values are calculated entirely on information from the previous time level, then the method is considered completely explicit. Restrictions on the time increment and the block size accompany calculations using the explicit method. If either is too large, the calculations are unstable (Wang and Anderson, 1982, p. 70). In a fully implicit scheme, the new space value is evaluated at the proceeding time level (Carnahan, *et al.*, 1969, p. 440). Although the implicit method has no restrictions on the time increment or block size, the computational work required can be cumbersome. By using the iterative ADI technique, the computational requirements are minimized and the advantages of the implicit method can be utilized.

The time levels are denoted throughout this chapter by the superscripts "n," "n*" and "nβ" for the initial time level, updated values after the explicit-implicit iteration and the updated values after the implicit-explicit iteration, respectively. An asterisk, "n*," in the superscript position signifies that the value is updated as soon as a new head value is available. The finite difference form of the Richards' equation used in this project is shown below.

$$\frac{\partial w_{a,b}^*}{\partial h} \frac{h_{a,b}^{n+1} + h_{a,b}^n}{\Delta t} \approx$$

$$\frac{(K_{a-1/2,b}^* h_{a-1,b}^{n+1}) - (K_{a-1/2,b}^n h_{a,b}^{n+1}) - (K_{a+1/2,b}^n h_{a,b}^{n+1}) + (K_{a+1/2,b}^n h_{a+1,b}^{n+1})}{(\Delta x)^2}$$

$$+$$

$$\frac{(K_{a,b-1/2}^* h_{a,b-1}^{n+1}) - (K_{a,b-1/2}^n h_{a,b}^{n+1}) - (K_{a,b+1/2}^n h_{a,b}^{n+1}) + (K_{a,b+1/2}^n h_{a,b+1}^{n+1})}{(\Delta z)^2}$$

$$+$$

$$\frac{(K_{a,b-1/2}^n - K_{a,b+1/2}^n)}{\Delta z}$$

7.3 The ADI Method

The main purpose of the ADI method is to reduce a large number of simultaneous equations to more simply solved tridiagonal matrices. Numerous sets of tridiagonal matrices are produced; however, each one can be solved directly using the Thomas algorithm (Wang and Anderson, 1982, pp. 96-98). Also note that the "G-B array method" of solution for the ADI method is identical to the Thomas algorithm. This "G-B array method" is discussed and applied in Peaceman and Rachford's original work (1955, p. 34) as well as in an ADI numerical model by Prickett and Lonquist (1971, pp. 6-7).

The ADI method essentially simplifies a two-dimensional problem into two, one-dimensional parts. First, the vertical components of the finite difference equation are considered implicit and the horizontal components explicit. For the second iteration within the same time level, the orientation of the implicit-explicit modes are reversed. The technique used in this work is actually an "iterative" ADI scheme. The iteration is not employed to solve sets of simultaneous equations, but rather to reach convergence between the two implicit-explicit steps of the solution within the same time level. Before advancing to the next time level, the values of the implicit-explicit and the explicit-implicit solutions are compared and checked for sufficient convergence. Iterations are performed during a single time increment. Comparisons are made between potential solutions instead of among numerous intermediate values as is done in most iterative procedures. The computational savings of this technique can be clearly seen.

An example of the first iteration in the series of two for an interior point is given below.

$$\begin{aligned}
 & [-(U K)_{a,b-1/2}^n] h_{a,b-1}^{n+\forall} + [(U K)_{a,b-1/2}^n + (U K)_{a,b+1/2}^n + 1] h_{a,b}^{n+\forall} \\
 & + [-(U K)_{a,b+1/2}^n] h_{a,b+1}^{n+\forall} = \\
 & [(U K)_{a-1/2,b}^{n+\forall*}] h_{a-1,b}^{n+\forall*} + [-(U K)_{a-1/2,b}^{n+\forall*} - (U K)_{a+1/2,b}^n + 1] h_{a,b}^n \\
 & + [(U K)_{a+1/2,b}^n] h_{a+1,b}^n + \frac{\partial h}{\partial w} \frac{\Delta t}{\Delta z} [K_{a,b-1/2}^n - K_{a,b+1/2}^n]
 \end{aligned}$$

The coefficient, $U = \frac{\text{time}}{(\Delta x)^2} \frac{\partial h}{\partial w}$, listed above is discussed in the chapter entitled "The Capillary Conductivity and Water Content Functions." A set of simultaneous equations in tridiagonal form are produced by the above formula. The Thomas algorithm, also known as the "B-G" array method, is used to solve the set directly, i.e., requiring only one iteration pass for each column (or row) of nodes. After solving the equations, all parameters with the asterisk superscript are updated with the new head values as they are calculated. The second iteration in the series for an interior point is shown next.

$$\begin{aligned}
& \left[- (U K)_{a-1/2,b}^{n+\gamma} \right] h_{a-1,b}^{n+\gamma+\beta} + \left[(U K)_{a-1/2,b}^{n+\gamma} + (U K)_{a+1/2,b}^{n+\gamma} + 1 \right] h_{a,b}^{n+\gamma+\beta} \\
& + \left[- (U K)_{a+1/2,b}^{n+\gamma} \right] h_{a+1,b}^{n+\gamma+\beta} = \left[(U K)_{a,b-1/2}^{n+\gamma+\beta^*} \right] h_{a,b-1}^{n+\gamma+\beta^*} \\
& + \left[- (U K)_{a,b-1/2}^{n+\gamma+\beta^*} - (U K)_{a,b+1/2}^{n+\gamma} + 1 \right] h_{a,b}^{n+\gamma} + \left[(U K)_{a,b+1/2}^{n+\gamma} \right] h_{a,b+1}^{n+\gamma}
\end{aligned}$$

Once again, all the parameters with an asterisk superscript are continuously updated. After each iteration, the new head values are compared to the old head values. If the cumulative difference between the two is below a given tolerance, then the time level is advanced. Also note the inclusion of the gravity term in the first equation of the series and its exclusion in the second equation. This demonstrates how the gravity term is used to account for the different rates in vertical and horizontal progression of moisture. A complete listing of discretization formulae for each case is given in Appendix C.

Most fluid dynamic numerical models have one fixed time increment for the entire simulation. With the iterative ADI technique, time is treated quite differently. After convergence occurs during a series of iterations in the ADI procedure, the time level is increased by addition of the next time increment. For example, the first time increment may be ten minutes, and the next time at which results are desired may be thirty minutes. The "delta" time for the first series of iterations would be .007 days and the "delta" time for the second time step would be .02 days. In most numerical models the second time step of thirty minutes would be obtained by three

sets of iterative procedures having a time step of 10 minutes each. In other words, the "delta" time used at each time level is actually an accumulation of all previous time increments plus the current one. The implicit-explicit iterations are performed for that time level until the head values stabilize for that point in time. The old head values from the previous series of iterations are used at the start of the next time level to expedite convergence. The flexibility of the iterative ADI approach toward matching empirical data can now be clearly seen. As mentioned previously, many investigators have proven the method is unconditionally stable (Douglas, 1955; Peacemon and Rachford, 1955; Carnahan, *et al.*, 1969; Wang and Anderson, 1982).

7.4 Weighting Factors

Finite difference formulas are approximations of equations that define continuous functions. The question arises as to how continuous parameters should be estimated or averaged in the finite difference scheme. In this case, the discretization is based on capillary head. Specific values for capillary conductivity and water content are also needed. These properties, especially in unsaturated flow, are extremely variable. At the very least, values should be averaged adjacent to the head node under consideration.

Two groups of researchers in three separate experiments have found the geometric mean weighting factor to be the most accurate averaging system for discrete solutions of unsaturated flow (Haverkamp and Vauclin,

1979, p. 182 and 1981, p. 19; Schnabel and Richie, 1984, p. 1008). The quantities used are block-centered. They are also known as interblock or internodal values. An example geometric mean formula is given below.

$$K_{a \pm 1/2} = (K_a \cdot K_{a \pm 1})^{1/2}$$

Haverkamp and Vauclin also found that large block sizes showed negligible effects on results when the geometric mean weighting factors were used (1979, p. 185).

In this model, the capillary conductivity and the water content values are calculated using the newest head value at each node. The values are then smoothed by the geometric mean procedure before application in the next set of simultaneous equations. This averaging style produces the best possible results from a discrete numerical solution.

7.5 Initial and Boundary Conditions

A propagation type numerical construction is used in this project. Propagation structures utilize pre-set initial conditions and open boundary conditions (Norrie and de Vries, 1973, p. 5). Declaring initial values and boundary values is necessary, mathematically, for well posedness of the parabolic equation (Holt, 1977, p. 4). Norrie and de Vries state that for a propagation framework: "...the solution marches out from the initial state guided and modified by the side boundary conditions..." (1973, p. 12).

Infiltration can be readily viewed as progressing in such a manner numerically.

Dirichlet type boundary conditions are applied in this numerical model. Head values are designated for the boundaries in Dirichlet's scheme. In this project, the initial boundary values were equivalent to those assigned to interior points. One study by Haverkamp and Vauclin (1981, p. 19) compared three models of unsaturated flow using Dirichlet conditions for one set of test runs and Neuman type (set flow across boundaries) in another. Their conclusions showed negligible differences among results using each type of boundary condition.

Dirichlet conditions are used for convenience here in view of initial and continuing field conditions. Before beginning the field experiment, no unusual events indicated differential wetting in the subsurface. Consequently, the soil was considered uniformly very dry (high capillary head potential). Additionally, Dirichlet conditions are well suited to this problem in view of the configuration of the infiltration source. A known constant head was maintained at the infiltration source throughout the field experiment.

The beginning and ending values of the head, capillary conductivity and water content arrays must also be defined. Bear in mind that the array points correspond to nodes in a vertical, profile lattice extending below the water source. The profile is oriented along strike and perpendicular to the infiltration source pipe. When the limit of the lattice is reached (an

array endpoint) for a head value, the value is set equal to the next adjacent value interior to the problem. In the cases of capillary conductivity and water content, which are calculated using the above weighting formula, the values are again set equal to the next adjacent interior value.

8.0 DISCUSSION OF INPUT PARAMETERS AND RESULTS

8.1 Explanation of Input/Output Data File Tables

Tables 4 through 8 list simulation test run input parameters and output values. The purpose of these listings is to simplify the process of assessing model results. Each table contains data file numbers, selected input parameters, example output values and comments on test run executions. The column headings are described briefly below in Table 3.

TABLE 3
DESCRIPTION OF COLUMN HEADINGS IN THE DATA FILE TABLES

"File Number;" for reference use, no two are duplicated.

"Function used;" which type of function was employed to calculate $w(h)$, $K(h)$ and $\partial h/\partial w$.

"Exponent;" refers to input parameters used for the $w(h)$, $K(h)$ and $\partial h/\partial w$ equations.

" $\partial h/\partial w$ Infl. (sat.);" the influence factor applied under saturated conditions.

"Grav. Infl. (sat.);" the influence factor applied to the gravity coefficients under saturated conditions.

(continued)

TABLE 3 (continued)

"HINIL and HSRC (cm);" the values assigned to the initial head values and the line source head values.

"Blksize (cm);" the size of the discretization blocks.

"Deltat (days);" the value assigned to DELTAT (see below).

"Incdelta;" the value assigned to INCDELTA (see below).

$$\text{DELTA} = \text{DELTA} + (\text{DELTA}) (\text{INCDELTA})$$

$$\text{TIME} = \text{TIME} + \text{DELTA}$$

"Ex. Time (days);" for the case of DELTAT = 0.5 and INCDELTA = 1.2, the 21.1 day time level or the highest time level reached reached is listed; for the case of DELTAT = 0.5 and INCDELTA = 1.1, the 38.5 day time level or the highest time level reached is listed.

"Ex. Depth (feet);" the depth to the midpoint of the discretization block containing the greatest head value, the top row excluded.

"Example Head (cbar);" the head value reported for the block described above; (1 cbar = 1.0213 cm); cm are considered equivalent to cbar for discussion purposes.

"Comments;" Yes or No, did the execution end prematurely? DECREASE is listed if any calculated head value drops below those assigned at the beginning of the simulation. HINIL, the initial head, was defined as -1000 cbar. INCREASE is listed if the calculated head is greater than the pressure head for the appropriate block. Pressure head is considered the distance from the line source to the midpoint of the block to which the head is indexed.

Tables 4 through 8 are given on the preceding pages.

TABLE 4
COMPUTER SIMULATION DATA FOR THE BROOKS AND COREY POWER FUNCTIONS

File Number	Exponent (E)	$\partial h/\partial w$ Infl. (sat.)	Grav. Infl. (sat.)	Blksize (cm)	Deltat (days)	Inc-delta	Ex. Time (days)	Ex. Depth (feet)	Example Head (cbars)	Comments
020	2.5	1	1	100	0.5	1.2	21.1	4.9	-17.5	Yes, INCREASE
021	1.0	1	1	100	0.5	1.2	21.1	4.9	-16.1	Yes, INCREASE
022	4.0	1	1	100	0.5	1.2	21.1	4.9	-27.1	Yes, INCREASE
023	2.5	1	1	70	0.5	1.2	21.1	3.4	-54.9	Yes, DECREASE
024	1.0	1	1	70	0.5	1.2	21.1	3.4	-30.5	Yes, DECREASE
025	4.0	1	1	70	0.5	1.2	21.1	3.4	-37.3	Yes, INCREASE
026	2.5	1	1	150	0.5	1.2	21.1	7.4	-183.5	No
027	1.0	1	1	150	0.5	1.2	21.1	7.4	-183.5	No
028	4.0	1	1	150	0.5	1.2	21.1	7.4	-183.5	No
029	2.5	1	1	100	0.5	1.1	38.5	4.9	-87.4	Yes, INCREASE
030	2.5	10	10	100	0.5	1.1	8.4	4.9	-119.2	Yes, INCREASE
031	2.5	10	10	100	0.5	1.2	9.3	4.9	-29.2	Yes, INCREASE
032	2.5	50	50	100	0.5	1.2	1.6	4.9	-400.7	Yes, DECREASE
033	2.5	10	10	70	0.5	1.2	4.0	3.4	-345.4	Yes, DECREASE
034	2.5	10	10	150	0.5	1.2	21.1	7.4	-39.5	Yes, INCREASE
035	1.0	10	10	100	0.5	1.2	9.3	4.9	-30.7	Yes, INCREASE
036	4.0	10	10	100	0.5	1.2	9.3	4.9	-91.6	Yes, INCREASE
037	1.0	1	1	100	0.5	1.1	38.5	4.9	-39.4	Yes, INCREASE
038	2.5	10	1	100	0.5	1.2	9.3	4.9	-28.3	Yes, INCREASE
039	2.5	10	1	100	0.5	1.1	18.1	4.9	-43.8	Yes, INCREASE

TABLE 5
COMPUTER SIMULATION DATA FOR THE VAN GENUCHTEN CLOSED FORM ANALYTICAL EQUATIONS

File Number	Exponent (N)	$\partial h/\partial w$ Infl. (sat.)	Grav. Infl. (sat.)	Blksize (cm)	Deltat (days)	Inc-delta	Ex. Time (days)	Ex. Depth (feet)	Example Head (cbars)	Comments
040	1.5	1	1	100	0.5	1.2	21.1	4.9	-46.6	Yes, INCREASE
041	3.0	1	1	100	0.5	1.2	9.3	4.9	-114.6	Yes, INCREASE
042	6.0	1	1	100	0.5	1.2	4.0	4.9	-517.9	Yes, DECREASE
043	1.5	1	1	70	0.5	1.2	9.3	3.4	-45.1	Yes, INCREASE
044	3.0	1	1	70	0.5	1.2	4.0	3.4	-150.6	Yes, INCREASE
045	6.0	1	1	70	0.5	1.2	4.0	3.4	-150.5	Yes, INCREASE
046	1.5	1	1	150	0.5	1.2	21.1	7.4	-185.7	Yes, INCREASE
047	3.0	1	1	150	0.5	1.2	21.1	7.4	-616.1	No
048	6.0	1	1	150	0.5	1.2	21.1	7.4	-613.8	No
049	1.5	1	1	100	0.5	1.1	18.1	4.9	-44.6	Yes, INCREASE
050	1.5	10	10	100	0.5	1.1	8.4	4.9	-158.2	Yes, DECREASE
051	1.5	10	10	100	0.5	1.2	9.3	4.9	-120.2	Yes, INCREASE
052	1.5	50	50	100	0.5	1.2	1.6	4.9	-400.6	Yes, DECREASE
053	1.5	10	10	70	0.5	1.2	4.0	3.4	-344.6	Yes, DECREASE
054	1.5	10	10	150	0.5	1.2	21.1	7.4	-179.8	Yes, INCREASE
055	3.0	10	10	100	0.5	1.2	9.3	4.9	-106.5	Yes, INCREASE
056	6.0	10	10	100	0.5	1.2	9.3	4.9	-349.0	Yes, DECREASE
057	1.1	1	1	100	0.5	1.1	38.5	4.9	-14.8	Yes, INCREASE
058	1.5	1	10	100	0.5	1.2	9.3	4.9	-17.0	Yes, INCREASE
059	1.5	1	10	100	0.5	1.1	8.4	4.9	-77.9	Yes, INCREASE

TABLE 6
COMPUTER SIMULATION DATA FOR THE CAMPBELL FUNCTION WITH POLYNOMIAL VARIATION

File Number	Exponent (E)	$\partial h/\partial w$ Infl. (sat.)	Grav. Infl. (sat.)	Blksize (cm)	Deltat (days)	Inc-delta	Ex. Time (days)	Ex. Depth (feet)	Example Head (cbars)	Comments
060	2.0	1	1	100	0.5	1.2	21.1	4.9	-16.4	No
061	0.5	1	1	100	0.5	1.2	21.1	4.9	-57.3	Yes, INCREASE
062	4.0	1	1	100	0.5	1.2	21.1	4.9	-26.5	No
063	2.0	1	1	70	0.5	1.2	21.1	3.4	-37.1	Yes, INCREASE
064	0.5	1	1	70	0.5	1.2	21.1	3.4	-74.1	Yes, DECREASE
065	4.0	1	1	70	0.5	1.2	21.1	3.4	-38.8	Yes, INCREASE
066	2.0	1	1	150	0.5	1.2	21.1	7.4	-234.4	No
067	0.5	1	1	150	0.5	1.2	21.1	7.4	-234.3	No
068	4.0	1	1	150	0.5	1.2	21.1	7.4	-184.4	No
069	2.0	1	1	100	0.5	1.1	38.5	4.9	-52.6	Yes, INCREASE
070	2.0	10	10	100	0.5	1.1	8.4	4.9	-119.2	Yes, INCREASE
071	2.0	10	10	100	0.5	1.2	9.3	4.9	-106.1	Yes, INCREASE
072	2.0	50	50	100	0.5	1.2	1.6	4.9	-400.7	Yes, DECREASE
073	2.0	10	10	70	0.5	1.2	4.0	3.4	-345.4	Yes, DECREASE
074	2.0	10	10	150	0.5	1.2	21.1	7.4	-168.5	Yes, INCREASE
075	0.5	10	10	100	0.5	1.2	9.3	4.9	-104.6	Yes, INCREASE
076	4.0	10	10	100	0.5	1.2	9.3	4.9	-110.2	Yes, INCREASE
077	2.0	1	1	100	0.5	1.2	21.1	4.9	-16.4	No
078	2.0	1	10	100	0.5	1.2	21.1	4.9	-55.7	Yes, INCREASE
079	2.0	1	10	100	0.5	1.1	18.1	4.9	-42.3	Yes, INCREASE

TABLE 7
COMPUTER SIMULATION DATA FOR RUNS WITH ZERO INFLUENCE FROM THE GRAVITY TERM

File Number	Function used	Exponent	$\partial h/\partial w$ Infl. (sat.)	Blksize (cm)	Deltat (days)	Inc-delta	Ex. Time (days)	Ex. Depth (feet)	Example Head (cbars)	Comments
080	BC ^a	2.5	1	100	0.5	1.2	0.0	0.0	0.0	Yes, DECREASE
081	BC	1.0	1	100	0.5	1.2	0.0	0.0	0.0	Yes, DECREASE
082	BC	4.0	1	100	0.5	1.2	0.0	0.0	0.0	Yes, DECREASE
083	VG ^b	1.5	1	100	0.5	1.2	21.1	4.9	-602.4	Yes, INCREASE
084	VG	3.0	1	100	0.5	1.2	0.5	4.9	-991.0	Yes, DECREASE
085	VG	6.0	1	100	0.5	1.2	0.0	0.0	0.0	Yes, DECREASE
086	CCH ^c	2.0	1	100	0.5	1.2	1.6	4.9	-962.8	Yes, DECREASE
087	CCH	0.5	1	100	0.5	1.2	0.0	0.0	0.0	Yes, DECREASE
088	CCH	4.0	1	100	0.5	1.2	21.1	4.9	-33.7	Yes, DECREASE
089	BC	2.5	10	100	0.5	1.2	0.0	0.0	0.0	Yes, DECREASE
090	VG	1.5	10	100	0.5	1.2	9.3	4.9	-154.8	Yes, DECREASE
091	CCH	2.0	10	100	0.5	1.2	9.3	4.9	-154.8	Yes, DECREASE
092	BC	2.5	1	100	0.5	1.1	0.0	0.0	0.0	Yes, DECREASE
093	VG	1.5	1	100	0.5	1.1	8.4	4.9	-160.3	Yes, DECREASE
094	CCH	2.0	1	100	0.5	1.1	1.6	4.9	-963.7	Yes, DECREASE.

^a Brooks and Corey Power Functions

^b Van Genuchten Closed Form Analytical Equations

^c Campbell Power Functions with the Clapp and Hornberger Polynomial Variation

TABLE 8
COMPUTER SIMULATION DATA FOR POSITIVE INITIAL HEAD VALUES

File Number	Function used	Exponent	Grav. Infl. (sat.)	HINIL and HSFC (cm)	Deltat (days)	Inc-delta	Ex. Time (days)	Ex. Depth (feet)	Example Head (cbars)	Comments
101	BC ^a	2.5	1	1.0 55.9	0.5	1.2	21.1	31.2	193.1	Did the execution end prematurely? DECREASE: Did the head decrease below the initial conditions. INCREASE: Did the head increase above calculated pressure head for that block? Yes, INCREASE
102	BC	2.5	1	100.0 100.0	0.5	1.2	9.3	34.4	200.9	Yes, INCREASE
103	BC	2.5	0	100.0 100.0	0.5	1.2	103.5	64.0	2.9	No
104	VG ^b	1.5	1	1.0 55.9	0.5	1.2	21.1	41.0	192.9	Yes, INCREASE
105	VG	1.5	1	100.0 100.0	0.5	1.2	9.3	34.4	200.9	Yes, INCREASE
106	VG	1.5	0	100.0 100.0	0.5	1.2	46.8	31.2	78.8	Yes, INCREASE
107	CCH ^c	2.0	1	1.0 55.9	0.5	1.2	21.1	31.2	193.1	Yes, INCREASE
108	OCH	2.0	1	100.0 100.0	0.5	1.2	9.3	34.4	200.9	Yes, INCREASE
109	OCH	2.0	0	100.0 100.0	0.5	1.2	103.5	64.0	-3.5	No

^a Brooks and Corey Power Functions

^b Van Genuchten Closed Form Analytical Equations

^c Campbell Power Functions with the Clapp and Hornberger Polynomial Variation

8.2 General Program Flow and Constraints

Head values for the entire profile are stored in two, two-dimensional arrays. One array contains the head values calculated for the column implicit calculations. The other array stores head values for the row implicit calculations. Appropriate head values are assigned to smaller working arrays that are then passed along to subroutines and functions. Selection of these head values depends on their proximity to boundaries. The boundary conditions are depicted by the discretization equations listed in Appendix C.

Internodal ($a \pm 1/2$ or $b \pm 1/2$) water content, capillary conductivity and $\partial h/\partial w$ values are always determined by the head values in two adjacent blocks. An exception occurs if the array index is on a boundary, in which case only a single head value is employed. If either head value is positive or greater than the value assigned to the bubbling point pressure head, h_{bub} ; the internodal terms take on values representative of saturated conditions.

If saturated conditions are indicated, the water content relative to saturated water content (porosity) is set equal to 1.0. A chain of events then takes place in which the capillary conductivity is defined by the saturated conductivity value, and the $\partial h/\partial w$ influence factor is set equal to the value provided at the beginning of the test run. The multiplication factors applied to $\partial h/\partial w$ in the sample runs were 1, 10 and 50.

If both head values are negative and below h_{bUB} , two capillary conductivity and two $\partial h/\partial w$ values are calculated from the head in each of the two blocks. Next, a geometric mean value is calculated for each parameter from the two values. These parameters are then applied as internodal coefficients. The coefficients are shown in the discretization equations in Appendix C.

Once all of the coefficients are calculated and stored in one dimensional arrays, the arrays are sent to the Thomas algorithm subroutine. The Thomas algorithm determines the solution of a tridiagonal system of equations by direct substitution. A prerequisite for application of the Thomas algorithm is dominance by the main diagonal terms over the super- and sub-diagonal ones. Results indicate that this criterion has been met, but no proof is provided. Next, the appropriate row or column is updated with the new head values calculated by the Thomas algorithm. Each column (or row) undergoes this process before the execution advances to the next iteration. In the first iteration where columns are implicit, both the column, two-dimensional array (HCOL) and the row, two-dimensional array (HROW) are updated. By doing this, the most recently calculated head is used in the next iteration where the rows are considered implicit.

Upon completing the set of two iterations, the absolute difference between each head value in HCOL and HROW is summed. Until the total sum is greater than the defined error tolerance and the defined maximum number of iterations has not been reached; another set of iterations occurs

within that same time level. When the maximum number of iterations is exceeded or the sum of the differences is below the tolerance, the time level is incremented. The head values are sent to the declared output file and the next set of iterations begins.

A gravity component is added to the explicit terms (right-hand-side terms) for the column implicit iteration. The parameters in the gravity component are shown below. The units are in centimeters.

$$\frac{\partial h / \partial w \text{ time } K}{\Delta z}$$

As previously described for the head coefficients, the gravity component procedure first tested for saturated conditions. If saturated conditions were indicated, the saturated conductivity value and the $\partial h / \partial w$ influence factor were applied in conjunction with the aforementioned parameters. Otherwise, two capillary conductivity and $\partial h / \partial w$ parameters were calculated according to their appropriate head values. The geometric mean of each pair were utilized in the equation.

Special consideration was provided for conductivity values near saturation. If the calculated conductivity was within two orders of magnitude of the saturated conductivity, the saturated conductivity was utilized in place of the calculated one. Increasing the conductivity near saturation enhances the gravity forces with respect to the capillary forces. As saturation is approached, the capillary forces no longer dominate flow migration.

In most test runs, the $\partial h/\partial w$ influence factor on the gravity component was equivalent to that which was applied to other coefficients. Special cases were tested where the gravity component was not included or the gravity component was given a greater influence multiplication factor. Data files 038, 039, 058, 059, 078 and 079 in Tables 4, 5 and 6 are examples of the gravity influence factor being greater than that of $\partial h/\partial w$. Table 7 shows the data files from runs involving no gravity components.

Program execution is terminated if one of two situations develops. Prior to executing any other calculations, the program checks the head values in the working array for erroneously high or low values. If the head value is greater than the pressure head for its assigned block, or if the head value is lower than the initially assigned head values; execution is discontinued. Head values in excess of pressure head are not considered feasible in the unconfined conditions of the field area. A decrease in head indicates that the strata is becoming drier. The initial head value setting of -1000 cbars denotes extremely dry conditions, and any decrease is not significant to the $w(h)$ or $K(h)$ calculations. If the head is permitted to increase or decrease without any controls, computationally unsound arithmetic operations will eventually occur, and the execution will be terminated by the computer system.

8.3 Input Parameters

A variety of input parameters were introduced to the model in over 100 test simulations. The empirically determined geologic parameters

such as saturated conductivity, residual water content and saturated water content were already discussed in the section entitled, "Porosity, Water Content and Hydraulic Conductivity Values." The values for these parameters were considered constant at $K_{sat} = 1.0 \cdot 10^{-3}$ cm/s, $w_{res} = 0.155$ and $w_{sat} = 0.42$. The bubbling point pressure was defined as -20.0 cm for all runs. The estimate of this parameter was based on the granular texture of the strata. No empirical evidence was available.

Head measurements of initial field conditions indicated suction pressures in excess of -2000 cbars. Realistically, the residual water content had been reached for head values below -1000 cbars, and the actual $w(h)$ and $K(h)$ values were not changing. Therefore, initial conditions were set at -1000 cbars. The lower limit for capillary conductivity was defined as 10^{-10} cm/s, and a lower bound for the $\partial h/\partial w$ value was defined as 0.001 cm. Values below those limits are insignificant to unsaturated flow rates in actual porous media systems. Recall also, that a numerically reasonable upper limit of 200 cm was placed on the $\partial h/\partial w$ term. This limit was primarily estimated by measuring slopes of the water content versus head graphs produced by the three types of functions applied in this project.

The pressure head in the line source was maintained at 22 inches (55.9 cm), and this head value was reassigned to the appropriate blocks in the first row after every iteration. Which blocks contain the source pressure head depends upon the input block size. Regardless of the defined

block size, however, the profile for each test run consisted of 20 blocks in both the horizontal and vertical directions.

The cumulative error tolerance was set at 200.0 cm. Given the 20 x 20 block profile arrangement, this tolerance allowed for a maximum difference of 0.5 cm between corresponding blocks from the column and row iterations. After observing test runs, this tolerance level was considered applicable.

Block sizes of 70, 100 and 150 cm were tested. The 100 cm size was utilized most frequently. Qualitative assessment of the results indicated that as the block size was decreased, the flow rate between blocks was enhanced as long as the $\partial h/\partial w$ influence factor was equal to one. For influence factor values greater than one, the flow rates decreased with decreasing block size. As block size is reduced, fundamental concepts of calculus would indicate that the model should better represent the theoretical system of differential equations. Increasing the influence factor violated this concept. This is a strong argument against increasing the $\partial h/\partial w$ influence at saturation.

The DELTAT and INCDELTA values were either 0.5 and 1.2 or 0.5 and 1.1, respectively. The 0.5 and 1.1 combination produced somewhat smaller time steps than the other combination did. Initial test runs indicated that taking smaller time steps (like those listed in the tables) encouraged somewhat higher flow rates. Note that this difference is not apparent by the information shown in the tables. Still, the gains in flow rates achieved

by using smaller time steps did not match the wetting rates observed in the field data.

8.4 Discussion of Output Data

Data from tensiometers C2 and C6 (see Table 2 in section 2.5) were considered for quantitative comparisons to the simulation output data. Measuring parallel to the dip of the beds, tensiometer C2 is eight feet and C6 is sixteen feet from the line source (see Figure 2). Both are placed in sandstone Unit 1. Note that "suction" pressure heads are reported in Table 2 and that their negative value is equivalent to the expression of head in this paper.

Table 4 lists the computer simulation data for the Brooks and Corey power functions. Overall, the head values obtained with an exponent of 1.0 more closely emulate the field data than those using exponents of 2.5 or 4.0. Notice especially, files 020, 021, 024, 031 and 035. None of the test runs satisfactorily model the field data. For example, data file 021 shows a capillary head of -16.1 cbars at a distance of 4.9 feet from the source after 21.1 days. Tensiometer C2 was already up to -8 cbars of head by day 9. The other four runs of note indicate still slower flow rates than those in 021.

Increasing the $\partial h/\partial w$ influence factor (which only affects parameters under saturated conditions) produced slower wetting rates in all the test runs except that of data file 034. The comparison of data files

021 and 035 indicates that increasing the influence factor one order of magnitude also decreased the calculated flow rate. Elevation of the influence factor to 50 produced a much slower flow rate, as seen in file 032. File 034 shows an improved result using an influence factor of 10 and a larger blocksize of 150 cm. This result emphasizes the possibility that blocksize affects the saturated head value applied in saturated blocks. This theory is deduced because test runs using 150 cm blocksize without the elevated influence factor exhibited very low flow rates.

Table 5 gives the computer simulation data for the Van Genuchten closed form analytical equations. The N value of 1.1 in test file 057 gave good results exhibiting a head of -35.7 cbars for the time of 18.1 days. Higher N values of 3.0 and 6.0 produced extremely slow flow rates.

The N value of 1.5, in combination with an influence factor of 10 on the gravity term (for saturated conditions), produced results matching the field data. The output value of -17.0 cbars for a time of 9.3 compares favorably with the -18 cbars recorded by tensiometer C2 on day 9. Note that in this test run the $\partial h/\partial w$ influence factor was given a value of unity. This test result is positive evidence in favor of gravity forces affecting flow in unsaturated models. This conclusion is reached because the field data was accurately simulated by enhancing the gravity component.

Table 6 gives the results from the test runs employing the Campbell power function and Clapp and Hornberger polynomial variation. The exponential value of 2.0 produced better results than exponents of 0.5 and

4.0. The data shown from test file 060 produced the best results. The indicated flow rates are still well below those displayed by the field data.

Overall, in Tables 4 through 6, the best results were obtained using a blocksize of 100 cm and $\partial h/\partial w$ influence factors of one. Very slow flow rates were indicated by all three functions for the larger blocksize of 150 cm. For all three functions, using an influence factor of 50 also gave very poor results. A head value of -400 cbars after 1.6 days of simulation were indicated in each case that applied the value of 50 as the influence factor (see files 032, 052 and 072). Additionally, the model indicated the blocks were becoming drier for these three test cases.

Table 7 shows the computer simulation data for runs that excluded the gravity component. In all but one case, file 083, the capillary head decreased below the initial setting before completing 127.0 days of flow. The flow rates predicted in data file 083 are sporadic. On day 21.1 at a depth of 4.9 feet, the highest head was -602.4 cbars. In contrast, for day 46.8 of the simulation, the highest head was 17.83 cbars at 4.9 feet and 149.5 cbars at 8.2 feet. The flow rate increased substantially during the period from 21.1 days to 46.8 days. This result is considered unreliable.

Seven out of fifteen test runs in Table 7 produced lower than initial head values before the first time level could be completed. Overall, when the gravity component was not added to the simulation runs, severe drying was indicated in the model. In conclusion, the theoretical equations and

numerical scheme utilized in this model are probably best suited to the inclusion of a gravity component.

Table 8 lists the computer simulation data for test runs involving all positive initial head conditions. The example data point was chosen for this table based on the greatest head value from the highest time level completed. Seven of the nine runs derived head values in excess of calculated pressure head before reaching the 103.5 day time level. The head values increased in a normal parabolic pattern from the line source. This pattern indicates that the numerical analysis of Richards' (1931) parabolic differential equation was probably valid. The conclusion of most importance here is that this model is not designed to emulate saturated, unconfined flow. If the model effectively simulated unconfined flow, the values would not have increased above the appropriate pressure head values.

The above conclusions indicate that this model is not reliable for calculating flow in blocks that become saturated. A majority of the modelling results are inaccurate because saturated conditions were encountered in the field experiment. What head values should be applied to saturated blocks in unsaturated models? This question is addressed in the chapter entitled "Conclusions."

9.0 CONCLUSIONS

Data file 057, employing the Van Genuchten closed form analytical $w(h)$ and $K(h)$ equations, was the only simulation that produced results matching the field data. Most other runs exhibited flow rates much slower than those indicated by the field data. Theories for the poor results of this modelling project are discussed below. The unknown value of head in saturated blocks and the undetermined influence of the gravity component are cited as the primary factors contributing to these results.

This project was an attempt to model an infiltration problem encompassing specific but not unusual conditions. A buried line source emitted water under 22 inches of head for over 120 days. Over time, the upper portions of the porous layers beneath the pipe became saturated. In most unsaturated flow tests that assume infiltration is transient, no parts of the strata reach saturation. Either the water inflow is insufficient or the test is not conducted until saturation is achieved. As mentioned in the introduction, unsaturated zone modelling is important to trace leachate that has escaped landfill cell containing systems. Clearly, liquids that seep into underlying strata are not necessarily restricted to amounts that would preclude saturation during leakage.

On the other hand, one could assume that saturation is reached in certain preferential flow paths; and, after a long period of time, steady

state conditions prevail. An outflow point is assumed under steady state conditions. In this case, that point would be an aquifer or an open water body. Waiting for free flowing leachate to reach a steady state, and therefore an additional water system, is not the preferred choice. The point of modelling the flow is to provide information for early efforts to stop leachate movement or divert its path from entering water systems.

Two cases of infiltration have been studied extensively elsewhere: that of exclusively transient, unsaturated flow and that of saturated or unsaturated flow under steady state conditions. The problem of drainage to a water table aquifer has also been studied. The draining liquids flow under capillary head and gravity forces until they reach the water table. At the water table, the pressure head or hydraulic head in the aquifer is considered the driving force for flow.

Reflect for a moment, and wonder what head applies to a single block that becomes saturated in known unsaturated conditions. Recall that in the actual physical situation, unsaturated flow is not regular and exhibits fingering flow paths. A pressure head value (the depth from the infiltration source to the midpoint of the saturated block) could be applied, or the head occurring in the model for that block could be employed. Neither has any physical foundation, and neither produced good results in the model tested herein.

Additionally, notice that the $\partial h/\partial w$ term is intrinsic to the unsaturated flow equation. What would be the value of this term, graphically, at saturation? The possible answers are infinity or an undefined value. Once saturated, the water content no longer changes. The head is still free to change hydraulically. What value should be assigned to $\partial h/\partial w$, at saturation, to be numerically consistent with the unsaturated flow equations being solved in the model? The results from this study indicate that $\partial h/\partial w$ should be given a value of unity if head is the independent variable and saturated conditions occur.

Three general methods were tested to determine the head and $\partial h/\partial w$ influence most appropriate for saturated blocks.

First, whatever head had been calculated during the previous iteration was utilized, and the $\partial h/\partial w$ term was considered equal to unity. The results varied from elevated head values that increased beyond the calculated pressure head for the saturated block, to insufficient head values that produced flow rates well below those encountered in the field. In some cases, data files 020, 021, 058 and 060, the capillary heads did increase (become less negative) in reasonably short periods of time. Nevertheless, the flow rates were lower than those displayed in the field data.

Secondly, the influence of the $\partial h/\partial w$ coefficient on each head term and gravity term was increased for saturated conditions. These

coefficients were multiplied by factors of 10 or 50 in several cases. In other cases, only the influence on the gravity term was increased one order of magnitude. With one exception, the blocks displayed either drainage below the initial head values or accumulations of pressure above theoretical pressure head. In that one case, data file 058, the input produced results matching the field data. When the pressure exceeded calculated pressure head, execution was terminated because excess pressures in unconfined conditions did not appear probable.

Finally, a special subroutine was constructed that substituted a pressure head value in each block deemed saturated. Note that these pressure head calculations were only applied to the right-hand-side of the equations where head is considered known. For every manipulation of the input parameters, the flow rate was much lower than that recorded in the field.

If the value of the head in a saturated block is so questionable, should saturation be determined by head? Yes, because head is the only choice if it is the only independent variable. In this project, the water content calculation is based on head. If the calculated water content equals or exceeds the porosity, the strata is considered saturated. The circularity of modelling the unsaturated process is seen here in these initial stages of calculations. The criteria for saturation is based on a value that becomes questionable if that same value indicates saturated conditions exist.

Possibly, in the situation of infiltration, including saturated blocks, the model should be based solely on water content. Conservation of mass principles and flux boundary conditions could be utilized. Still, the capillary conductivities would be dependent on the "unknown" water contents. As already cited in section 3.5 concerning hysteresis, the $K(w)$ function displays little or no hysteresis. This may be an advantage, especially in rewetting situations, because the $K(h)$ and $w(h)$ functions exhibit significant hysteretic variability. Bear in mind that the same questions concerning threshold moisture effects on the $w(h)$ functions apply to the $K(w)$ functions. However, the uncertainty of the saturated head value is totally circumvented. At saturation, the water content equals the porosity and the capillary conductivity equals the saturated conductivity.

Gravity, in this researcher's opinion, is an important consideration no matter which approach is chosen for an unsaturated flow model. The effect of gravity is not clearly known whether the capillary head or the water content is declared as the independent variable. Table 6 shows the results of simulation runs that excluded the gravity term. In seven cases, data files 080, 081, 082, 085, 087, 089 and 092, certain blocks appeared to dry out before one set of iterations in a given time level could be completed. All other test runs lacking the gravity term did not show any resemblance to the field data.

One goal of this project was to test the ADI method for convergence if the gravity term was added to one set of iterations and not the other during a given time level. The gravity component was included, explicitly, when the columns in this profile model were calculated in the implicit sense. Gravity was not added to the right-hand-side of the equation (explicit side) when the rows (horizontal direction) were viewed implicitly. The convergence of this technique was displayed for numerous ranges of parameter input. This is not to say the technique is unconditionally stable. However, this work does show that under reasonable unsaturated conditions, applying the gravity influence to the vertical gradient and not the horizontal one will give numerically stable results in the ADI method.

The results from this project raise important questions for future research in the modelling of unsaturated flow. At this time, a generally applicable model for unsaturated flow is considered unreliable by some researchers and impossible by others. Numerous studies have been and are currently being conducted on the functional relationships among capillary head, capillary conductivity and water content. This project shows that the transition of forces between unsaturated and saturated volumes must be accurately described to apply these functions in models of unsaturated flow.

10.0 REFERENCES CITED

- Ahuja, L. R., 1973, "A Numerical Similarity Analysis of Infiltration Into Crusted Soils", Water Resources Research, Vol. 9, No. 4, pp. 987-994.
- Amerman, C. R., 1969, "Finite Difference Solutions of Unsteady, Two-Dimensional, Partially Saturated Porous Media Flow", Ph.D. Thesis, Purdue University, Lafayette Indiana, 221 p.
- Averjanov, S. F., 1950, "About Permeability of Subsurface Soils in the Case of Incomplete Saturation", Eng. Collect., 7.
- Bear, J., D. Zaslavsky and S. Irmay, 1968, Physical Principles of Water Percolation and Seepage, France, Unescd.
- Bear, Jacob, 1972, Dynamics of Fluids in Porous Media, New York, American Elsevier Publishing Company, Inc.
- Bodman, G. B., and E. A. Colman, 1943, "Moisture and Energy Conditions During Downward Entry of Water into Soils", Soil Science Society of America Proc., 8, pp. 116-122.
- Bouwer, H., 1964, "Unsaturated Flow in Groundwater Hydraulics", Proc. American Soc. Civil Engr., No. HY5, 90, pp. 121-144.
- Bresler, E., 1973, "Simultaneous Transport of Solutes and Water Under Transient Unsaturated Flow Conditions, Water Resources Research, Vol. 9, No. 4, pp. 975-986
- Brooks, R. H., and A. T. Corey, 1964, "Hydraulic Properties of Porous Media", Hydrol. Pap. 3, Colo. State Univ., Fort Collins.
- Brooks, R. H., and A. T. Corey, 1966, "Properties of Porous Media Affecting Fluid Flow", J. Irrig. Drain. Div. Amer. Soc. Civil Eng., 92 (IR2), pp. 61-88.
- Buckingham, E., 1907, "Studies in the Movement of Soil Moisture", U.S. Dept. Agric. Soils Bur. Bul. 38, 61 pp.
- Burdine, N. T., 1953, "Relative Permeability Calculation From Size Distribution Data", Amer. Soc. Agric. Eng., 10, pp. 400-404.

- Burejev, L. N., and Z. M. Burejeva, 1969, "Some Numerical Methods for Solving Problems of Non-Steady Seepage in Non-Homogeneous Anisotropic Soils", in (see ref. Rijtema and Wassink, editors), pp. 500-503.
- Campbell, G. S., 1974, "A Simple Method for Determining Unsaturated Conductivity from Moisture Retention Data", Soil Science, Vol. 117, No. 6, pp. 311-314.
- Carnahan, B., H. Luther and J. Wilkes, 1969, Applied Numerical Methods, New York, John Wiley and Sons.
- Childs, E. C., and N. Collis-George, 1950, "The Permeability of Porous Materials", Proc. Royal Soc. London, 201A, pp. 392-405.
- Clapp, R. B., and G. M. Hornberger, 1978, "Empirical Equations for Some Soil Hydraulic Properties", Water Resources Research, Vol. 14, No. 4, pp. 601-604.
- Colman, E. A., and G. B. Bodman, 1944, "Moisture and Energy Conditions During Downward Entry of Water into Moist and Layered Soils", Proc. Soil Science Society of America, 9, pp. 3-11.
- Dames & Moore and Kaman Tempo, 1987, "Kettleman Hills Vadose Zone Demonstration", by Kaman Sciences Corporation, Temp Division and Dames and Moore Corporation, California.
- Dane, J.H., and F.H. Mathis, 1981, "An Adaptive Finite Difference Scheme for the One-Dimensional Water Flow Equation", Soil Science Soc. Amer. J., Vol. 45, pp. 1048-1054.
- _____, and S. Hruska, 1983, "In-Situ Determination of Soil Hydraulic Properties During Drainage", Soil Science Soc. Amer. J., Vol. 47, pp. 619-624.
- Dewiest, R. J. M., 1969, Flow Through Porous Media, New York, Academic Press.
- Diment, G. A., K. K. Watson and P. J. Blennerhasset, 1982, "Stability Analysis of Water Movement in Unsaturated Porous Materials. 1. Theoretical Considerations", Water Resources Research, Vol. 18, No. 4, pp. 1248-1254.

Douglas, Jim (Jr.), 1955, "On the Numerical Integration of

$$\frac{\partial^2 m}{\partial x^2} + \frac{\partial^2 m}{\partial y^2} = \frac{\partial m}{\partial t} \text{ By Implied Methods"}, \text{ J. Soc. Indust. Apl. Math (SIAM), Vol. 3, No. 1, pp. 42-65.}$$

Elrick, D. E., J. H. Scandrett and E. E. Miller, 1959, "Tests of Capillary Flow Scaling", Soil Science Soc. Amer. Proc., 23, pp. 329-332.

Everett, L. G., and L. G. McMillion, 1985, "Operational Ranges for Suction Lysimeters", Ground Water Monitoring Review, pp. 51-60.

Freeze, R. A., and J. A. Cherry, 1979, Ground Water, New Jersey, Prentice-Hall Press.

Green, N. H., and C. A. Ampt, 1911, "Studies on Soil Physic, 1. Flow of Air and Water Through Soils", J. Agric. Science, Vol. 4, No. 1.

Green, R. E., and J. C. Corey, 1971, "Calculation of Hydraulic Conductivity: A Further Evaluation of Some Predictive Methods", Soil Science Soc. Amer. Proc., Vol. 35, pp. 3-8.

Hanks, R. J., and S. A. Bowers, 1962, "Numerical Solution of the Moisture Flow Equation for Infiltration Into Layered Soils", Proc. Soil Science Soc. Amer., 26, pp. 530-534.

Haverkamp, R., and M. Vauclin, 1979, "A Note on Estimating Finite Difference Interblock Hydraulic Conductivity Values for Transient Unsaturated Flow Problems", Water Resources Research, Vol. 15, No. 1, pp. 181-187,

_____, and M. Vauclin, 1981, "A Comprehensive Study of Three Forms of the Richard Equation Used for Predicting One-Dimensional Infiltration in Unsaturated Soils", Soil Science Soc. Amer. J., Vol. 45, pp. 13-20.

Hillel, D., 1982, Introduction to Soil Physics, San Francisco, Academic Press.

Holt, M., 1977, Numerical Methods in Fluid Dynamics, New York, Springer-Verlag.

- Hornberger, G. M., I. Remson and A. A. Fungaroli, 1969, "Numeric Studies of a Composite Soil Moisture Ground-Water System", Water Resources Res., 5, pp. 797-802.
- Irmay, S., 1954, "On the Hydraulic Conductivity of Unsaturated Soils", EOS Trans. AGU, Vol. 35, No. 3, pp. 463-470.
- Johnson, T. M., K. Cartwright and R. M. Schuller, 1981, "Monitoring of Leachate Migration in the Unsaturated Zone in the Vicinity of Sanitary Landfills", Ground Water Monitoring Review, pp. 55-63.
- Klute, A., 1952, "A Numerical Method for Solving the Flow Equation for Water in Unsaturated Material", Soil Science, Vol. 73, pp. 105-116.
- _____, and G. E. Wilkinson, 1958, "Some Tests of the Similar Media Concept of Capillary Flow: I. Reduced Capillary Conductivity and Moisture Characteristic Data", Soil Science Soc. of Amer. Proc., Vol. 22, pp. 278-281.
- Kraijenhoff Van De Leur, D. A., 1962, "Some Effects of the Unsaturated Zone on Nonsteady Free-Surface Groundwater Flow as Studied in a Scaled Granular Model", J. Geophysical Res., Vol. 67, pp. 4347-4362.
- Laliberte, G. E., and R. H. Brooks, 1967, "Hydraulic Properties of Disturbed Soil Materials Affected by Porosity", Soil Science Soc. Amer. Proc., Vol. 31, pp. 451-454.
- Luthin, J. N., A. Orhun and G. S. Taylor, 1975, "Coupled Saturated-Unsaturated Transient Flow in Porous Media: Experimental and Numeric Model", Water Resources Research, Vol. 11, No. 6, pp. 973-978.
- Mein, R. G., and C. L. Larson, 1973, "Modeling Infiltration During Steady Rain", Water Resources Research, Vol. 9, No. 2, pp. 384-
- Meredith/Boli & Associates, Inc., 1985, State Siting Criteria Equivalency Assessment for Chemical Waste Management, Inc.'s Kettleman Hills Facility, Beverly Hills, CA.
- Miller, E. E., and R. D. Miller, 1956, "Physical Theory for Capillary Flow Phenomena", J. of Applied Physics, Vol. 27, No. 4, pp. 324-332.

- Millington, R. J., and J. P. Quirk, 1961, "Permeability of Porous Solids", Trans. Faraday Soc., 57, pp. 1200-1206.
- Mualem, Yechezkel, 1976a, "A New Model for Predicting The Hydraulic Conductivity of Unsaturated Porous Media", Water Resources Research, Vol. 12, No. 3, pp. 513-522.
- _____, 1976b, "Hysteretical Models for Prediction of The Hydraulic Conductivity of Unsaturated Porous Media", Water Resources Research, Vol. 12, No. 6, pp. 1248-1254.
- _____, 1978, "Hydraulic Conductivity of Unsaturated Porous Media: Generalized Macroscopic Approach", Water Resources Research, Vol. 14, No. 2, pp. 325-334.
- _____, and G. Dagan, 1978, "Hydraulic Conductivity of Soils: Unified Approach to the Statistical Models", Soil Science Soc. Amer. J., Vol. 42, pp. 392-395.
- _____, and A. Klute, 1984, "A Predictor-Corrector Method for Measurement of Hydraulic Conductivity and Membrane Conductance", Soil Science Soc. Amer. J., Vol. 48, pp. 993-1000.
- Narasimhan, T. N., and P. A. Witherspoon, 1976, "An Integrated Finite Difference Method for Analyzing Fluid Flow in Porous Media", Water Resources Res., Vol. 12, No. 1, pp. 57-64.
- _____, and P. A. Witherspoon, 1977, Numerical Model for Saturated-Unsaturated Flow in Deformable Porous Media, 1. Theory", Water Resources Res., Vol. 13, No. 3, pp. 657-
- _____, S. P. Neuman and P. A. Witherspoon, 1978, "Finite Element Method for Subsurface Hydrology Using a Mixed Explicit-Implicit Scheme", Water Resources Res., Vol. 14, No. 5, pp. 863-877.
- Nelson, R. W., "Steady Darcian Transport of Fluids in Heterogeneous Partially Saturated Porous Media, 1. Mathematical and Numerical Formulation", HW-72335, 1, AEC Res. Develop. Dept., June, 1962.
- Neuman, S. P., 1976, "Wetting Front Pressure Head in the Infiltration Model of Green and Ampt", Water Resources Res., Vol. 12, No. 3, pp. 564-566.

- _____, and T. N. Narasimhan, 1977, "Mixed Explicit-Implicit Iterative Finite Element Scheme for Diffusion-Type Problems, I, Theory", Int. J. Numer. Methods Eng., 11, pp. 309-323.
- Norrie, Douglas H., Gerard de Vries, 1973, The Finite Element Method Fundamentals and Applications, New York, Academic Press.
- Peaceman, D. W., H. H. Rachford, Jr., 1955, "The Numerical Solution of Parabolic and Elliptic Differential Equations", J. Soc. Indust. Appl. Math. (SIAM), Vol. 3, No.1, pp. 28-41.
- Philip, J. R., 1969a, "A Linearization Technique for the Study of Infiltration", in (see ref. Rijtema and Wassink, editors), pp. 471-478.
- _____, 1969b, "Absorption and Infiltration in Two- and Three-Dimensional Systems", in (see ref. Rijtema and Wassink, editors), pp. 503-525.
- Prickett, T. A., and C. G. Lonquist, 1971, Selected Digital Computer Techniques for Groundwater Resource Evaluation, Illinois State Water Survey, Bulletin 55.
- Raats, P. A. C., 1970, "Steady Infiltration From a Line Source and Furrows", Soil Science Soc. of Amer. Proc., Vol. 34, pp. 704-714.
- Reeder, J. W., D. L. Freyberg, J. B. Franzini and I. Remson, 1980, "Infiltration Under Rapidly Varying Surface Water Depths", Water Resources Res., Vol. 16, No. 1, pp. 97-104.
- Reichardt, K., P. Libardi and D. Nielsen, 1975, "Unsaturated Hydraulic Conductivity Determination by a Scaling Technique", Soil Science, Vol. 120, No. 3, pp. 165-168.
- Reisenauer, A. E., 1963, "Methods for Solving Problems of Multi Dimensional, Partially Saturated Steady Flow in Soils", J. of Geophysical Res., Vol. 68, No. 20, pp. 5725-5733.
- Remson, I., R. L. Drake, S. S. Mc Nary and E. M. Wallo, 1965, "Vertical Drainage of an Unsaturated Soil", Proc. ASCE. J. Hydr. Div., 91 (HY1), pp. 55-74.
- Richards, L. A., 1931, "Capillary Conduction of Liquids Through Porous Mediums", Physics (J. of Applied Physics), Vol. 1, pp. 318-333.

- Rijtema, P. E. (editor), and H. Wassink (editor), 1969, Water in the Unsaturated Zone Proceedings of the Wageningen Symposium, Volumes 1 and 2, Paris, International Association of Scientific Hydrology.
- Rogers, J. S., and A. Klute, 1971, "The Hydraulic Conductivity-Water Content Relationship During Nonsteady Flow Through a Sand Column", Soil Science Soc. Amer. Proc., Vol. 35, pp. 695-700.
- Rubin, J., 1968, "Theoretical Analysis of Two-Dimensional, Transient Flow of Water in Unsaturated and Partly Unsaturated Soils", Soil Science Soc. of Amer. Proc., Vol. 32, pp. 607-615.
- _____, 1969, "Numerical Analysis of Poned Rainfall Infiltration", in (see ref. Rijtema and Wassink, editors), pp. 440-451.
- _____, and R. Steinhardt, 1963, "Soil-Water Relations During Rain Infiltration: 1, Theory", Proc. Soil Science Soc. Amer., Vol. 27, pp. 246-251.
- Schnabel, R. R., and E. B. Richie, 1984, "Calculation of Internodal Conductances for Unsaturated Flow Simulations: A Comparison", Soil Science Soc. Amer. J., Vol. 48, pp. 1006-1010.
- Schuh, W. M., and J. W. Bauder, 1986, "Effect of Soil Properties on Hydraulic Conductivity - Moisture Relationships", Soil Science Soc. Amer. J., Vol. 50, pp. 848-855.
- Selim, H. M., and K. Kirkham, 1973, "Unsteady Two-Dimensional Flow of Water in Unsaturated Soils Above an Impervious Barrier", Soil Science Amer. Proc., Vol. 37, pp. 489-495.
- Singh, Rameshwar, 1965, Unsteady and Unsaturated Flow in Soils in Two Dimensions, Department of Civil Engineering, Standford University, Technical Report No. 54, 130 pp.
- Sisk, S. W., 1986, Ground-Water Monitoring Evaluation. Chemical Waste Management, Inc., Kettleman Hills Facility, U. S. E. P. A., Denver, CO.
- Sposito, G., 1978, "The Statistical Mechanical Theory of Water Transport Through Unsaturated Soil, 2. Deviation of the Buckingham-Darcy Flux Law", Water Resources Research, Vol. 14, No. 3, pp. 479-484.

- Stephens, D. B., K. R. Rehfeldt, 1985, "Evaluation of Closed-Form Analytical Models to Calculate Conductivity in a Fine Sand", Soil Science Soc. Amer. J., Vol. 49, pp. 12-19.
- Straub, W. A., and D. R. Lynch, 1982, "Models of Landfill Leaching: Moisture Flow and Inorganic Strength", Proc ASCE, J. Env. Engr. Div., 108 (EE2), pp. 231-250.
- Supplement to RCRA Part B Permit Application, Chemical Waste Management, Inc., Kettleman Hills Facility, 1985, Vol. IV.
- Swartzendruber, D., 1969, "Flow of Water in Unsaturated Soils", in Dewiest, R. J. M. (editor), Flow Through Porous Media, New York, Academic Press.
- Talsma, T., 1970, "Hysteresis in Two Sands and the Independent Domain Model", Water Resources Research, Vol. 6, No. 3, pp. 964-970.
- Taylor, G. S., 1974, "Digital Computers and Drainage Problem Analysis, 2", Drainage for Agric., Agron, Monogr. Ser., Vol 17, J. van Schilfgaarde (editor), Amer. Soc. of Agronomy, pp. 567-586.
- _____, and J. N. Luthin, 1969, "Computer Methods for Transient Analysis of Water Table Aquifers", Water Resources Res., Vol. 5, No. 1, pp. 144-152.
- Topp, G. C., 1971, "Soil Water Hysteresis in Silt Loam and Clay Loam Soils", Water Resources Research, Vol. 7, No. 4, pp. 914-920.
- Ungs, M., R. W. Cleary, L. Boersma and S. Yingiajaval, 1976, "The Qualitative Description of Transfer of Water and Chemical Through Soils", in R. S. Loehr (editor), Land as a Waste Management Alternative, Proc. Cornell Agricultural Waste Management Conf., Ann Arbor Publ., Ann Arbor, Michigan, pp. 109-150.
- Van Bavel, C. H. M., G. B. Stirk and K. J. Brust, 1968, "Hydraulic Properties of a Clay Loam Soil and the Field Measurement of Water Uptake by Roots: I. Interpretation of Water Content and Pressure Profiles", Soil Science Amer. Proc., Vol. 32, pp. 310-317.

- Van der Ploeg, R. R., and P. Benecke, 1974, "Unsteady, Unsaturated, N-dimensional Moisture Flow in Soil: A Computer Simulation Program", Soil Science Soc. Amer. Proc., Vol. 38, No. 6, pp. 881-885.
- Van Genuchten, M. Th., 1980, "A Closed-Form Equation for Predicting the Hydraulic Conductivity of Unsaturated Soils", Soil Science Soc. Amer. J., Vol. 44, pp. 892-898.
- Wang, Flora Chu, and V. Lakshminarayana, 1968, "Mathematical Simulation of Water Movement Through Unsaturated Non-Homogeneous Soils", Soil Science Soc. Amer. Proc., Vol. 32, pp. 329-334.
- Wang, Herbert F., and Mary P. Anderson, 1982, Introduction to Groundwater Modelling: Finite Difference and Finite Element Methods, San Francisco, W.H. Freeman and Company.
- Ward, A., L. G. Wells, and R. E. Phillips, 1983, "Characterizing Unsaturated Hydraulic Conductivity of Western Kentucky Surface Mine Spoils and Soils", Soil Science Soc. Amer. J., Vol. 47, pp. 847-854.
- Warrick, A. W., J. W. Biggar, and D. R. Nielsen, 1971, "Simultaneous Solute and Water Transfer for an Unsaturated Soil", Water Resources Research, Vol. 7, No. 5, pp. 1216-1225.
- _____, G. J. Mullen, and D. R. Nielsen, 1977, "Scaling Field-Measured Soil Hydraulic Properties Using a Similar Media Concept", Water Resources Research, Vol. 13, No. 3, pp. 355-362.
- Whisler, F. D., and A. Klute, 1969, "Analysis of Infiltration into Stratified Soil Columns", in (see ref. Rijtema and Wassink, editors), pp. 451-470.
- Wilkinson, G. E., and A. Klute, 1959, "Some Tests of the Similar Media Concept of Capillary Flow: II. Flow Systems Data", Soil Science Soc. Amer. Proc., Vol. 23, pp. 434-437.
- Wilson, L. G., 1981, "Monitoring in the Vadose Zone Part I: Storage Changes", Ground Water Monitoring Review, pp. 32-41.
- _____, 1983, "Monitoring in the Vadose Zone: Part III, Detecting Pollutant Movement", Ground Water Monitoring Review, pp. 155-166.

Zachmann, D. W., 1978, "A Mathematical Treatment of Infiltration from a Line Source Into an Inclined Porous Medium", Soil Science Soc. Amer. J., Vol. 42, pp. 685-688.

_____, and A. W. Thomas, 1973, "A Mathematical Investigation of Steady Infiltration from Line Sources", Soil Science Soc. Amer. Proc., Vol. 37, pp. 495-500.

11.1 APPENDIX A

EXAMPLE DIFFERENTIAL FORMS OF THE RICHARDS' EQUATION

USED IN OTHER ADI MODELS

11.1 APPENDIX A

EXAMPLE DIFFERENTIAL FORMS OF THE RICHARDS' EQUATION
USED IN OTHER ADI MODELS

Selim and Kirkham, 1973, p. 490.

$$\frac{\partial w}{\partial t} = \frac{\partial}{\partial x} D(w) \frac{\partial w}{\partial x} + \frac{\partial}{\partial z} D(w) \frac{\partial w}{\partial z} - \frac{\partial K(w)}{\partial z}$$

where: $D(w) = -K \frac{\partial h}{\partial x}$

Luthin, *et al.*, 1975, p. 973.

$$\frac{K}{r} \left[\frac{\partial(H+z)}{\partial r} \right] + \frac{\partial}{\partial r} \left[\frac{K \partial(H+z)}{\partial r} \right] + \frac{\partial}{\partial z} \left[\frac{K \partial(H+z)}{\partial z} \right] = \frac{\partial w}{\partial H} \frac{\partial H}{\partial t}$$

where: r denotes radial distance from a pumping well

Prickett and Lonquist, 1971, p. 3.

$$\frac{\partial}{\partial x} \left[T \frac{\partial h}{\partial x} \right] + \frac{\partial}{\partial y} \left[T \frac{\partial h}{\partial y} \right] = S \frac{\partial h}{\partial t} + Q$$

where: T = aquifer transmissivity
 S = aquifer storage coefficient
 Q = net groundwater withdrawal rate per unit area

Rubin, 1968, p. 608.

$$\frac{\partial w}{\partial t} = \frac{\partial}{\partial x} \left[K(H-z) \frac{\partial H}{\partial x} \right] + \frac{\partial}{\partial z} \left[K(H-z) \frac{\partial H}{\partial z} \right]$$

11.2 APPENDIX B

GRAPHS OF WATER CONTENT, CAPILLARY CONDUCTIVITY
AND CAPILLARY HEAD RELATIONSHIPS

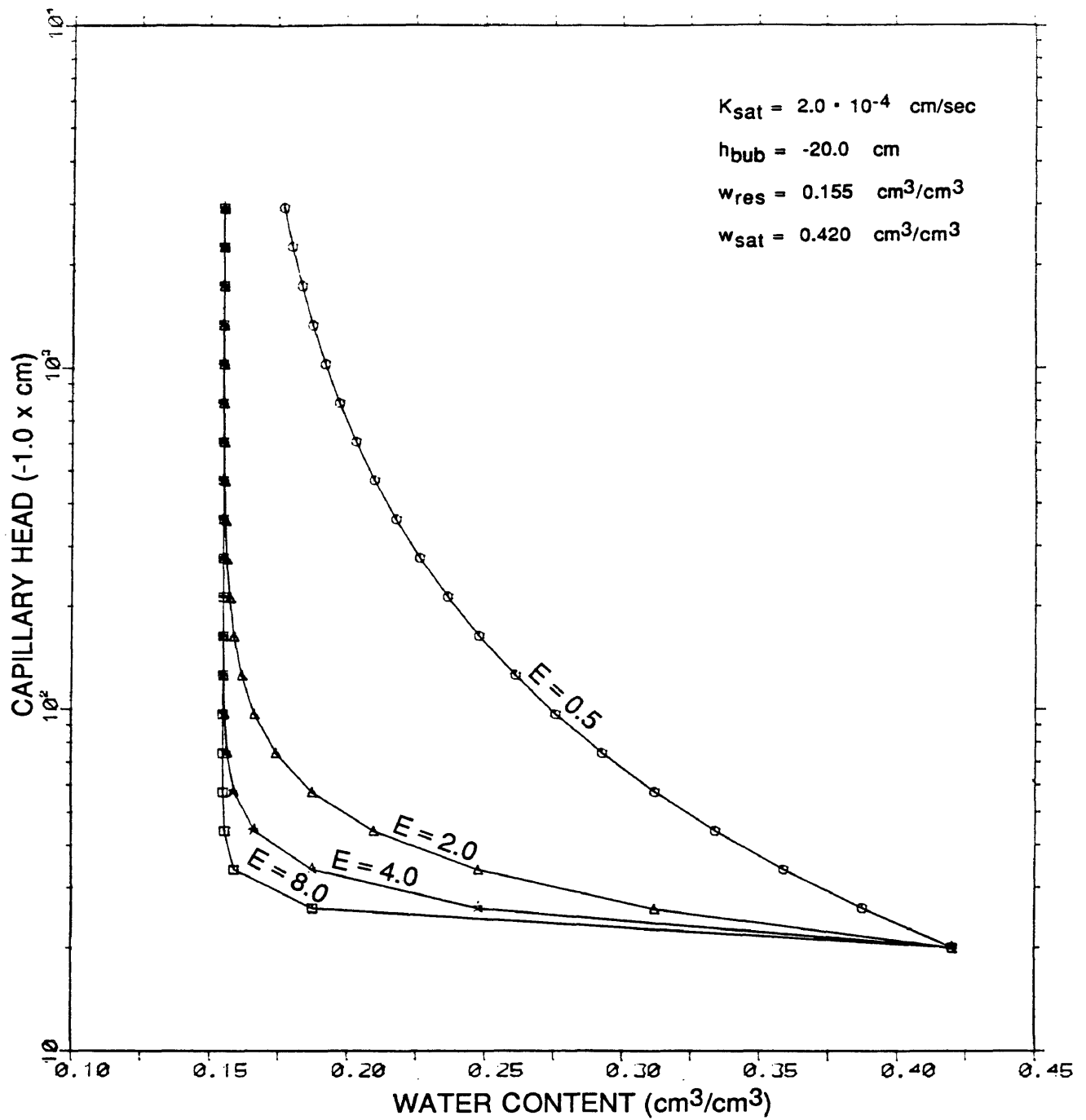


Figure 3
 WATER CONTENT VERSUS CAPILLARY HEAD
 BROOKS AND COREY, AVERJANOV AND MUALEM POWER EQUATIONS

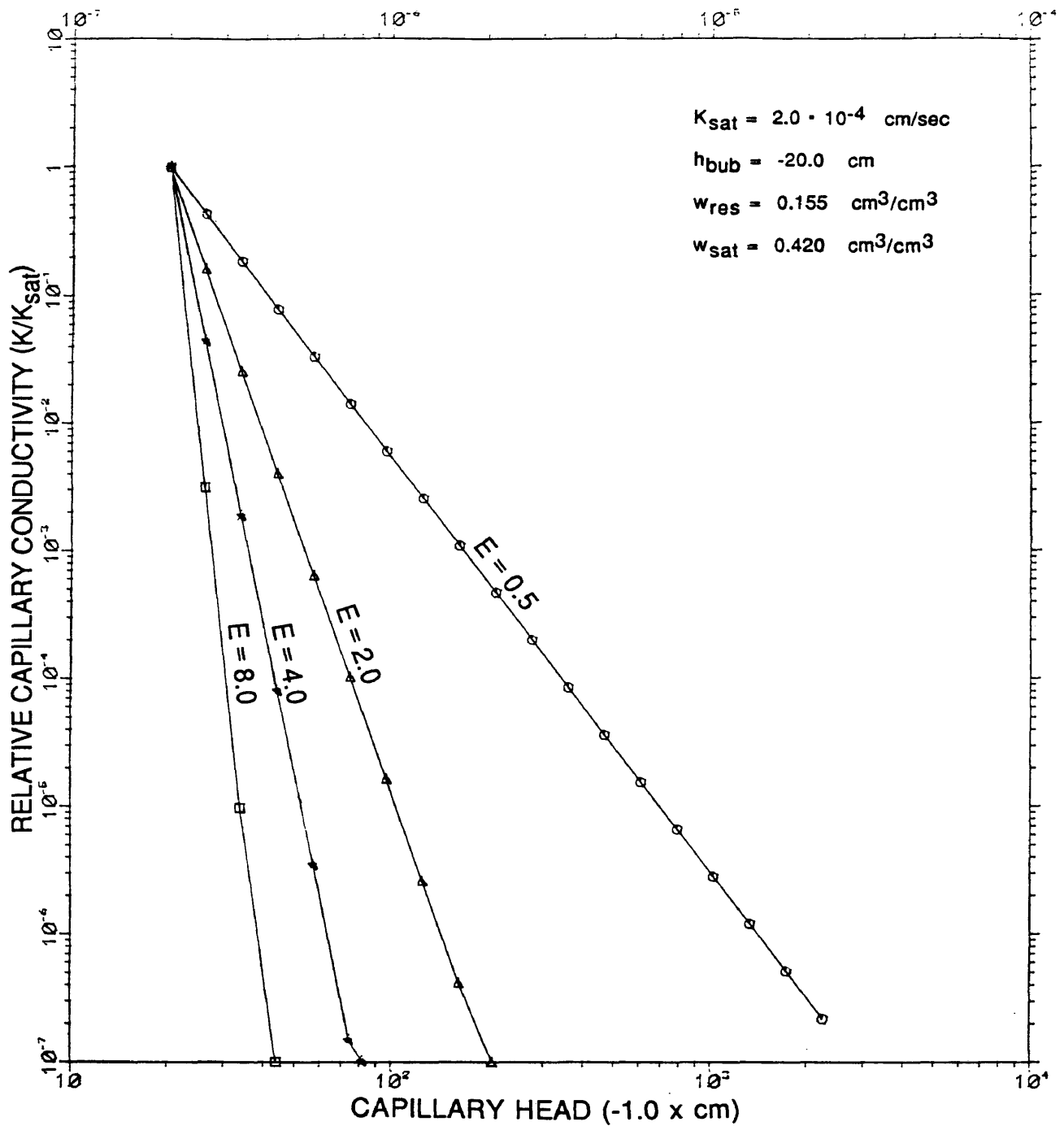


Figure 4
 CAPILLARY HEAD VERSUS CAPILLARY CONDUCTIVITY
 BROOKS AND COREY, AVERJANOV AND MUALEM POWER EQUATIONS

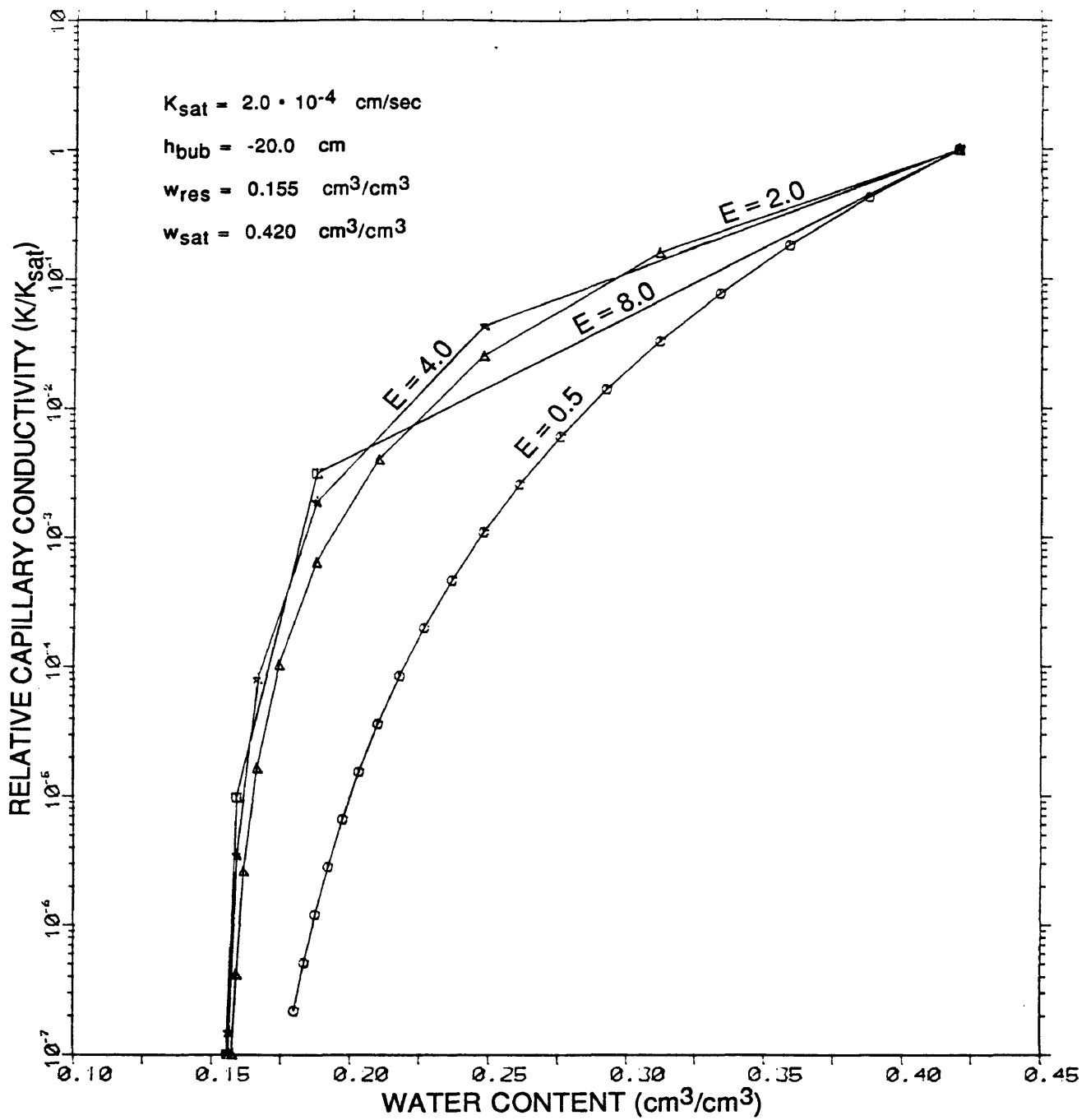


Figure 5
 WATER CONTENT VERSUS CAPILLARY CONDUCTIVITY
 BROOKS AND COREY, AVERJANOV AND MUALEM POWER EQUATIONS

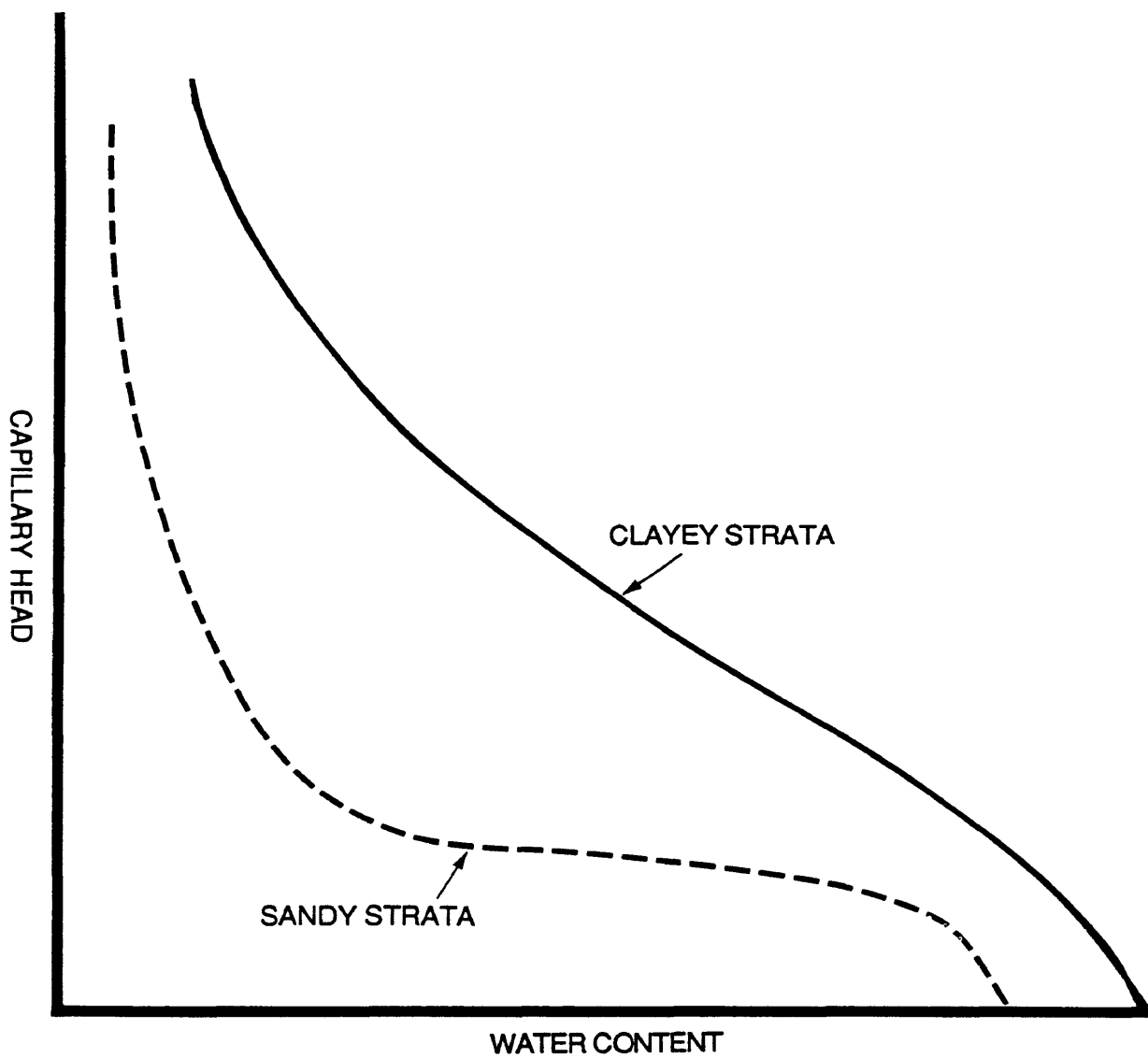


Figure 6
RELATIVE SHAPE OF THE WATER CONTENT VERSUS CAPILLARY HEAD CURVES
FOR COMPARISON TO GENERATED CURVES
(Modified from: Hillel, 1982, p. 76)

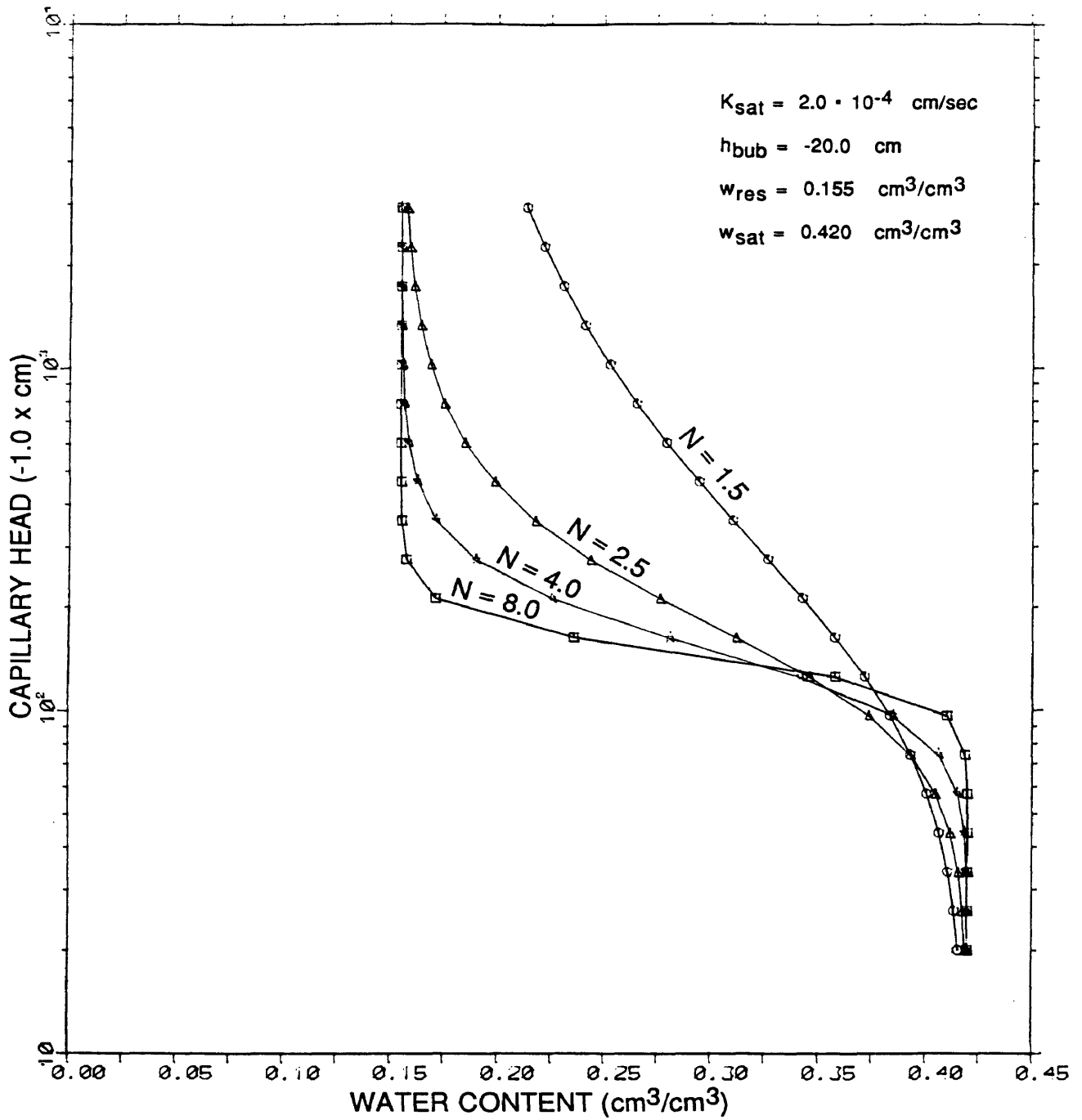


Figure 7
WATER CONTENT VERSUS CAPILLARY HEAD
VAN GENUCHTEN CLOSED FORM ANALYTICAL EQUATIONS ($\alpha = 0.007$)

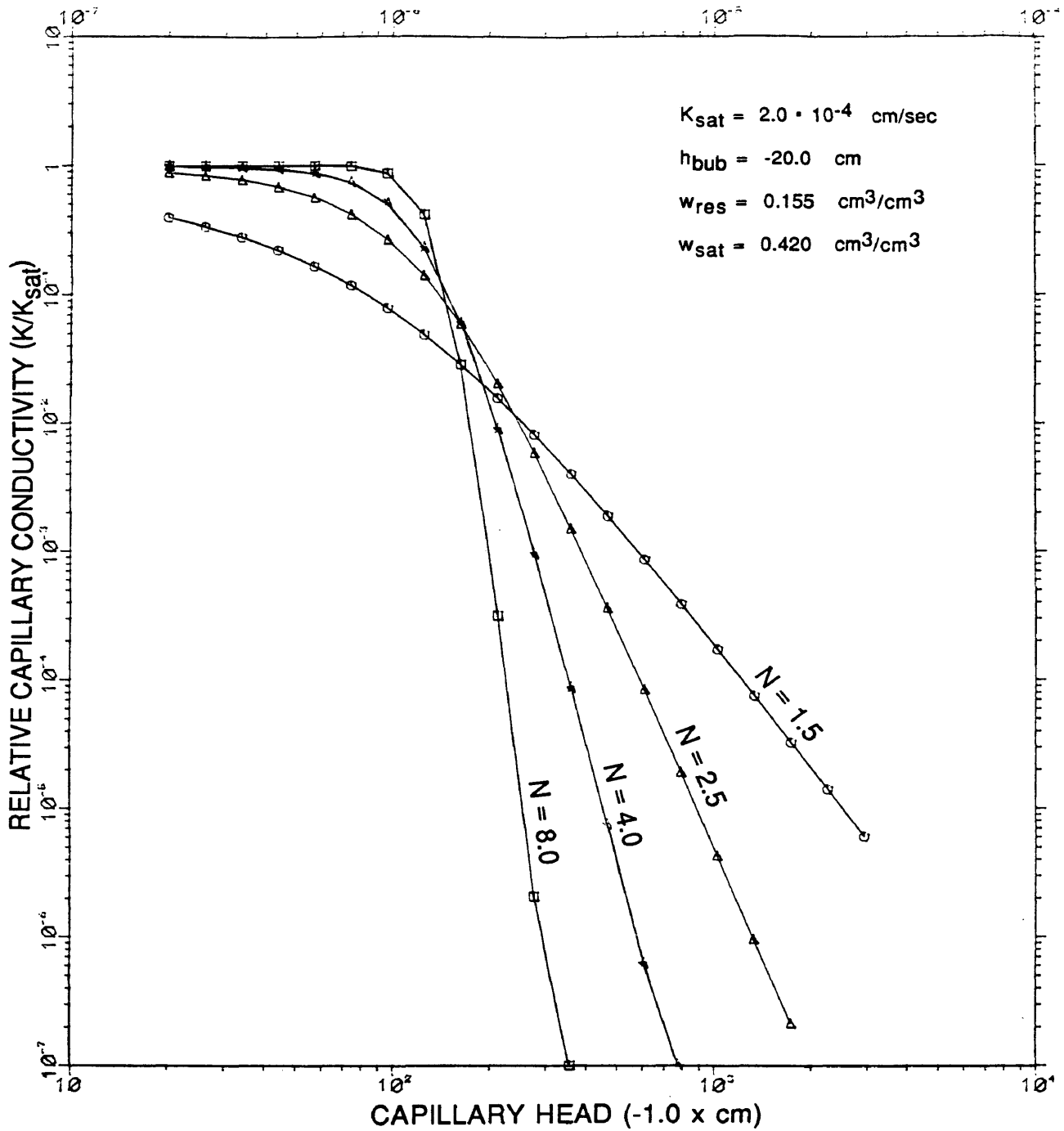


Figure 8
 CAPILLARY HEAD VERSUS CAPILLARY CONDUCTIVITY
 VAN GENUCHTEN CLOSED FORM ANALYTICAL EQUATIONS ($\alpha = 0.007$)

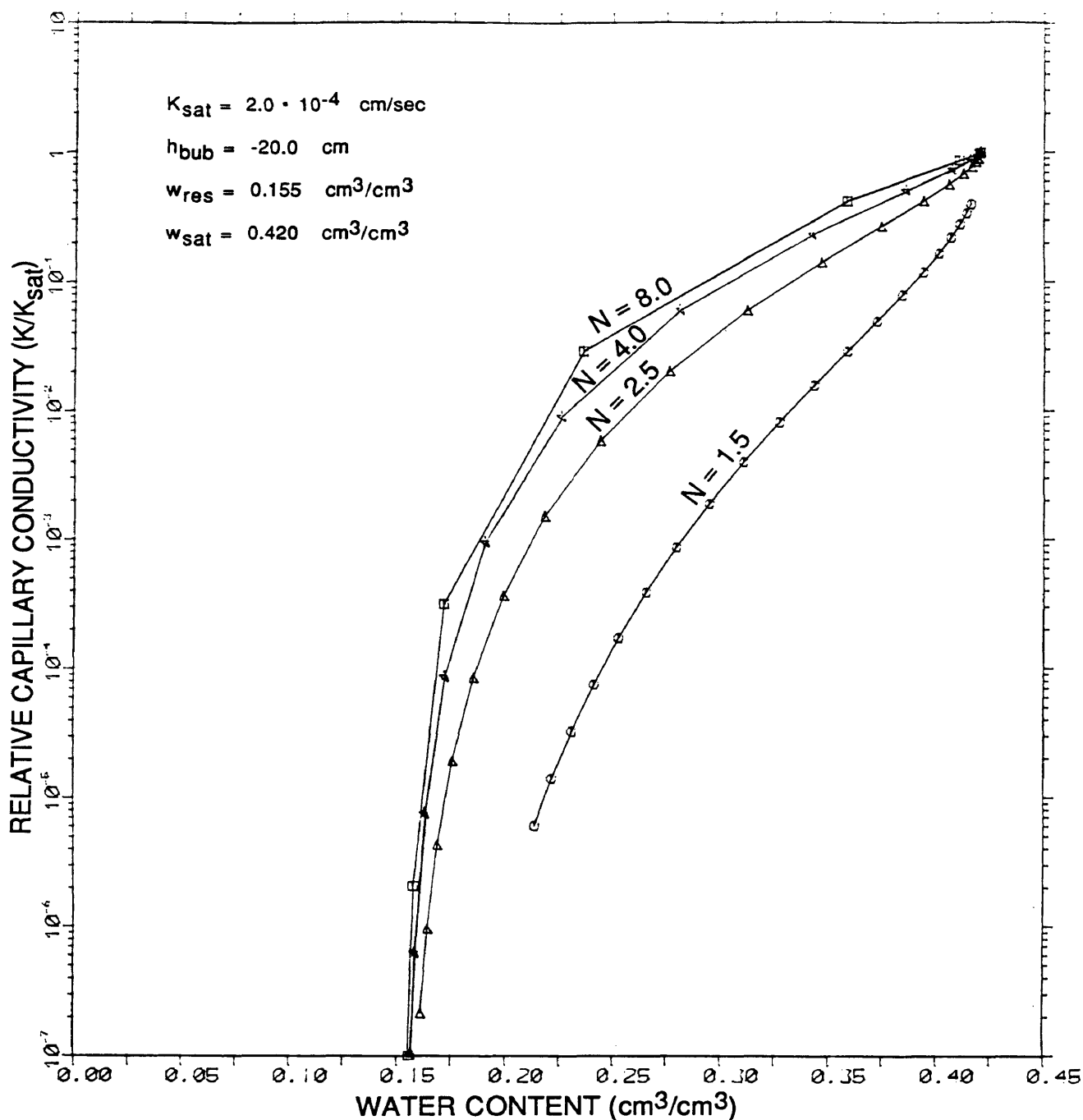


Figure 9
 WATER CONTENT VERSUS CAPILLARY CONDUCTIVITY
 VAN GENUCHTEN CLOSED FORM ANALYTICAL EQUATIONS ($\alpha = 0.007$)

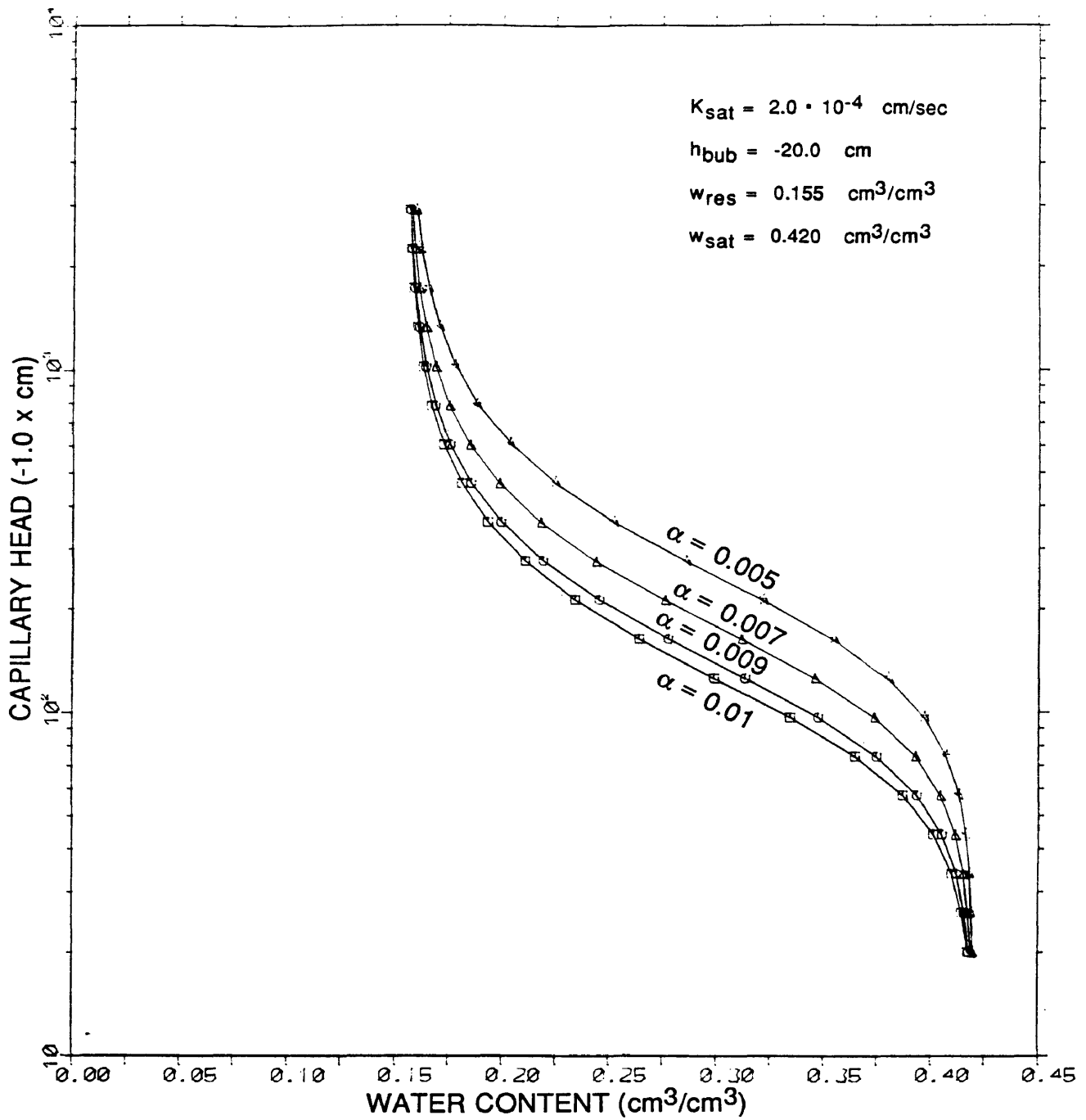


Figure 10
 WATER CONTENT VERSUS CAPILLARY HEAD
 VAN GENUCHTEN CLOSED FORM ANALYTICAL EQUATIONS ($N = 2.5$)

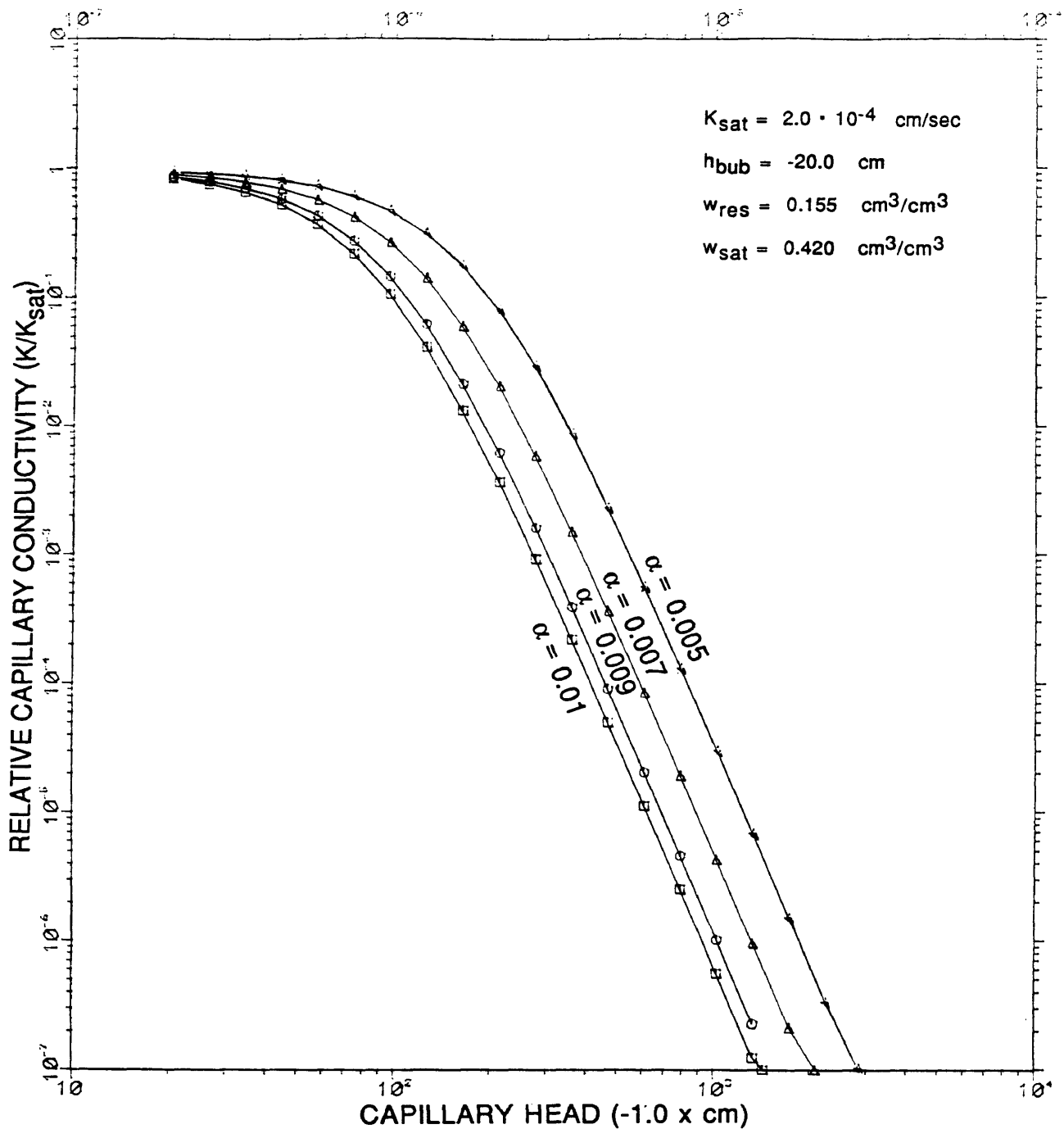


Figure 11
 CAPILLARY HEAD VERSUS CAPILLARY CONDUCTIVITY
 VAN GENUCHTEN CLOSED FORM ANALYTICAL EQUATIONS (N = 2.5)

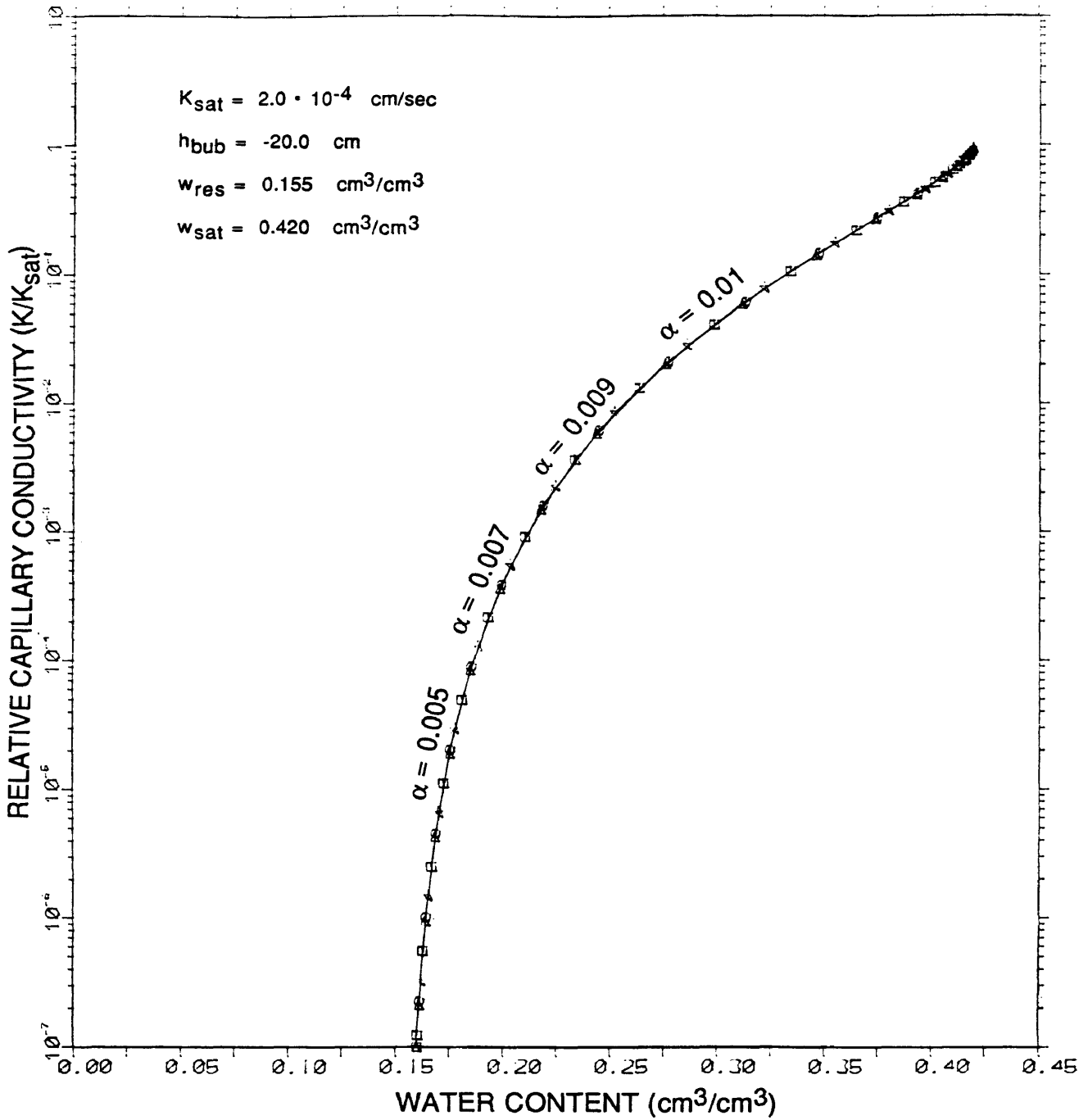


Figure 12
 WATER CONTENT VERSUS CAPILLARY CONDUCTIVITY
 VAN GENUCHTEN CLOSED FORM ANALYTICAL EQUATIONS (N = 2.5)

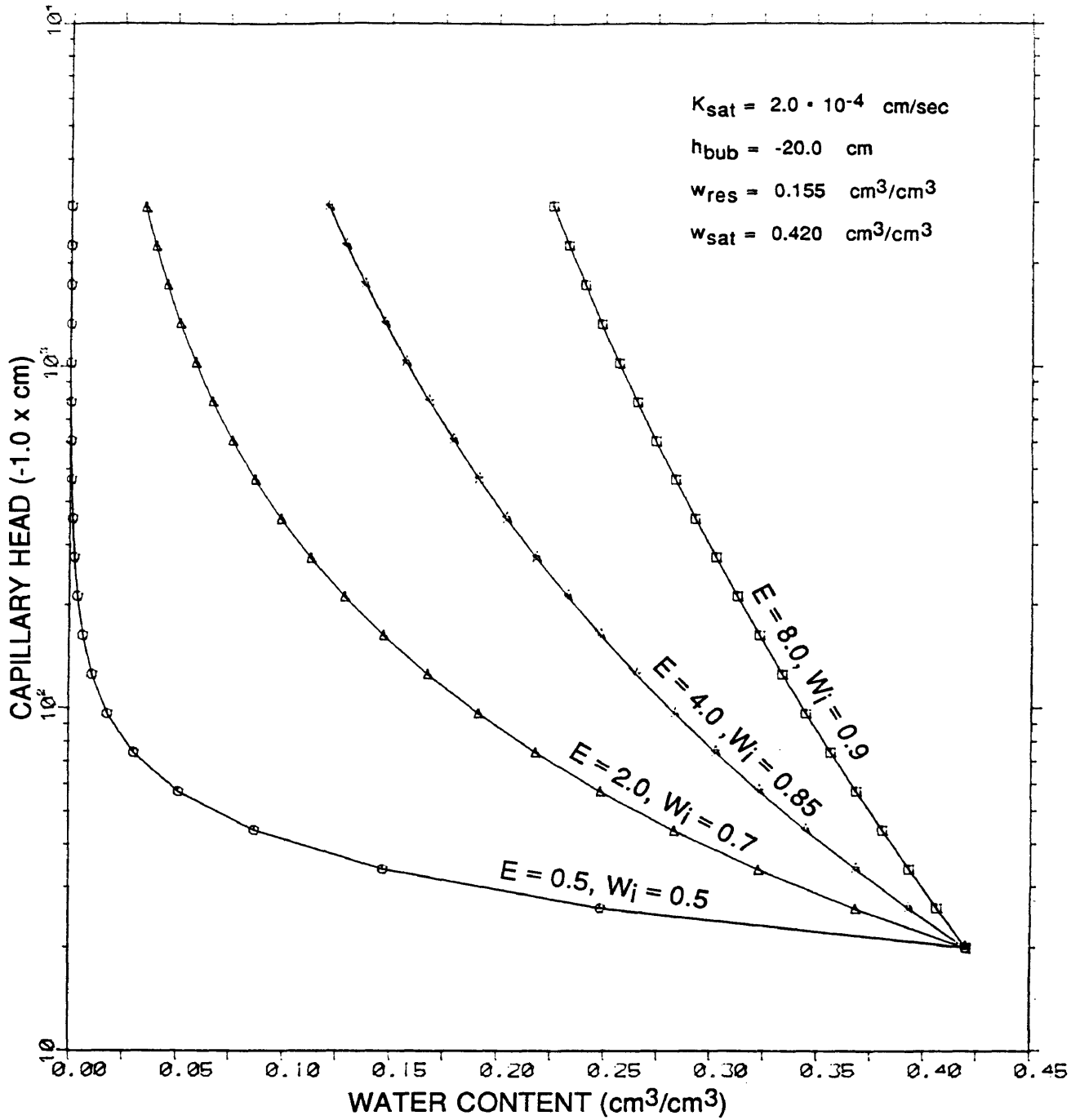


Figure 13
WATER CONTENT VERSUS CAPILLARY HEAD
CAMPBELL POWER EQUATIONS WITH THE CLAPP AND HORNBERGER
POLYNOMIAL VARIATION

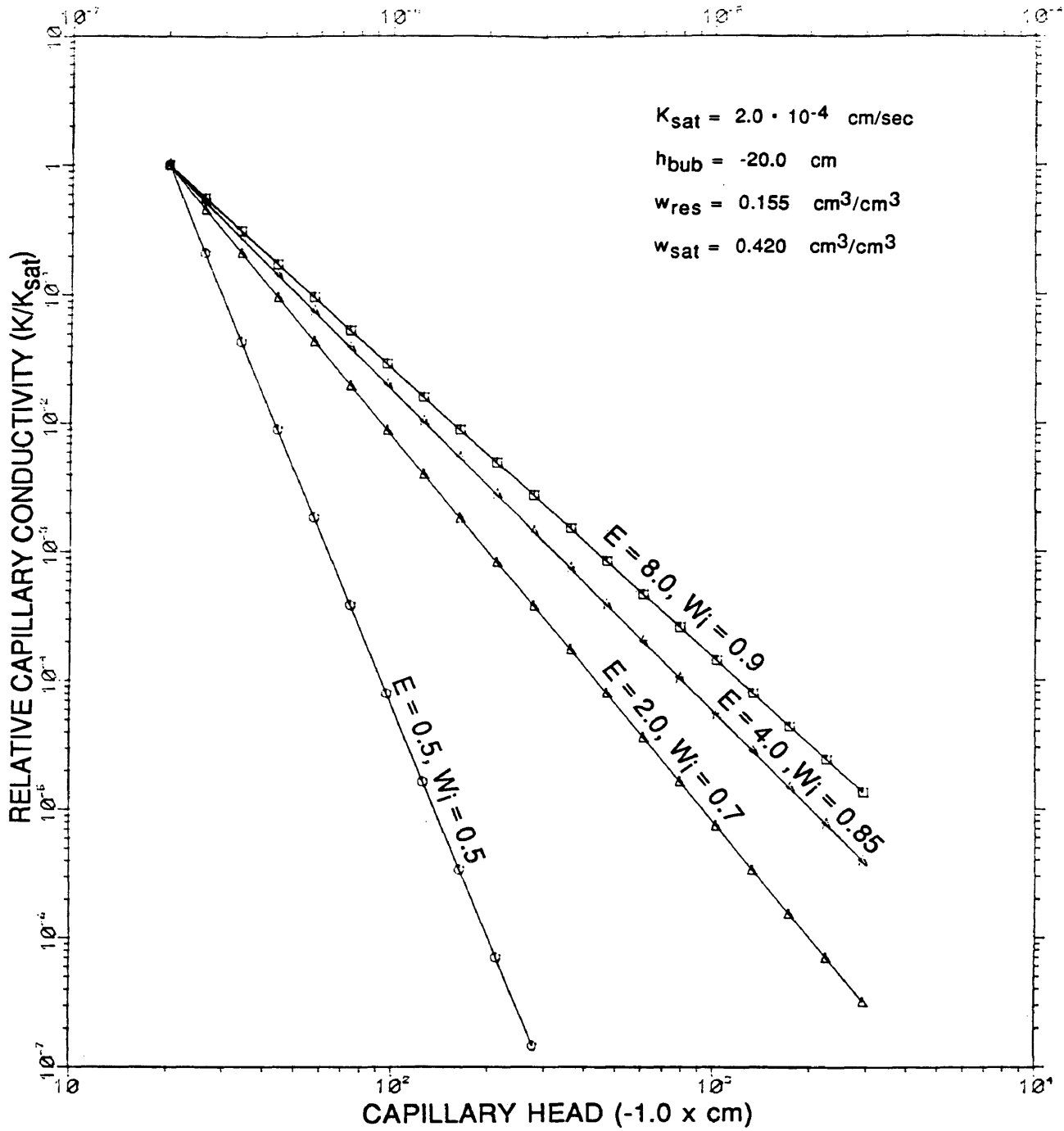


Figure 14
 CAPILLARY HEAD VERSUS CAPILLARY CONDUCTIVITY
 CAMPBELL POWER EQUATIONS WITH THE CLAPP AND HORNBERGER
 POLYNOMIAL VARIATION

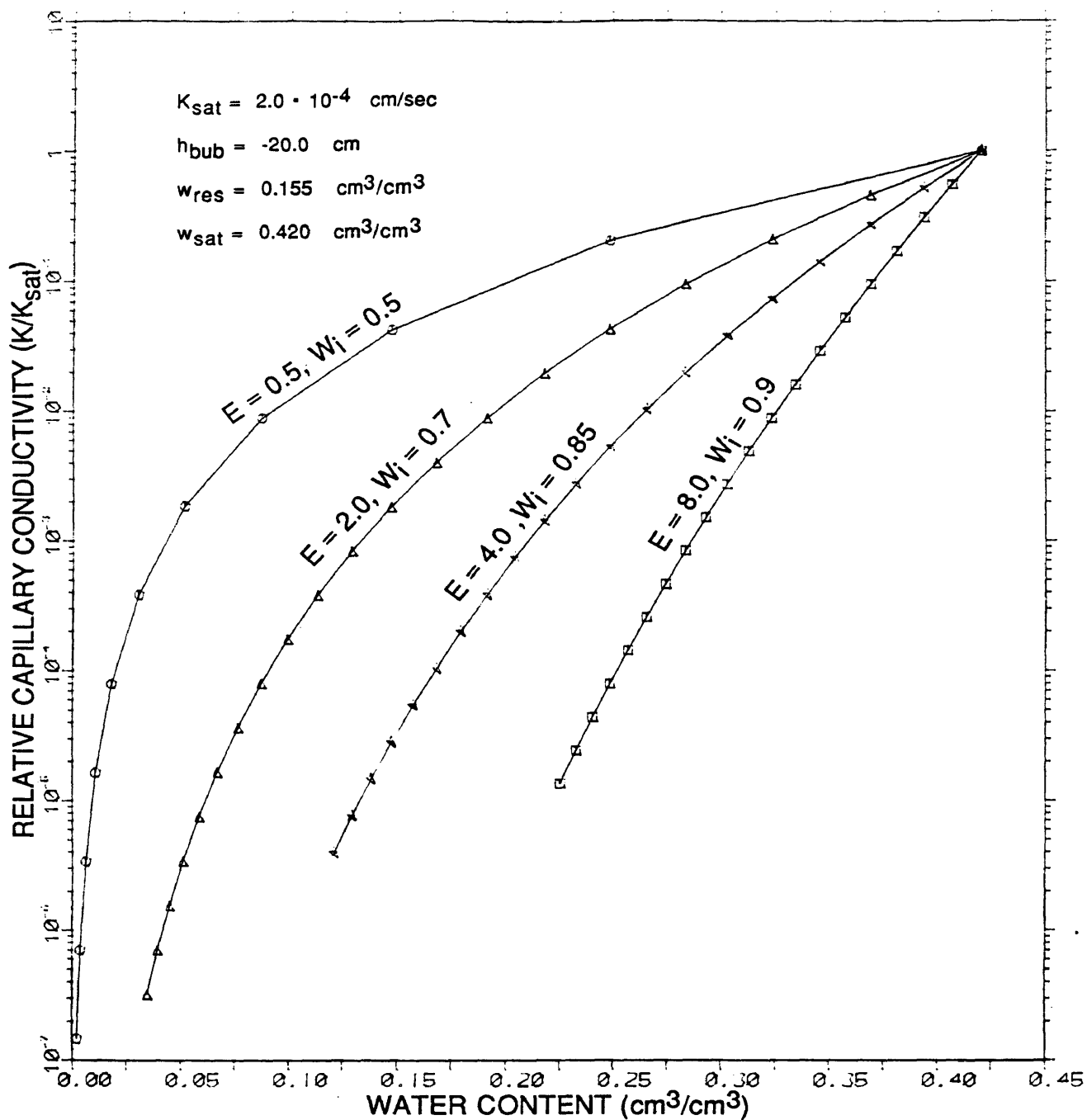


Figure 15
 WATER CONTENT VERSUS CAPILLARY CONDUCTIVITY
 CAMPBELL POWER EQUATIONS WITH THE CLAPP AND HORNBERGER
 POLYNOMIAL VARIATION

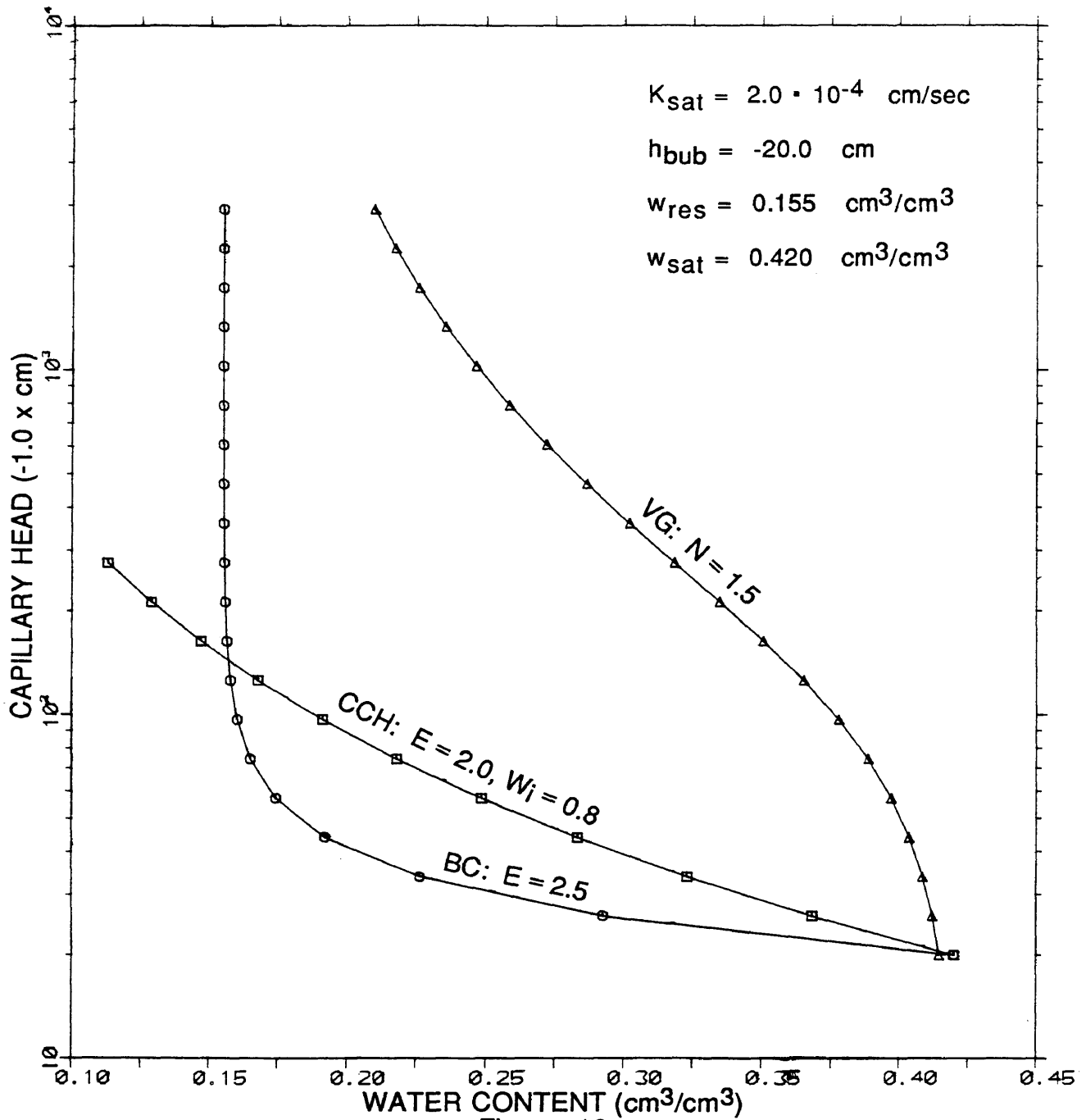


Figure 16

WATER CONTENT VERSUS CAPILLARY HEAD

THREE TYPES OF FUNCTIONS REPRESENTED FOR COMPARISON

- BC: BROOKS AND COREY, AVERJANOV AND MUALEM POWER EQUATIONS
- VG: VAN GENUCHTEN CLOSED FORM ANALYTICAL EQUATIONS ($\alpha = 0.008$)
- CCH: CAMPBELL POWER EQUATIONS WITH THE CLAPP AND HORNBERGER POLYNOMIAL VARIATION

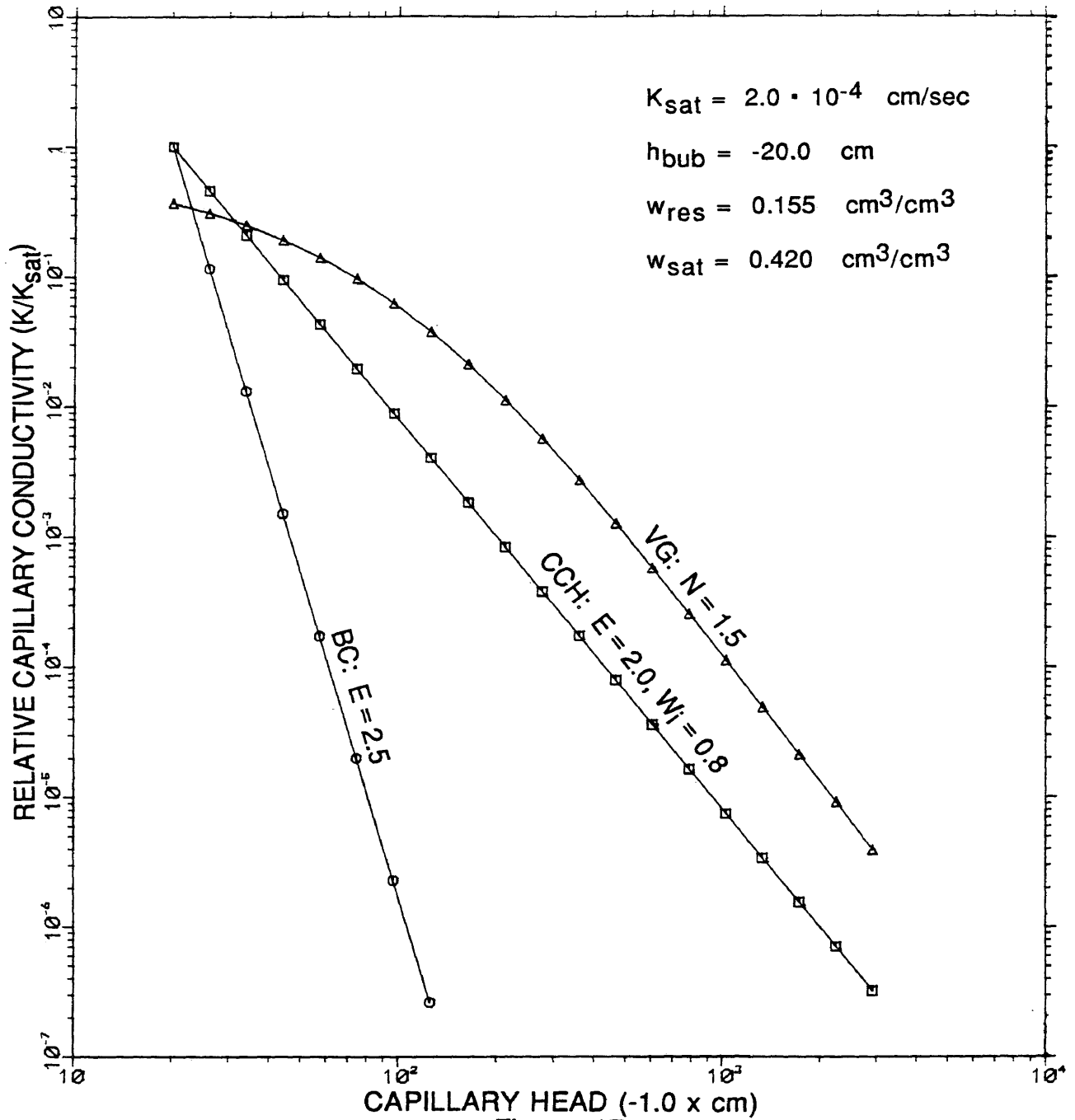


Figure 17

CAPILLARY HEAD VERSUS CAPILLARY CONDUCTIVITY

THREE TYPES OF FUNCTIONS REPRESENTED FOR COMPARISON

- BC: BROOKS AND COREY, AVERJANOV AND MUALEM POWER EQUATIONS
- VG: VAN GENUCHTEN CLOSED FORM ANALYTICAL EQUATIONS ($\alpha = 0.008$)
- CCH: CAMPBELL POWER EQUATIONS WITH THE CLAPP AND HORNBERGER POLYNOMIAL VARIATION

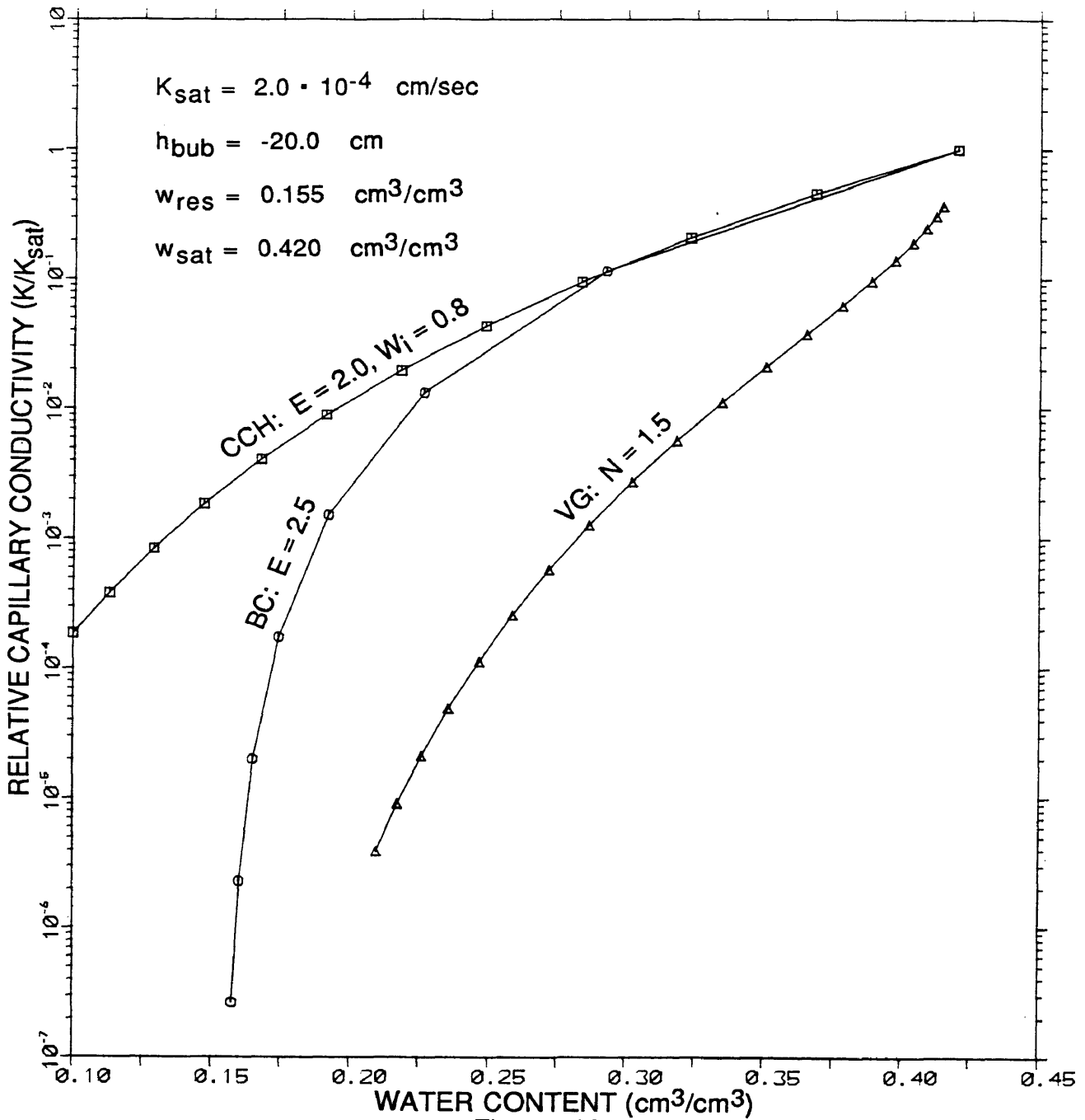


Figure 18

WATER CONTENT VERSUS CAPILLARY CONDUCTIVITY

THREE TYPES OF FUNCTIONS REPRESENTED FOR COMPARISON

- BC: BROOKS AND COREY, AVERJANOV AND MUALEM POWER EQUATIONS
- VG: VAN GENUCHTEN CLOSED FORM ANALYTICAL EQUATIONS ($\alpha = 0.008$)
- CCH: CAMPBELL POWER EQUATIONS WITH THE CLAPP AND HORNBERGER POLYNOMIAL VARIATION

11.3 APPENDIX C
DISCRETIZATION EQUATIONS REPRESENTED BY THE MODEL

APPENDIX C

DISCRETIZATION EQUATIONS REPRESENTED BY THE MODEL

Notation:

Superscripts: denote time levels.

- "n" initial time level,
- " γ " values updated after the column implicit - row explicit iteration,
- " β " values updated after the row implicit - column explicit iteration,
- "*" the value is updated as soon as a new head value is available.

Subscripts: denote block location in array storage indices

- "a" column index
- "b" row index
- " $x \pm 1/2$ " internodal block location, calculated by finding the geometric mean between values in adjacent blocks; $X_{a, b \pm 1/2} = (X_a \cdot X_b)^{1/2}$.

Coefficients:

$$U = \frac{\text{time}}{(\text{block size})^2} \frac{\partial h}{\partial w}$$

- h = capillary head,
- w = water content,
- K = capillary conductivity.

INDICES: $b = 1, a = 1$ column implicit

$$\left[(U K)_{a,b}^n + (U K)_{a,b+1/2}^n + 1 \right] h_{a,b}^{n+\Delta} + \left[-(U K)_{a,b+1/2}^n \right] h_{a,b+1}^{n+\Delta} =$$

$$\left[-(U K)_{a,b}^n - (U K)_{a+1/2,b}^n + 1 \right] h_{a,b}^n + \left[(U K)_{a+1/2,b}^n \right] h_{a+1,b}^n + \frac{\partial h}{\partial w} \frac{\Delta t}{\Delta z} \left[K_{a,b}^n - K_{a,b+1/2}^n \right]$$

INDICES: $1 < b < b_{\max}, a = 1$ Column implicit

$$\left[-(U K)_{a,b-1/2}^n \right] h_{a,b-1}^{n+\Delta} + \left[(U K)_{a,b-1/2}^n + (U K)_{a,b+1/2}^n + 1 \right] h_{a,b}^{n+\Delta} + \left[-(U K)_{a,b+1/2}^n \right] h_{a,b+1}^{n+\Delta} =$$

$$\begin{aligned} & \left[-(U K)_{a,b}^n - (U K)_{a+1/2,b+1}^n \right] h_{a,b}^n \\ & + \left[(U K)_{a+1/2,b}^n \right] h_{a+1,b}^n + \frac{\partial h}{\partial w} \frac{\Delta t}{\Delta z} \left[K_{a,b-1/2}^n - K_{a,b+1/2}^n \right] \end{aligned}$$

INDICES: $b = b_{\max}, a = 1$ column implicit

$$\begin{aligned} & \left[-(U K)_{a,b-1/2}^n \right] h_{a,b-1}^{n+\Delta} + \left[(U K)_{a,b-1/2}^n + (U K)_{a,b+1}^n \right] h_{a,b}^{n+\Delta} \\ & = \left[-(U K)_{a,b}^{n+\Delta} - (U K)_{a+1/2,b+1}^n \right] h_{a,b}^n \\ & + \left[(U K)_{a+1/2,b}^n \right] h_{a+1,b}^n + \frac{\partial h}{\partial w} \frac{\Delta t}{\Delta z} \left[K_{a,b-1/2}^n - K_{a,b}^n \right] \end{aligned}$$

INDICES: $b = 1, 1 < a < a_{\max}$ column implicit

$$\begin{aligned} & \left[(U K)_{a,b}^n + (U K)_{a,b+1/2}^n + 1 \right] h_{a,b}^{n+\Delta} \\ & + \left[-(U K)_{a,b+1/2}^n \right] h_{a,b+1}^{n+\Delta} = \end{aligned}$$

$$\begin{aligned} & \left[(U K)_{a-1/2,b}^{n+\forall^*} \right] h_{a-1,b}^{n+\forall^*} + \left[-(U K)_{a-1/2,b}^{n+\forall^*} - (U K)_{a+1/2,b}^n + 1 \right] h_{a,b}^n \\ & + \left[(U K)_{a+1/2,b}^n \right] h_{a+1,b}^n + \frac{\partial h}{\partial w} \frac{\Delta t}{\Delta z} \left[K_{a,b}^n - K_{a,b+1/2}^n \right] \end{aligned}$$

INDICES: $1 < b < b_{\max}$, $1 < a < a_{\max}$ column implicit

$$\begin{aligned} & \left[-(U K)_{a,b-1/2}^n \right] h_{a,b-1}^{n+\forall} + \left[(U K)_{a,b-1/2}^n + (U K)_{a,b+1/2}^n + 1 \right] h_{a,b}^{n+\forall} \\ & + \left[-(U K)_{a,b+1/2}^n \right] h_{a,b+1}^{n+\forall} \\ & = \left[(U K)_{a-1/2,b}^{n+\forall^*} \right] h_{a-1,b}^{n+\forall^*} + \left[-(U K)_{a-1/2,b}^{n+\forall^*} - (U K)_{a+1/2,b}^n + 1 \right] h_{a,b}^n \\ & + \left[(U K)_{a+1/2,b}^n \right] h_{a+1,b}^n + \frac{\partial h}{\partial w} \frac{\Delta t}{\Delta z} \left[K_{a,b-1/2}^n - K_{a,b+1/2}^n \right] \end{aligned}$$

INDICES: $b = b_{\max}$, $1 < a < a_{\max}$ column implicit

$$\begin{aligned}
 & \left[-(U K)_{a,b-1/2}^n \right] h_{a,b-1}^{n+\Delta} + \left[(U K)_{a,b-1/2}^n + (U K)_{a,b}^n + 1 \right] h_{a,b}^{n+\Delta} \\
 = & \left[(U K)_{a-1/2,b}^{n+\Delta^*} \right] h_{a-1,b}^{n+\Delta^*} + \left[-(U K)_{a-1/2,b}^n - (U K)_{a+1/2,b}^n + 1 \right] h_{a,b}^n \\
 & + \left[(U K)_{a+1/2,b}^n \right] h_{a+1,b}^n + \frac{\partial h}{\partial w} \frac{\Delta t}{\Delta z} \left[K_{a,b-1/2}^n - K_{a,b}^n \right]
 \end{aligned}$$

INDICES: $b = 1, a = \text{amax}$ column implicit

$$\begin{aligned}
 & \left[(U K)_{a,b}^n + (U K)_{a,b+1/2}^n + 1 \right] h_{a,b}^{n+\Delta} + \left[-(U K)_{a,b+1/2}^n \right] h_{a,b+1}^{n+\Delta} \\
 = & \left[(U K)_{a-1/2,b}^{n+\Delta^*} \right] h_{a-1,b}^{n+\Delta^*} + \left[-(U K)_{a-1/2,b}^n - (U K)_{a,b}^n + 1 \right] h_{a,b}^n \\
 & + \frac{\partial h}{\partial w} \frac{\Delta t}{\Delta z} \left[K_{a,b}^n - K_{a,b+1/2}^n \right]
 \end{aligned}$$

INDICES: $1 < b < \text{bmax}, a = \text{amax}$ column implicit

$$\begin{aligned}
& \left[-(U K)_{a,b-1/2}^n h_{a,b-1}^{n+\gamma} + \left[(U K)_{a,b-1/2}^n + (U K)_{a,b+1/2}^n + 1 \right] h_{a,b}^{n+\gamma} \right. \\
& \quad \left. + \left[-(U K)_{a,b+1/2}^n \right] h_{a,b+1}^{n+\gamma} \right] \\
= & \left[(U K)_{a-1/2,b}^{n+\gamma*} h_{a-1,b}^{n+\gamma*} + \left[-(U K)_{a-1/2,b}^n - (U K)_{a,b}^n + 1 \right] h_{a,b}^n \right. \\
& \quad \left. + \frac{\partial h}{\partial w} \frac{\Delta t}{\Delta z} \left[K_{a,b-1/2}^n - K_{a,b+1/2}^n \right] \right]
\end{aligned}$$

INDICES: $b = b_{\max}$, $a = a_{\max}$

columns implicit

$$\begin{aligned}
& \left[-(U K)_{a,b-1/2}^n h_{a,b-1}^{n+\gamma} + \left[(U K)_{a,b-1/2}^n + (U K)_{a,b}^n + 1 \right] h_{a,b}^{n+\gamma} \right. \\
= & \left[(U K)_{a-1/2,b}^{n+\gamma*} h_{a-1,b}^{n+\gamma*} + \left[-(U K)_{a-1/2,b}^{n+\gamma*} - (U K)_{a,b}^n + 1 \right] h_{a,b}^n \right. \\
& \quad \left. + \frac{\partial h}{\partial w} \frac{\Delta t}{\Delta z} \left[K_{a,b-1/2}^n - K_{a,b}^n \right] \right]
\end{aligned}$$

INDICES: $a = 1$, $b = 1$

row implicit

$$\begin{aligned} & \left[(U K)_{a,b}^{n+\gamma} + (U K)_{a+1/2,b+1}^{n+\gamma} \right] h_{a,b}^{n+\gamma+\beta} + \left[- (U K)_{a+1/2,b}^{n+\gamma} \right] h_{a+1,b}^{n+\gamma+\beta} \\ & = \left[- (U K)_{a,b}^{n+\gamma} - (U K)_{a,b+1/2}^{n+\gamma} + 1 \right] h_{a,b}^{n+\gamma} + \left[(U K)_{a,b+1/2}^{n+\gamma} \right] h_{a,b+1}^{n+\gamma} \end{aligned}$$

INDICES: $1 < a < \text{amax}, b = 1$ row implicit

$$\begin{aligned} & \left[- (U K)_{a-1/2,b}^{n+\gamma} \right] h_{a-1,b}^{n+\gamma+\beta} + \left[(U K)_{a-1/2,b}^{n+\gamma} + (U K)_{a+1/2,b+1}^{n+\gamma} \right] h_{a,b}^{n+\gamma+\beta} \\ & \quad + \left[- (U K)_{a+1/2,b}^{n+\gamma} \right] h_{a+1,b}^{n+\gamma+\beta} \\ & = \left[- (U K)_{a,b}^{n+\gamma} - (U K)_{a,b+1/2}^{n+\gamma} + 1 \right] h_{a,b}^{n+\gamma} + \left[(U K)_{a,b+1/2}^{n+\gamma} \right] h_{a,b+1}^{n+\gamma} \end{aligned}$$

INDICES: $a = \text{amax}, b = 1$ row implicit

$$\begin{aligned} & \left[-(U K)_{a-1/2,b}^{n+\gamma} \right] h_{a-1,b}^{n+\gamma+\beta} + \left[(U K)_{a-1/2,b}^{n+\gamma} + (U K)_{a,b+1}^{n+\gamma} + 1 \right] h_{a,b}^{n+\gamma+\beta} \\ & = \left[-(U K)_{a,b}^{n+\gamma} - (U K)_{a,b+1/2}^{n+\gamma} + 1 \right] h_{a,b}^{n+\gamma} + \left[(U K)_{a,b+1/2}^{n+\gamma} \right] h_{a,b+1}^{n+\gamma} \end{aligned}$$

INDICES: $a = 1, 1 < b < b_{\max}$ row implicit

$$\begin{aligned} & \left[(U K)_{a,b}^{n+\gamma} + (U K)_{a+1/2,b+1}^{n+\gamma} \right] h_{a,b}^{n+\gamma+\beta} + \left[-(U K)_{a+1/2,b}^{n+\gamma} \right] h_{a+1,b}^{n+\gamma+\beta} \\ & = \left[(U K)_{a,b-1/2}^{n+\gamma+\beta^*} \right] h_{a,b-1}^{n+\gamma+\beta^*} \\ & + \left[-(U K)_{a,b-1/2}^{n+\gamma+\beta^*} - (U K)_{a,b+1/2}^{n+\gamma} + 1 \right] h_{a,b}^{n+\gamma} + \left[(U K)_{a,b+1/2}^{n+\gamma} \right] h_{a,b+1}^{n+\gamma} \end{aligned}$$

INDICES: $1 < a < a_{\max}, 1 < b < b_{\max}$ row implicit

$$\begin{aligned}
& \left[-(U K)_{a-1/2,b}^{n+\gamma} \right] h_{a-1,b}^{n+\gamma+\beta} + \\
& \left[(U K)_{a-1/2,b}^{n+\gamma} + (U K)_{a+1/2,b}^{n+\gamma} + 1 \right] h_{a,b}^{n+\gamma+\beta} + \left[-(U K)_{a+1/2,b}^{n+\gamma} \right] h_{a+1,b}^{n+\gamma+\beta} \\
& = \left[(U K)_{a,b-1/2}^{n+\gamma+\beta^*} \right] h_{a,b-1}^{n+\gamma+\beta^*} \\
& + \left[-(U K)_{a,b-1/2}^{n+\gamma+\beta^*} - (U K)_{a,b+1/2}^{n+\gamma} + 1 \right] h_{a,b}^{n+\gamma} + \left[(U K)_{a,b+1/2}^{n+\gamma} \right] h_{a,b+1}^{n+\gamma}
\end{aligned}$$

INDICES: $a = \text{amax}, 1 < b < \text{bmax}$ row implicit

$$\begin{aligned}
& \left[-(U K)_{a-1/2,b}^{n+\gamma} \right] h_{a-1,b}^{n+\gamma+\beta} + \left[(U K)_{a-1/2,b}^{n+\gamma} + (U K)_{a,b}^{n+\gamma} + 1 \right] h_{a,b}^{n+\gamma+\beta} \\
& = \left[(U K)_{a,b-1/2}^{n+\gamma+\beta^*} \right] h_{a,b-1}^{n+\gamma+\beta^*} \\
& + \left[-(U K)_{a,b-1/2}^{n+\gamma+\beta^*} - (U K)_{a,b+1/2}^{n+\gamma} + 1 \right] h_{a,b}^{n+\gamma} + \left[(U K)_{a,b+1/2}^{n+\gamma} \right] h_{a,b+1}^{n+\gamma}
\end{aligned}$$

INDICES: $a = 1, b = \text{bmax}$ row implicit

$$\begin{aligned} & \left[(U K)_{a,b}^{n+\gamma} + (U K)_{a+1/2,b}^{n+\gamma} + 1 \right] h_{a,b}^{n+\gamma+\beta} + \left[-(U K)_{a+1/2,b}^{n+\gamma} \right] h_{a+1,b}^{n+\gamma+\beta} \\ & = \left[(U K)_{a,b-1/2}^{n+\gamma+\beta^*} \right] h_{a,b-1}^{n+\gamma+\beta^*} + \left[-(U K)_{a,b-1/2}^{n+\gamma} - (U K)_{a,b}^{n+\gamma} + 1 \right] h_{a,b}^{n+\gamma} \end{aligned}$$

INDICES: $1 < a < \text{amax}, b = \text{bmax}$ row implicit

$$\begin{aligned} & \left[-(U K)_{a-1/2,b}^{n+\gamma} \right] h_{a-1,b}^{n+\gamma+\beta} + \left[(U K)_{a-1/2,b}^{n+\gamma} + (U K)_{a+1/2,b}^{n+\gamma} + 1 \right] h_{a,b}^{n+\gamma+\beta} \\ & + \left[-(U K)_{a+1/2,b}^{n+\gamma} \right] h_{a+1,b}^{n+\gamma+\beta} \\ & = \left[(U K)_{a,b-1/2}^{n+\gamma+\beta^*} \right] h_{a,b-1}^{n+\gamma+\beta^*} + \left[-(U K)_{a,b-1/2}^{n+\gamma} - (U K)_{a,b}^{n+\gamma} + 1 \right] h_{a,b}^{n+\gamma} \end{aligned}$$

INDICES: $a = \text{amax}, b = \text{bmax}$ row implicit

$$\begin{aligned}
& \left[-(U K)_{a-1/2,b}^{n+\gamma} \right] h_{a-1,b}^{n+\gamma+\beta} + \left[(U K)_{a-1/2,b}^{n+\gamma} + (U K)_{a,b}^{n+\gamma} + 1 \right] h_{a,b}^{n+\gamma+\beta} \\
& = \left[(U K)_{a,b-1/2}^{n+\gamma+\beta^*} \right] h_{a,b-1/2}^{n+\gamma+\beta^*} + \left[-(U K)_{a,b-1/2}^{n+\gamma+\beta^*} - (U K)_{a,b}^{n+\gamma} + 1 \right] h_{a,b}^{n+\gamma}
\end{aligned}$$